Analysis of the Function of Rice Homeobox Genes.

Yutaka Sato

Division of Chemical and Cellular Regulation,
Research Institute for Biochemical Regulation,
Graduate School of Bioagricultural Sciences,
Nagoya University, Nagoya, Japan

January, 1998

CONTENTS

Chapter 1

General Introduction

Although most plant development occurs after embryogenesis, the basic body plan in the vascular plant is generated during embryogenesis (Meinke, 1995; Jürgens et al., 1994). Like all sexually reproducing organisms, the vascular plant begins its existence as a single cell, the fertilized egg or zygote. This cell proliferates to be an embryo with some organs and tissues. Early in the embryogenesis, axes patterns which contribute the basic organization of a plant body are formed: namely the apical-basal pattern and the radial pattern. Based on the regional information of these axes, the shoot apical meristem (SAM) and the root apical meristem are developed during embryogenesis (Jürgens, 1995).

After seed germination, the shoot and root apical meristems retain some properties of embryonic cells and continue to produce the post embryonic shoot and root systems of the adult plant. The entire ground portion of a plant body is constructed by piling up a shoot unit called phytomere which consists of an axillary bud, a leaf, and a stem. SAM continuously produces these units keeping itself as collection of indeterminate stem cell (Steeves and Sussex, 1989).

After the phase change of the SAM has occurred, most flowering plants transform the vegetative shoot apical meristem into the inflorescence meristem from which determinate reproductive or floral meristems are arisen. Floral meristems produce floral organs which become sepals, petals, stamens, and carpels. Thus, plants continuously perform organogenesis throughout the life cycle even after embryogenesis. Organogenesis after embryogenesis is a distinct feature of plant development, comparing to the development of higher animals (Walbot, 1985). In the animal embryo, all the organs and tissues are formed at least in rudimentary forms during embryogenesis. Just enlargement of the body and/or its maintenance in a functionally efficient state only occur in postembryonic development of animal bodies.

The process of axis establishment during embryogenesis has been the focus of the developmental biology, regardless of plant or animal materials (Jürgens, 1995; Lawrence and Morata, 1994). Recent advances in studies on animal embryogenesis have established the genetic programs by which genes control patterning (Gehring et al., 1994; Lawrence and Morata, 1994). Some important concepts on the molecular mechanisms governing the developmental processes have been derived from the studies on the *Drosophila* embryogenesis (Lawrence and Struhl, 1996). The studies on developmental processes of many other eukaryotic organisms often depend on such concepts. (1) There is a set of genes controlling the program of the developmental processes. (2) Through this program, regional information over a wide range is transmitted to localized, region specific information. (3) This process is mediated by the cascade of transcriptional regulations and/or signal transductions. (4) Before any visible differentiation of organs, a set of transcriptional regulators which control the expression of genes involved in the organogenesis are expressed as if they mark the regions of the future organogenesis. (5) Families of related genes often specify related developmental processes.

Recent advances in the molecular genetic studies on the determination of a floral organ identity or the maintenance of indeterminacy of the SAM indicate the existence of molecular mechanisms in plant development similar to that governing the developmental process in animals (Bowman et al., 1991; Clark et al., 1996). From a number of homeotic mutations affecting floral organ identities, Bowman et al., (1991) established a genetic model for the determination of floral organ identities. It has been revealed that most of the floral homeotic genes are encoded by a family of MADS box genes (Coen and Meyerowitz, 1991). Also in the analysis of the indeterminacy in the SAM, it has been suggested that genes designated *CLV1* and *STM* function in the competitive manner for the maintenance of the indeterminate cells in the SAM

(Clark et al., 1996). It has been revealed that *CLV1* encodes a receptor kinase and this suggests the involvement of a signal transduction pathway via extra cellular ligands to the SAM activity (Clark et al., 1997). Also it has been revealed that *STM* encodes a *KNOTTED*-type homeobox gene and it may function in the meristem maintenance (Long et al., 1996). Though they are still fragmental evidences, these two examples of molecular mechanisms governing plant development suggest that it is possible to apply the concepts of the molecular mechanisms governing the animal patterning to that of plant development.

Homeotic mutations of the fruit fly, *Drosophila melanogaster*, in which entire body parts (albeit non functional) develop in inappropriate locations, such as the replacements of halters with wings, antennae with legs, or mouth parts with legs, have been very useful in addressing the molecular genetic mechanisms underlying the body plan of *Drosophila* (for review, see Hayashi and Scott, 1990). Homeotic genes are therefore thought to play a crucial role in positional specification. Molecular cloning of *Drosophila* homeotic genes has revealed that they share a conserved 180 bp DNA sequence element called the homeobox (McGinnis et al., 1984; Scott and Weiner, 1984). The homeobox encodes a conserved 60 amino acid sequence referred to as the homeodomain which interacts with specific DNA sequences. Through the DNA binding property of the homeodomain, the products of homeobox genes are believed to regulate the expression of batteries of target genes as transcriptional factors (Affolter et al., 1990; Andrew et al., 1992). The evolutionary conservation of the homeobox sequence has enabled the identification in many organisms of homeobox genes and gene families that are potentially important regulators of development (Scott et al., 1989). Recently, it has been revealed that homeobox gene families also exist in higher plants.

In higher plants, the first homeobox gene was cloned by transposon tagging from the maize *Knotted1* (*Kn1*) mutant as *KNOTTED1* (*KN1*) gene (Vollbrecht et al., 1991). In the *Kn1* mutant, abnormal arrangements of lateral veins, sporadical outgrowths called knots, and ligule displacement are observed in leaf blades . It has been revealed that *Kn1* is a dominant mutation caused by ectopic expression of *KN1* in leaves, and that its ectopic expression results in the disorganization of the developmental program of leaf blades (Smith and Hake, 1994).

Many homeobox genes have been cloned from various plant species in an effort to address the biological functions of homeobox genes in plant development. Based on amino acid sequence similarities within the homeodomain or conserved protein motifs outside of the homeodomain, plant homeobox genes have been classified into five groups (Kerstetter et al., 1994; Lu et al., 1996). These include the KNOTTED-type homeodomain proteins, homeodomain zipper proteins (HD-ZIP), plant homeodomain finger proteins (PHD-finger), the GLABRA2 homeodomain protein, and the BELL1 homeodomain protein. In animals, families of related homeobox genes often specify related developmental processes (Gehring et al., 1994). Based on the observations that KNOTTED-type homeodomain proteins are expressed around the SAM and overexpression of these genes affects the developmental program of the leaf blades, it has been suggested that genes of this class are involved in maintenance of the SAM and/or the development of lateral organs from it (Smith et al., 1992).

I am interested in elucidating the role of KNOTTED-type homeobox genes in plant development, especially in monocotyledonous plants. Toward this goal, I have isolated a family of KNOTTED-type homeobox genes from rice. Recently rice has become a model system in monocotyledonous plants for plant biologists, mainly because of the accumulated mutants, the feasibility of efficient transformation, the creation of a highly saturated molecular genetic

map, and the large-scale analysis of expressed sequence tags (Izawa and Shimamoto, 1996). So the isolation and characterization of KNOTTED-type genes from rice will permit further molecular and genetic analyses of this class of homeobox genes.

In this thesis, I have analyzed the functions of two KNOTTED-type rice homeobox genes, *OSH1* and *OSH15* with several approaches.

As I mentioned, ectopic expression of KNOTTED-type homeobox genes including *OSH1* in transgenic plants resulted in the abnormal leaf morphologies. This phenomenon has been explained that the developmental program of leaves are disorganized by ectopic expression of the homeobox genes. The relation between misexpression of homeobox genes and the cellular basis of these abnormal leaf morphologies were unknown, because the transgenes were expressed ubiquitously by the Cauliflower Mosaic virus *35S* promoter in the previous studies. In chapter 2, I tried to analyze when and where *OSH1* acts for induction of the abnormal leaf morphologies in transgenic tobacco plants. In chapter 3, in order to analyze the function of *OSH1* in wild-type rice, I determined the expression pattern of *OSH1* during embryogenesis by *in situ* hybridization analysis. In chapter 4, from the ectopic expression experiments in transgenic tobacco plants and the analysis of expression pattern through almost all the rice life cycle, I discussed the pleiotropic function of *OSH15* during rice development. In order to determine the *bona fide* function of a gene of interest, it is a crucial step to identify loss-of-function mutations. I have identified the loss-of-function mutations in *OSH15*. In chapter 5, I analyzed the phenotype of these mutants and discussed the function of *OSH15* during rice development.

References

Affolter, M., Schier, A., and Gehring, W. J. (1990) Homeodomain proteins and regulation of gene expression. *Current Opin. Cell Biol.* **2,** 485-495.

Andrew, D. J., and Scott, M. P. (1992) Downstream of the homeotic genes. *New Biologist* **4,** 5-15.

Bowman, J, L., Smyth, D. R., and Meyerowitz, E. M. (1991) Genetic interactions among floral homeotic genes of *Arabidopsis*. *Development* **112**, 1-20.

Clark, S. E., Jacobsen, S. E., Levin, J. Z., and Meyerowitz, E. M. (1996) The *CLAVATA* and *SHOOT MERISTEMLESS* loci competitively regulate meristem activity in *Arabidopsis*. *Development* **122**, 1567-1575.

Clark, S. E., Williams, R. W., and Meyerowitz, E. M. (1997) The *CLAVATA1* Gene Encodes a Putative Receptor Kinase That Controls Shoot and Floral Meristem Size in Arabidopsis. *Cell* **89**, 575-585.

Coen, E. S., and Meyerowitz, E. M. (1991) The war of whorls: Genetic interactions controlling flower development. *Nature* **353**, 31-37.

Gehring, W. J., Affolter, M., and Bürglin, T. (1994) HOMEODOMAIN PROTEINS. *Annu. Rev. Biochem.* **63,** 487-526.

Hayashi, S., and Scott, M. (1990) What determines the specificity of action of *Drosophila* homeodomain proteins? *Cell* **63,** 883-894.

Izawa, T. and Shimamoto, K. (1996) Becoming a model plant: the importance of rice to plant science. *Trends plant sci.* **1**, 95-99.

Jürgens, G., Ruiz, T., and Berleth, T. (1994) EMBRYONIC PATTERN FORMATION IN FLOWERING PLANTS. *Annu. Rev. Genet.* **28**, 351-371.

Jürgens, G. (1995) Axis Formation in Plant Embryogenesis: Cues and Clues. *Cell* **81**, 467-470.

Kerstetter, R., Vollbrecht, E., Lowe, B., Veit, B., Yamaguchi, J. and Hake, S. (1994) Sequence Analysis and Expression Patterns Divide the Maize *knotted1*-like Homeobox Genes into Two Classes. *Planat Cell* **6**, 1877-1887.

Lawrence, P. A. and Morata, G. (1994) Homeobox genes: Their Function in Drosophila Segmentation and Pattern Formation. *Cell* **78**, 181-189.

Lawrence, P. A., and Struhl, G. (1996) Morphogens, Compartments, and Pattern: Lessons from Drosophila? *Cell* **85**, 951-961.

Long, J. A., Moan, E. I., Medford, J. I. and Barton, M. K. (1996) A member of the KNOTTED class of homeodomain proteins encoded by the *STM* gene of *Arabidopsis*. *Nature* **379**, 66-69.

Lu, P., Porat, R., Nadeau, J. A. and O'Neill, S. D. (1996) Identification of a Meristem L1 Layer-Specific Gene in Arabidopsis That Is Expressed during Embryonic Pattern Formation and Defines a New Class of Homeobox Genes. *Plant Cell* **8**, 2155-2168.

McGinnis, W., Levine, M. S., Hafen, E., Kuroiwa, A., and Gehring, W. J. (1984) A conserved DNA sequence in homeotic genes of the *Drosophila* Antennapedia and bithorax complexes. *Nature* **308,** 428-433.

Meinke, D. W. MOLECULAR GENETICS OF PLANT EMBRYOGENESIS. *Annu. Rev. Plant Phsiol. Plant Mol. Biol.* **46**, 369-394.

Scott, M. P., Tamkun, J. W., and Hartzell, G. W. III (1989) The structure and function of the homeodomain. *BBA Rev. Cancer* **989,** 25-48.

Scott, M. P., and Weiner, A. J. (1984) Structural relationships among genes that control development: sequence homology between the *Antennapedia*, *Ultrabithorax*, and *fushi tarazu* loci of Drosophila. *Proc. Natl. Acad. Sci. USA* **81,** 4115-4119.

Smith, L. G., Greene, B., Veit, B., and Hake, S. (1992) A dominant mutation in the maize homeobox gene, *Knotted-1*, causes its ectopic expression in leaf cells with altered fates. *Development* **116,** 21-30.

Smith, L. G. and Hake, S. (1994) Molecular genetic approaches to leaf development: *Knotted* and beyond. *Can. J. Bot.* **72**, 617-625.

Steeves, T. A. and Sussex, I. M. (1989) Patterns in Plant Development. Cambridge University Press.

Vollbrecht, E., Veit, B., Sinha, N., and Hake, S. (1991) The developmental gene *Knotted-1* is a member of a maize homeobox gene family. *Nature* **350**, 241-243.

Walbot, V. (1985) On the life strategies of plant and animals. *Trends Genet.* **1**, 165-169.

Chapter 2

Abnormal cell divisions in leaf primordia caused by the expression of the rice homeobox gene *OSH1* lead to altered morphology of leaves in transgenic tobacco.

Introduction

The molecular mechanisms which underlie the body plan of living organisms have long been a fundamental question of biology. Homeotic mutants of the fruit fly, *Drosophila melanogaster*, in which whole (albeit nonfunctional) body parts develop in inappropriate locations, in effect replacing halters with wings, antennae with legs, or mouth parts with legs have been very useful in addressing this question (for review, see Hayashi and Scott, 1990). Homeotic genes are therefore thought to play a crucial role in positional specification. Molecular cloning of *Drosophila* homeotic genes has revealed that they share a conserved 180 bp DNA sequence element called the homeobox (McGinnis et al., 1984; Scott and Weiner, 1984). The homeobox encodes a conserved 60 amino acid sequence referred to as the homeodomain which interacts with specific DNA sequences. Through the DNA binding property of the homeodomain, the products of homeobox genes are believed to regulate the expression of batteries of target genes as transcriptional factors (Affolter et al., 1990; Andrew et al., 1992).

The evolutionary conservation of the homeobox sequence has enabled the identification in many organisms of homeobox genes and gene families that are potentially important regulators of development (Scott et al., 1989). One useful means of investigating the function of homeobox genes has been the analysis of dominant gain-of-function homeotic mutations resulting from over-expression of the cloned genes in vivo. For example, the function of the mouse *Hox* gene, *Hox1.1*, which contains a *Drosophila antennapedia* type homeobox sequence, was investigated by expressing a *Hox1.1* construct under the control of an ubiquitously expressed promoter (Kessel et al., 1990). Although the embryos were not viable, a number of transformations of cervical vertebrae into more posterior body segments were observed. Jegalian and De Robertis (1992) also generated a transgenic mouse ectopically expressing

the human *Hox3.3* gene, and found homeotic transformations of the skeleton. These results demonstrate that over-expression of the cloned genes in transformants is one of the useful means for investigating the function of homeobox genes.

Recently, homeobox genes have been cloned from several species of higher plants, maize (Vollbrecht et al. 1991; Bellmann and Werr, 1992), *Arabidopsis* (Ruberti et al., 1991; Mattsson et al., 1992; Schena and Davis, 1992; Carabelli et al., 1993; Schindler, et al., 1993), and rice (Matsuoka et al., 1993). By analogy with the functional roles of animal homeobox genes, plant homeobox genes are thought to encode transcriptional regulators that play important roles in developmental processes (Schena and Davis, 1992). As in the case of animal homeobox genes, experiments using transgenic organisms are a powerful means of understanding the function of the cloned homeobox genes in plants. Schena et al. (1993) succeeded in generating transgenic *Arabidopsis* which alter the expression of a homeobox gene, *HAT4*, and observed morphological alterations in those transgenic plants. Based on these observations, they predicted that *HAT4* functions as a master regulator of developmental rate. Sinha et al (1993) have also produced transgenic tobacco plants transformed with a maize homeobox gene, *KN1*, and observed altered phenotypes in transformants such as abnormally shaped leaves, loss of apical dominance, and severe dwarfism. Based on these observations they proposed that the *KN1* homeobox gene plays a role in determining cell fate.

We reported that overexpression of a rice homeobox gene, *OSH1*, causes altered morphology including abnormally shaped leaves and flowers of transgenic *Arabidopsis* and tobacco, and suggested that *OSH1* acts as a regulator of leaf morphological development (Kano-Murakami et al., 1993; Matsuoka et al., 1993). In these experiments, the introduced homeobox genes were driven by the cauliflower mosaic virus 35S promoter (35S promoter) in the transgenic plants. The 35S promoter constitutively drives the

transgene expression in almost all organs of the transformants, and this made it difficult to decide which components of transgene expression were necessary or sufficient for development of aberrant morphological features. We have recently found that an *OSH1* transgene controlled by the promoter of a tobacco pathogenesis-related protein 1a (*PR1a*) morphologically alters transgenic tobacco plants, even though transgene expression is undetectable in fully-developed leaves (Kano-Murakami et al., 1993).

Northern analysis using the *PR1a* cDNA indicates this gene is not expressed in healthy tobacco tissue (Matsuoka et al., 1988), however, *PR1a* is specifically induced in response to pathogenic infection as well as some chemical inducers (Ohashi and Matsuoka, 1985). I chose the *PR1a* promoter for *OSH1* transgene expression expecting to be able to induce *OSH1* expression using chemical inducers. Contrary to my expectations, the *PR1a-OSH1* constructs result in abnormal phenotypes without chemical treatment, and interestingly *OSH1* expression is undetectable in the leaves of transformants that have aberrant morphology. *OSH1* expression was observed in the shoot apices of these plants, however, indicating that ectopic expression of *OSH1* in the shoot apex is sufficient to alter the morphology of developing leaves. The only abnormal phenomenon I observed in shoot apical meristem tissue expressing the *OSH1* transgene was periclinal division in regions where anticlinal division would normally occur. All the other abnormal phenomena I observed occurred in tissues which do not express *OSH1*. Thus it appears that the abnormal morphological features induced by *OSH1* are attributable to the occurrence of abnormal periclinal division in the shoot apical meristem.

Experimental Procedures

Construction of chimeric genes

A cDNA clone encoding rice *OSH1* was introduced into the XbaI/SacI site of pBI121 (Clontech Lab. Inc., CA, USA) to construct 35S-*OSH1* (Matsuoka et al, 1993). The promoters of the NOS and *PR1a* genes were each amplified by PCR using 5' primers containing HindIII recognition sites (positions -256 and -902, respectively) and 3' primers with XbaI recognition sites (positions +37 and +29, respectively). The PCR products were cloned into the HindIII-XbaI site of pUC119, and the sequences were analyzed to confirm that nucleotide substitution had not occurred during PCR. Both promoters which were cloned into pUC119 were used to replace the 35S promoter of the 35S-*OSH1* construct at the HindIII-XbaI site to produce the NOS-*OSH1* and *PR1a-OSH1* constructs.

Transformation and regeneration of tobacco

The fusion constructs were then introduced into *Agrobacterium tumefaciens* LBA4404 by electroporation. Transformation of *Nicotiana tabacum* cv. Samsun NN was according to the leaf disc method as previously reported (Matsuoka and Sanada, 1991). Transformants were selected in medium containing 100 mg/L of kanamycin.

Northern blot analysis

Total RNA was separately prepared from various organs for Northern blot analysis. Each RNA preparation was transferred to nitrocellulose membranes and hybridized to the entire *OSH1* insert. Hybridization with a labeled cDNA insert was performed in 50% formamide, 5 x SSC (1 x SSC is 0.15 M NaCl, 15 mM sodium citrate), 6 x Denhardt's solution (1 x Denhardt's solution is 0.02% Ficoll, 0.02% PVP, 0.02% BSA), 0.5% SDS, and 0.1 mg/mL salmon

sperm DNA at 62°C for 20 Hr. Each filter was washed with 0.1 x SSC and 0.1% SDS at 55°C for 3 Hr.

Histology and *in situ* hybridization

Plant material was fixed in 4% (w/v) paraformaldehyde and 0.25% glutaraldehyde in 0.1 M sodium phosphate buffer, pH 7.4 overnight at 4°C, dehydrated through a graded ethanol series and then a *t*-butanol series (Sass, 1958), and finally embedded in Paraplast Plus (Sherwood Medical). Microtome sections (7-10 μm thick) were applied to glass slides treated with Vectabond (Vector Labs). The sections were deparaffinized in xylene, rehydrated through a graded ethanol series and dried overnight prior to staining with hematoxylin. *In situ* hybridization with digoxigenin-labeled sense or antisense RNA was conducted according to the method of Kouchi and Hata (1993).

Results

Limited expression of *OSH1* in shoot apices alters the morphology of transgenic tobacco leaves

OSH1 transgene expression under the promoters of the nopaline synthetase gene (NOS) and 35S in tobacco transformants resulted in aberrant morphology including wrinkled leaves with thick blades and short midveins, dwarfism, loss of apical dominance, and formation of ectopic shoots on tiny disc-shaped leaves, as reported previously (Kano-Murakami et al., 1993). The severity of the aberrant morphology differed in each transformed line but almost all NOS-*OSH1* transformants had less severe phenotypes than 35S-*OSH1* transformants. The severity of the phenotype of a given transformant correlated with the level of *OSH1* expression in fully-developed leaves; e.g. high level of *OSH1* expression was associated with ectopic shoots on disc-like leaves and severe dwarfism, while plants with low level expression had wrinkled leaves.

In *PR1a-OSH1* transformants, however, no such correlation was observed (Fig. 2-1). I divided the *PR1a-OSH1* transformants into four phenotypic categories; plants with the mild phenotype have wrinkled leaves. The intermediate plants have elongated stems with slender leaves and wrinkled older leaves. The severe plants are dwarfs and the leaves have deep sinuses. I describe the phenotype of the fourth group as being "shooty". These plants are severe dwarfs with axillary buds which develop into vegetative stems, rather than remaining dormant. Shooty leaves are not wrinkled but are tiny and often form ectopic shoots. I was unable to detect expression of the transgene in fully-developed leaves of the mild, intermediate or severe transformants.

PR1a gene expression in tobacco does not occur in leaves under normal conditions (Matsuoka et al., 1988), but occurs during stress conditions

such as virus infection (Antoniw et al., 1980), wounding (Ohashi and Matsuoka, 1985), and treatment with some chemicals (Antoniw and White, 1980), therefore lack of *PR1a-OSH1* expression in fully-developed leaves is not an unexpected result. High level expression of the transgene was detected in shooty plants; however, interestingly, the endogenous *PR1a* gene is also highly expressed in these plants. Constitutive expression of the *PR1a* gene was also observed in the 35S-*OSH1* transformants (data not shown). Production of the OSH1 protein by the NOS promoter did not induce the expression of the *PR1a* gene (data not shown) suggesting that the OSH1 product does not work as a direct regulator of the *PR1a* expression. My recent results demonstrate that the high amount of OSH1 product causes some physiological stresses,such as changes in levels of some phytohormones. These stresses may result in the induction of PR1a promoter activity.

It is noteworthy that severe phenotypes were observed even in transformants showing no detectable expression of the transgene in fully-developed leaves(Fig. 2-1i). Northern blot analysis with a higher quantity of RNA (10μg) also supported no or very low level of expression of *OSH1* in developed leaves in PR1a-*OSH1* transformants(Fig. 2-2). This indicates that *OSH1* expression in a given leaf of PR1a-*OSH1* transformants is not necessary for that leaf to develop an abnormal morphology. Furthermore, when *OSH1* expression in the fully-developed leaves was induced by salicylic acid, a chemical inducer of the *PR1a* promoter, no visibele effect was observed (data not shown). This further suggests that expression of *OSH1* during a limited time period or in a limited area is sufficient for producing altered leaf morphology. To explore this question further, I performed Northern blot hybridization analysis using RNA isolated from various organs of a severe T2 transformant line, that do not express the transgene in developed leaves (Fig. 2-2). RNAs of about 1.6 kb were detected in vegetative and

reproductive meristems, corresponding to the size of the *OSH1* clone that I used to construct the transgene.

I also analyzed temporal and spatial expression of the transgene in T2 transgenic plants with the severe phenotype by *in situ* hybridization (Fig. 2-3). I tested five transgenic plants and found the same results in all the lines. Expression of the transgene was observed in cross sections of the shoot apices of transformed lines (Fig. 2-3A). Hybridization signals occurred mainly in shoot apical meristems (sam) and leaf buttresses (P1 and P2 in Fig. 2-3A) and the youngest leaf primordium (P3 in Fig. 2-3A). In more mature leaf primordia (P4 and P5) faint signals were observed in the vascular strands of the developing midveins. Under the same conditions, no hybridization signals were obtained with the sense probe in any part of the shoot apical region (Fig. 2-3B). In longitudinal sections through the shoot apex, hybridization signals were found in shoot apical meristems, P1 leaf buttresses, in the provascular tissues of leaf primordia and in the procambium of the stems (Fig. 2-3C). No signal was detected in cross sections of leaf primordia located 1-2 mm below the shoot apical meristem (Fig. 2-3D), indicating that *PR1a-OSH1* gene expression occurs only in shoot apical meristems, leaf buttresses and very young leaf primordia. Recent studies of endogenous *PR1a* expression in untransformed tobacco (T_0) indicated the same expression pattern as observed for the *PR1a-OSH1* transgene (Murakami et al. unpublished results). This result also indicates that the expression of *OSH1* by the *PR1a* promoter does not affect its own expression pattern in transformants with the severe phenotype.

Leaf growth in phenotypically severe transformants

Northern analysis and *in situ* hybridization demonstrated that the *OSH1* transgene is expressed only in shoot apical meristems and very young leaf primordia, and therefore, the altered morphology observed in mature leaves

must be a consequence of unusual leaf development patterns initiated by *OSH1* gene expression. I followed leaf development in T_0 tobacco and in several transformed lines by placing marks at 1 mm intervals on relatively normally-shaped leaves of 5-15 mm in length and observing the pattern formed by the spots during development. A typical result is shown in Fig. 2-4. In this leaf, the growth of the right side of the blade was arrested relative to that of the left side, and asymmetrical growth of the leaf blade resulted in curvature of the midvein to the right. Anisotropic growth occurred in most areas of this leaf, particularly in the basal region, however, the most abnormal growth was observed in the basal region to the right of the midvein. A limited area of the leaf margin in this region expanded to form a lobe. The left margin of the leaf was initially entire, however within 3 days the margin was sinuate and thereafter became undulate. Such abnormal expansion of the leaf blade was observed in all the leaves I tested, indicating that the expression of *OSH1* in leaf primordia causes anisotropic expansion of the leaf blade.

I also measured leaf growth in length and width in the severe transformants and in T_0 plants (Fig. 2-5). Transformant leaf growth in length is similar to that of T_0 plants up to the 2-3 cm stage (Fig. 2-5A). Beyond this point, leaves in transformed lines lengthened at a slower rate. Leaf growth in width was slower than that of T_0 plants at all stages of development measured (Fig. 2-5B). These results correspond with the observations presented in Fig. 2-4, and confirm that *OSH1* expression arrests lateral expansion and lengthening of leaf blades. These observations also indicate that the programs governing lateral growth are affected more severely by *OSH1* expression in young leaves than that governing longitudinal growth.

I also observed the morphology of the young leaves surrounding the shoot apex (less than 20 mm in length, Fig. 2-6). The leaf blades of T_0 plants expand symmetrically at the same rate, and the lateral veins arise symmetrically in an organized manner at an oblique angle to the midvein

(which is almost constant) to form a pinnate venation system. In the severe transformants asymmetrical leaf blade expansion is evident in leaves of 3.5 mm in length and becomes more pronounced with further development. As mentioned above, the midveins of some leaves curve due to this asymmetry. The formation of lateral veins was also disorganized in the leaves of severe transformants. For example, as shown in Fig. 2-6, the angles of the lateral veins to the midvein varied in a leaf of 19 mm in length and the number of veins differed between the left and right sides of the leaf blade. Consequently, this leaf did not form the pinnate venation system observed in the leaves of T_0 plants (Fig. 2-6). In T_0 tobacco, the first three or four veins arise simultaneously in the leaf blade when the leaf is 1 mm in length, and by the time the leaf has reached a length of 3 mm, all six or seven major lateral veins have been initiated (Poethig and Sussex, 1985). Abnormal development of the lateral veins was observed in transformant leaves of 3-5 mm length, in that only one or two lateral veins were present on each side of the leaf blade. Therefore, in leaves of the severe transformants, the formation of lateral veins is not only disorganized but fewer lateral veins are initiated.

The above observations demonstrate that some abnormal phenomena in the external morphology have already occurred by the time a leaf has reached a length of about 3 mm. I observed the anatomy of leaf primordia of the severe transformants. In T_0 tobacco, the leaf blade consists of six to seven cell layers which generate from the upper to the lower layers the upper epidermis, the palisade mesophyll, the middle spongy mesophyll, the lower spongy mesophyll, and the lower epidermis (McHale, 1993, Fig. 2-7A). In contrast to T_0 tobacco leaves, transformant leaves did not show clear cell lineages except in the outer-most layers, which generate the upper and lower epidermis (Fig. 2-7B). The leaf blades were thicker than those of T_0 tobacco leaves due to the intercalation of cells into the cell layers to disrupt the lineage of these layers. In more mature leaves, the cell lineages were severely

disrupted; for example, the leaf blade shown in Fig. 2-7C is comprised of more than ten cells stacked near the basal region to form very thick blade. In some sections of the leaf blades, I observed abnormal clusters of meristematic cells indicated by arrowheads in Fig. 2-7D. Radial cell clusters observed in cross sections of T_0 tobacco leaf blades develop to veins. However, cell clusters such as those shown in Fig. 2-7D never extended longitudinally in the blades of transformant leaves.

The six cell layers in T_0 tobacco leaf blades are maintained during lateral expansion of the leaf blade by a strict pattern of anticlinal division of each cell relative to the blade surface (McHale, 1993, Fig. 2-7E). At the initiation of leaf blade formation in the transformants, I observed abnormal periclinal divisions in the mesophyll cell layers (indicated by white arrowheads in Fig. 2-7F and 2-7G). These divisions occurred sporadically in leaf blades, thickening the leaf blade and disorganizing the cell layers. *In situ* hybridization indicates that *OSH1* is expressed in emerging blades of the transformants at this stage, thus *OSH1* either directly or indirectly causes these periclinal divisions to occur.

Discussion

In previous studies, we reported that the expression level of the *OSH1* transgene in leaves with aberrant morphology correlated with the severity of the abnormality of the leaves and suggested that the expression levels affected the degree of these abnormalities in transgenic plants (Matsuoka et al., 1993). Sinha et al. (1993) reported similar observations, suggesting that the severity of the phenotypes of transgenic tobacco depended on the levels of KN1 protein, a maize homeobox protein. Interestingly, *OSH1* expression in developing or fully-developed leaf blades is not necessary for these aberrations to occur. *PR1a-OSH1* transformants display all of the same morphological abnormalities observed in NOS-*OSH1* transformants, even though the *PR1a* promoter drives the expression of *OSH1* only in shoot apical meristems and very young leaf primordia, demonstrating that limited *OSH1* expression is sufficient to induce severe morphological aberrations, which are evident much later, in well-developed leaves.

In the present studies, I used *PR1a-OSH1* transformants to investigate the function of *OSH1*, because limited expression of the transgene makes it easy to eliminate indirect phenomena caused by the secondary or tertiary effects of *OSH1* expression, which occur in tissues in which *OSH1* is not expressed. If abnormal development occurs in a tissue which does not express the transgene, this must be due to an indirect effect of transgene expression. In the 35S-*OSH1* transformants, it is difficult to distinguish between direct and indirect consequences, because the 35S promoter constitutively drives *OSH1* expression in almost all tissues.

The only abnormal phenomenon that I observed in tissues expressing the *OSH1* gene was periclinal division of mesophyll cells at blade initiation. According to the observations of McHale (1993), the tobacco leaf blade starts as six superimposed cell layers by the cell division of the inner and outer cells

of the midrib. The six cell layers are classified into three cell lineages, L1, L2, and L3. The outer-most cell layer, L1, forms the upper and lower epidermis, and the L2 cell layer contributes two cell layers to the expanding blade, the upper (palisade) and lower (spongy) mesophyll. The L3 cell layer forms the spongy mesophyll, the inner-most cell layers in leaf blades. These cell layers are all established and maintained by a strict pattern of anticlinal division relative to the leaf blade surface during blade initiation. In T_0 tobacco plants, I observed well-organized cell lineage as reported by McHale at blade initiation and at various stages of development (Fig. 2-7 A and E). The strict cell division pattern was disrupted in transgenic tobaccos. The L2 and L3 cells often divided periclinally relative to the blade surface (Fig. 2-7 F and G). These periclinal divisions did not occur continuously throughout the cell layers, but occurred sporadically, disrupting the L2 and L3 cell lineages and consequently disrupting the organized cell layers in leaf blades. Indeed, the more mature leaf blades of transformed lines were composed of irregular cell layers and were thicker with more than the six cell layers observed in T_0 leaves (Fig. 2-7 B and C).

There is a negative correlation between the frequency of periclinal division and the lateral expansion of leaf blades. The higher the frequency of periclinal division, the more lateral expansion of the leaf blades was arrested. Thus, the difference in the lateral expansion between the right and left sides of a given leaf blade can be explained by the difference in the frequency of periclinal division. If higher rates of periclinal division occur in the right side of the blade than in the left side, the blade expansion of the right side becomes slower than that of the left side and consequently the midvein develops a curve to the right. A similar observation was reported for the *fat* mutant of *Nicotiana sylvestris,* namely, that abnormal periclinal divisions in leaf blades arrest lateral leaf blade expansion (McHale, 1993). The leaves of the *fat* mutant show a deficiency in lateral development and attain just over half the

width of the wild type. The leaf blade of the mutant contains extra cell layer(s) resulting from abnormal periclinal divisions in L2 and L3 founder cells during blade initiation and expansion. This generates a blade approximately twice the normal thickness and causes the arrest of lateral development. These observations for the *fat* mutant support my findings and interpretations in the *PR1a-OSH1* transformed lines and also indicate that arrest of lateral leaf blade development is not a direct effect of the *OSH1* expression but a result of abnormal periclinal cell division that occurs at the stage of blade initiation.

The molecular mechanisms controlling the orientation of cell division in higher plants are unclear, however, it has been pointed that microtubules play a crucial part in influencing the site and plane of cell division (for review, see Gunning, 1982). One of the earliest signs of orientation of cell division is the congregation of microtubules in a discrete band circling the cell to form a preprophase band (Gunning and Sammut, 1990). This preprophase band of microtubules predicts where the new cell wall will join the old one when the cell later divides. It is possible, therefore, that the *OSH1* product may interfere with the regulation of microtubule alignment resulting in periclinal division of mesophyll cells during leaf blade initiation. The *fat* gene may be one of the target genes of the *OSH1* product, or perhaps, vice versa. The expression of the *OSH1* gene in transformed lines may result in ectopic expression or suppression of genes which regulate microtubule alignment, consequently resulting in abnormal leaf blade development.

I also observed abnormal lateral vein formation and/or arrest in the early stages of leaf development in the *PR1a-OSH1* transformed lines. According to the observations of Poethig and Sussex (1985), lateral provascular strands first appear in the leaf blade when the leaf is 1 mm long, and by the time the leaf has reached a length of 3 mm, all six or seven major lateral veins have been initiated. Then, lateral veins extend from the midrib toward the margin, to form a pinnate venation system (Avery, 1933). In

transgenic tobacco, lateral vascular differentiation was severely arrested relative to that of T_0 leaves. Moreover, there are fewer veins in mature leaves than in T_0 leaves and the orientation of the veins in the leaf blade is irregular, those in T_0 leaves are well organized in a pinnate venation with a constant oblique angle to the midvein. At this stage, *OSH1* expression is quite low, so the failure to develop normal vascular tissue is probably not a direct consequence of *OSH1* expression. Vascular tissues originate from inner mesophyll cells. Therefore, the aberrant venation pattern in these transformed lines is probably due to the occurrence of periclinal cell division in the inner mesophyll cells and the resulting disruption of the inner mesophyll cell layers. The abnormal arrangement of inner mesophyll cells may also arrest the differentiation of mesophyll cells into vascular strands.

From several structural studies on *OSH1,* I have predicted that *OSH1* is a rice counterpart of the maize *KN1* gene, and therefore the biological function of *OSH1* in rice is thought to be similar to that of *KN1* in maize. Indeed, tobacco plants overexpressing *OSH1* and *KN1* from the 35S promoter exhibit similar abnormalities in leaf morphology, loss of apical dominance, severe dwarfism, and ectopic formation of shoot meristems on the surface of small leaves (Kano-Murakami et al., 1993; Sinha et al., 1993). Smith et al., (1992) have hypothesized that *KN1* may function to oppose determination, the process by which cells become committed to their developmental fates, manifested in patterns of cell division and growth, and ultimately in cellular differentiation. This hypothesis corresponds well with my observation that *OSH1* expression changes the orientation of mesophyll cell division in the process of leaf blade development, and consequently affects the differentiation of lateral veins from mesophyll cells. Based on the observation that the down-regulation of *KN1* within the shoot apical meristem occurs just prior to the emergence of a leaf primordium, these authors also suggest that the *KN1* gene may play a role in the switching of an indeterminate organ, the

undifferentiated shoot meristem, to a differentiated organ, a leaf primordium (Sinha et al., 1993). This contrasts with my observations in that leaf primordium development appeared to occur normally until the stage of leaf blade initiation, thus the transition from undifferentiated shoot meristem to differentiated leaf primordium was unaffected. The ectopic expression of *OSH1* from the 35S promoter in transgenic rice also does not disrupt the development of leaf primordia (Matsuoka unpublished result), suggesting that this result is not due to abnormalities associated with expression of a monocot gene in a dicot plant. We have recently observed *OSH1* expression in rice plants by *in situ* hybridization, and it mainly occurs in developing vascular strands of stems but not in the shoot apical meristem or in leaf primordia (Matsuoka et al., 1995). These observations indicate that the biological role of *OSH1* in rice is not related to the development of a determined organ (a leaf) from an undetermined organ (the shoot apical meristem). In contrast to *OSH1, KN1* expression in maize mainly occurs in indeterminate organs such as the shoot apical meristem and the tassel inflorescence, while its expression is absent in the presumed position of the incipient leaf (Jackson et al., 1994). Why such differences were observed between the *OSH1* and *KN1* expression patterns is presently unclear, but it is possible that their functions differ, even though the genes are very similar in structure and result in very similar aberrant morphological features in transgenic tobacco overexpressing these genes.

Summary

Transgenic tobacco plants carrying a rice homeobox gene, *OSH1*, controlled by the promoter of a gene encoding a tobacco pathogenesis-related protein (*PR1a*) were generated. The transgenic tobacco lines were morphologically abnormal, with wrinkled and/or lobed leaves. Histological analysis indicated arrest of lateral leaf blade expansion often resulting in asymmetric and anisotropic growth of leaf blades. Other notable abnormalities include abnormal or arrested development of lateral veins. Interestingly, *OSH1* expression was undetectable in mature leaves with these aberrant morphological features. Thus, *OSH1* expression in mature leaves is unnecessary for abnormal leaf development. Northern blot analysis and *in situ* hybridization indicate *PR1a-OSH1* gene expression only in the shoot apical meristem and in very young leaf primordia. Therefore, the aberrant morphological features are an indirect consequence of ectopic *OSH1* gene expression. The only abnormality observed in tissues expressing the transgene was periclinal (rather than anticlinal) division in mesophyll cells during blade initiation. This generates thicker leaf blades and disrupts the mesophyll cell layers, from which vascular tissues differentiate. The *OSH1* product appears to affect the mechanism controlling the orientation of the plane of cell division, resulting in abnormal periclinal mesophyll cell division, which in turn results in the gross morphological abnormalities observed in the transgenic lines.

References

Affolter, M., Schier, A., and Gehring, W. J. (1990) Homeodomain proteins and regulation of gene expression. *Current Opin. Cell Biol.* **2,** 485-495.

Andrew, D. J., and Scott, M. P. (1992) Downstream of the homeotic genes. *New Biologist* **4,** 5-15.

Antoniw, J. F., Ritter, C. E., Pierpoint, W. S., and Van Loon, L. C. (1980) Comparison of three pathogenesis-related proteins from plants of two cultivars of tobacco infected with TMV. *J. gen. Virol.* **47,** 79-87.

Antoniw, J. F., and White, R. F. (1980) The effects of aspirin and polyacrylic acid on soluble leaf proteins and resistance to virus infection in five cultivars of tobacco. *Phytopath Z.* **98,** 331-341.

Avery, G. S. (1933) Structure and development of the tobacco leaf. *Am. J. Bot.* **20,** 565-592.

Bellmann, R., and Werr, W. (1992) Zmhox1a, the product of a novel maize homeobox gene, interacts with the *Shrunken* 26 bp *feedback* control element. *EMBO J.* **11,** 3367-3374.

Carabelli, M., Sessa, G., Baima, S., Moralli, G., and Ruberti, I. (1993) The *Arabidopsis Athb-2* and *-4* gens are strongly induced by far-red-rich light. *Plant J.* **4,** 469-479.

Gunning, B. E. S. (1982) The cytokinetic apparatus; its development and spatial regulation. In *The Cytoskeleton in Plant Growth and Development*, C.W. Lloyd, ed (New York: Academic Press), pp. 229-292.

Gunning, B. E. S., and Sammut, M. (1990) Rearrangements of microtubules involved in establishing cell division planes start immediately after DNA synthesis and are completed just before mitosis. *Plant Cell* **2,** 1273-1283.

Hayashi, S., and Scott, M. (1990) What determines the specificity of action of *Drosophila* homeodomain proteins? *Cell* **63,** 883-894.

Jackson, D., Veit, B., and Hake, S. (1994) Expression of maize *KNOTTED1* related homeobox genes in the shoot apical meristem predicts patterns of morphogenesis in the vegetative shoot. *Development* **120,** 405-413.

Jegalian, B. G., and De Robertis, E. M. (1992) Homeotic transformations in the mouse induced by overexpression of a human *Hox3.3* transgene. *Cell* **71,** 901-910.

Kano-Murakami, Y., Yanai, T., Tagiri, A., and Matsuoka, M. (1993) A rice homeotic gene, *OSH1* , causes unusual phenotypes in transgenic tobacco. *FEBS Lett.* **334,** 365-368.

Kessel, M., Balling, R., and Gruss, P. (1990) Variations of cervical vertebrae after expression of a *Hox-1.1* transgene in mice. *Cell* **61,** 301-308.

Kouchi, H., and Hata, S. (1993) Isolation and characterization of novel nodulin cDNAs representing genes expressed at early stages of soybean nodule development. *Mol. Gen. Genet.* **238,** 106-119.

Matsuoka, M., Asou, S., and Ohashi, Y. (1988) Regulation mechanisms of the synthesis of pathogenesis-related proteins in tobacco leaves. *Plant Cell Physiol.* **29,** 1185-1192.

Matsuoka, M., Ichikawa, H., Saito, A., Tada, Y., Fujimura, T., and Kano-Murakami, Y. (1993) Expression of a rice homeobox gene causes altered morphology of transgenic plants. *Plant Cell* **5,** 1039-1048.

Matsuoka, M., and Sanada, Y. (1991) Expression of photosynthetic genes from the C4 plant, maize, in tobacco. *Mol. Gen. Genet.* **225,** 411-419.

Matsuoka, M., Tamaoki, M., Tada, Y., Fujimura, T., Tagiri, A., Yamamoto, N., and Kano-Murakami, Y. (1995) Expression of rice

OSH1 gene is localized in developing vascular strands and its ectopic expression in transgenic rice causes altered morphology of leaf. *Plant Cell Rep.* **14,** 555-559.

Mattsson, J., Söderman, E., Svenson, M., Borkird, C., and Engström, P. (1992) A new homeobox-leucine zipper gene from *Arabidopsis thaliana*. *Plant Mol. Biol.* **18,** 1019-1022.

McGinnis, W., Levine, M. S., Hafen, E., Kuroiwa, A., and Gehring, W. J. (1984) A conserved DNA sequence in homeotic genes of the *Drosophila* Antennapedia and bithorax complexes. *Nature* **308,** 428-433.

McHale, N. A. (1993) *LAM-1* and *FAT* genes control development of the leaf blade in Nicotiana sylvestris. *Plant Cell* **5,** 1029-1038.

Ohashi, Y., and Matsuoka, M. (1985) Synthesis of stress proteins in tobacco leaves. *Plant Cell Physiol.* **26,** 473-480.

Poethig, R. S., and Sussex, I. M. (1985) The developmental morphology and growth dynamics of the tobacco leaf. *Planta* **165,** 158-169.

Ruberti, I., Sessa, G., Lucchetti, S., and Morelli, G. (1991) A novel class of plant proteins containing a homeodomain with a closely linked leucine zipper motif. *EMBO J.* **10,** 1787-1791.

Sass, A. E. (1958) Botanical micro technique, 3rd edn., Iowa State University Press, Ames.

Schena, M., and Davis, R. W. (1992) HD-zip proteins: members of an Arabidopsis homeodomain protein superfamily. *Proc. Natl. Acad. Sci. USA* **89,** 3894-3898.

Schena, M., Lloyd, A. M., and Davis, R. W. (1993) The *HAT4* gene of *Arabidopsis* encodes a developmental regulator. *Genes Dev.* **7,** 367-379.

Schindler, U., Beckmann, H., and Cashmore, A. R. (1993) *HAT3.1*, a novel *Arabidopsis* homeodomain protein containing a conserved cysteine-rich region. *Plant J.* **4,** 137-150.

Scott, M. P., Tamkun, J. W., and Hartzell, G. W. III (1989) The structure and function of the homeodomain. *BBA Rev. Cancer* **989,** 25-48.

Scott, M. P., and Weiner, A. J. (1984) Structural relationships among genes that control development: sequence homology between the *Antennapedia*, *Ultrabithorax*, and *fushi tarazu* loci of Drosophila. *Proc. Natl. Acad. Sci. USA* **81,** 4115-4119.

Sinha, N. R., Williams, R. E., and Hake, S. (1993) Overexpression of the maize homeo box gene, *KNOTTED-1*, causes a switch from determinate to indeterminate cell fates. *Genes Dev.* **7,** 787-795.

Smith, L. G., Greene, B., Veit, B., and Hake, S. (1992) A dominant mutation in the maize homeobox gene, *Knotted-1*, causes its ectopic expression in leaf cells with altered fates. *Development* **116,** 21-30.

Vollbrecht, E., Veit, B., Sinha, N., and Hake, S. (1991) The developmental gene *Knotted-1* is a member of a maize homeobox gene family. *Nature* **350**, 241-243.

Figures

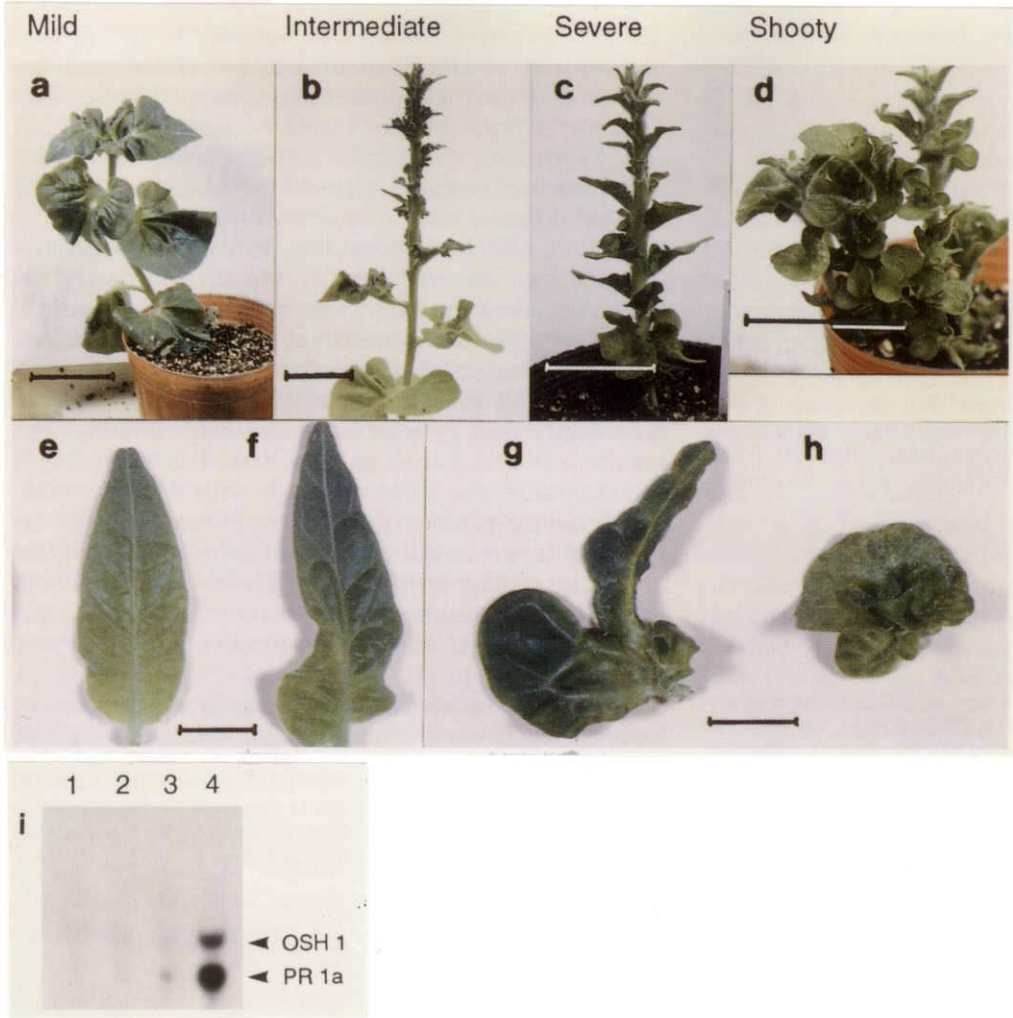

Fig. 2-1. Phenotypes of plants transformed with the *PR1a-OSH1* construct and expression of the *OSH1* and *PR1a* transcripts in mature leaves.
(a and e) The mild phenotype with wrinkled leaves. (b and f) The intermediate phenotype shows elongated stems and slender leaves. (c and g) The severe phenotype shows dwarfism and deeply lobed leaves. (d and h) The shooty phenotype shows severe dwarfism and ectopic shoots on disc-like leaves, as do the 35S-*OSH1* transformants. (i) Northern blot analysis of each phenotype was performed with three micrograms of total RNA. Lane 1, 2, 3, and 4 correspond to the mild, intermediate, severe, and shooty phenotypes, respectively. The positions of the *OSH1* and *PR1a* transcripts are shown at the right. Bars indicate 5 cm in (a-d) and 1 cm in (e-h).

Fig. 2-2. Expression of the *OSH1* transgene in various organs of the *PR1a-OSH1* transformants with the severe phenotype.
Total RNA (10 μg) from the organ indicated was loaded in each lane. The positions of the 28S and 18S rRNAs are shown on the right. Y. Lf, young leaves; O.Lf, old leaves; St, stem; VSA, vegetative shoot apices; RSA, reproductive shoot apices.

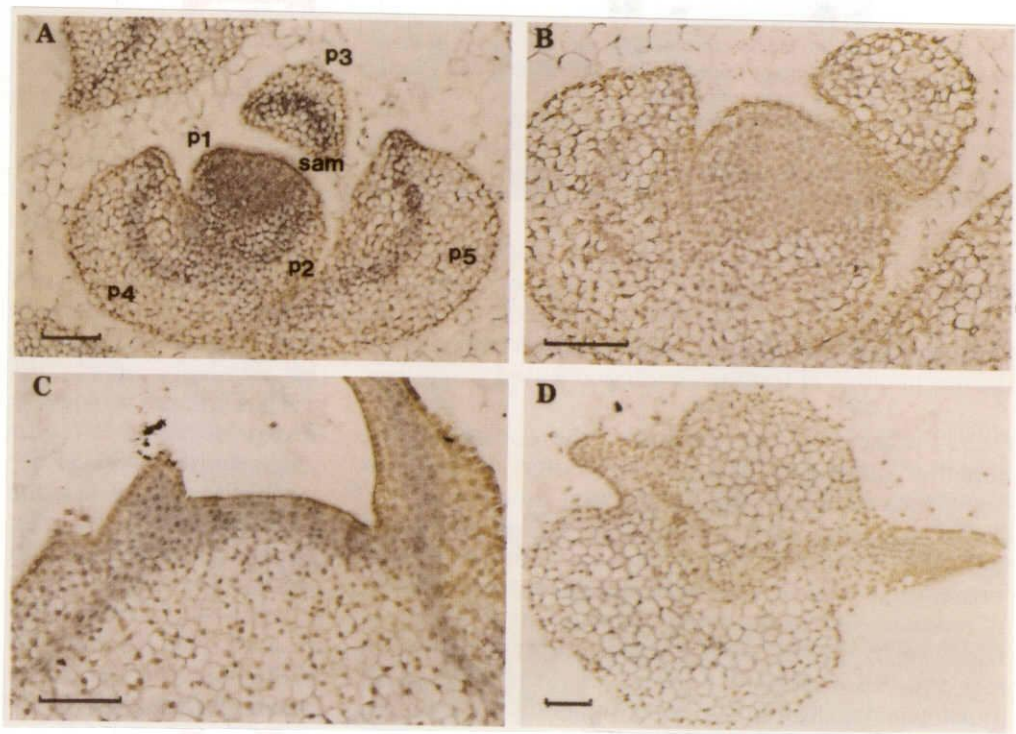

Fig. 2-3. Localization of the *OSH1* transcript in shoot apex by *in situ* hybridization.

Positive hybridization signals are indicated by blue to violet color. (A, B) Cross sections of a vegetative shoot apex of transgenic tobacco hybridized with the antisense and sense probes, respectively. sam, shoot apical meristem; P1-5, leaf primordia 1-5, respectively. (C) Longitudinal section of a vegetative shoot apex of transgenic tobacco hybridized with the antisense probe. (D) Cross section of a leaf P5 primordium of transgenic tobacco with the antisense probe. All transgenic lines were of the severe phenotype. Bars indicate 0.1 mm in all panels.

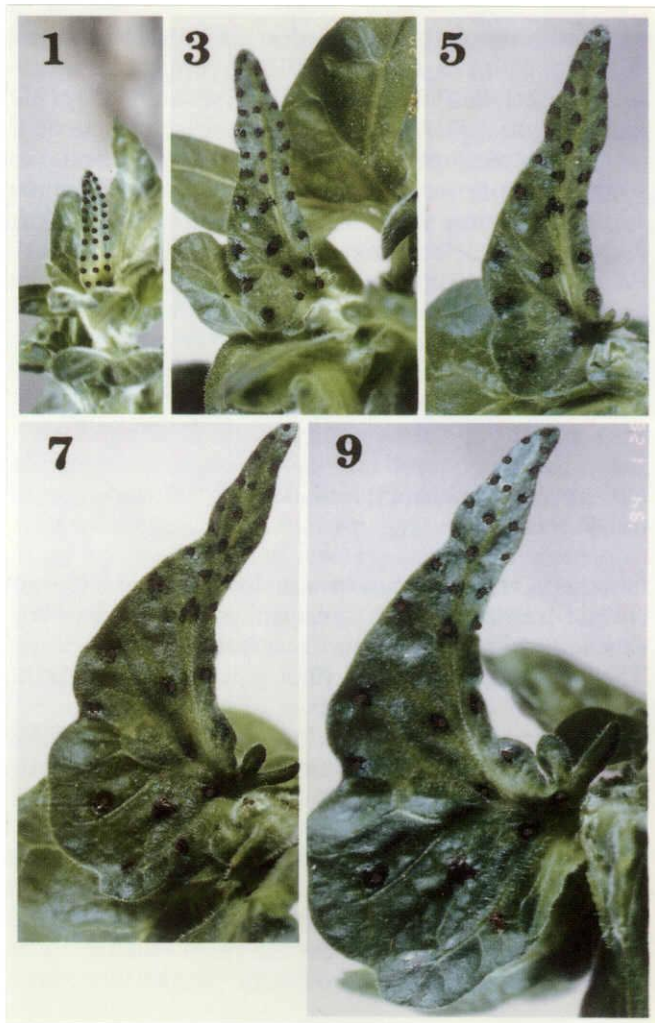

Fig. 2-4. The growth of a transgenic tobacco leaf (severe phenotype) from 1 cm in length for 10 days.

The leaf blade was marked with dots when the leaf was 1 cm long and photographs taken on the indicated number of days after marking are shown. The photographs show the actual sizes of the leaves.

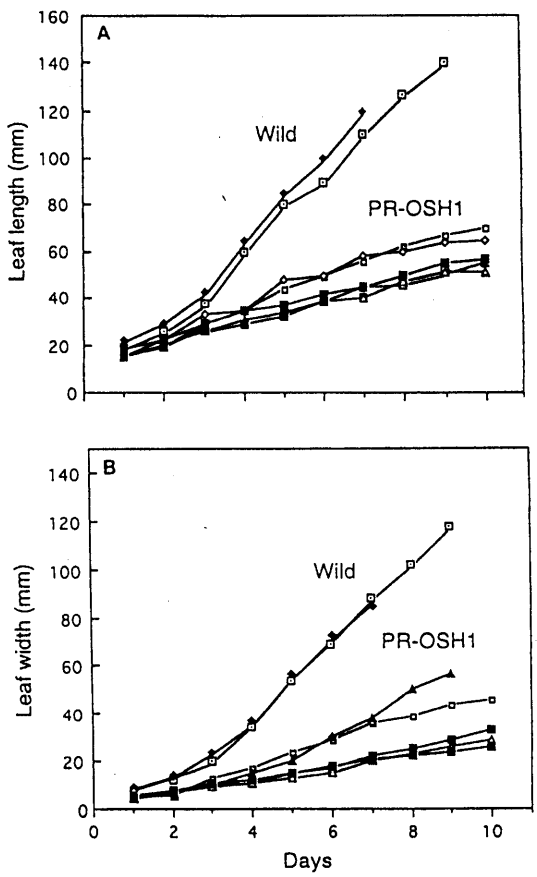

Fig. 2-5. Leaf growth in transgenic (PR-*OSH1*) and T_0 (wild) tobacco from 2 cm in length for 10 days. Each line indicates the growth of a single leaf on a different transformed line.

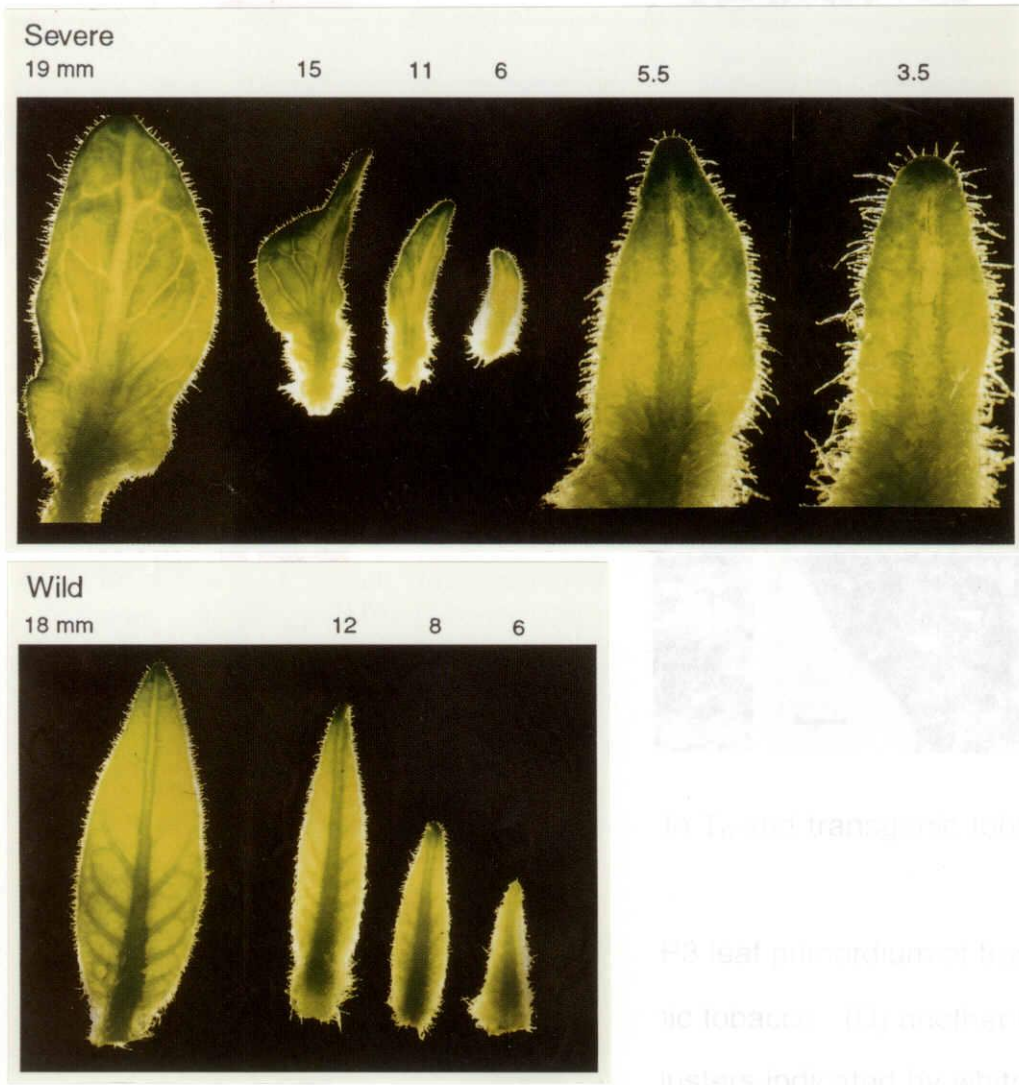

Fig. 2-6. Leaf morphology in T_0 and transgenic tobacco.

The upper and lower panels show the leaves of transgenic tobacco with the severe phenotype and T_0 (wild) tobacco, respectively. The length of each leaf is indicated above each panel. The T_0 (wild) leaves have a typical pinnate venation system, while the transformant leaves have disorganized venation.

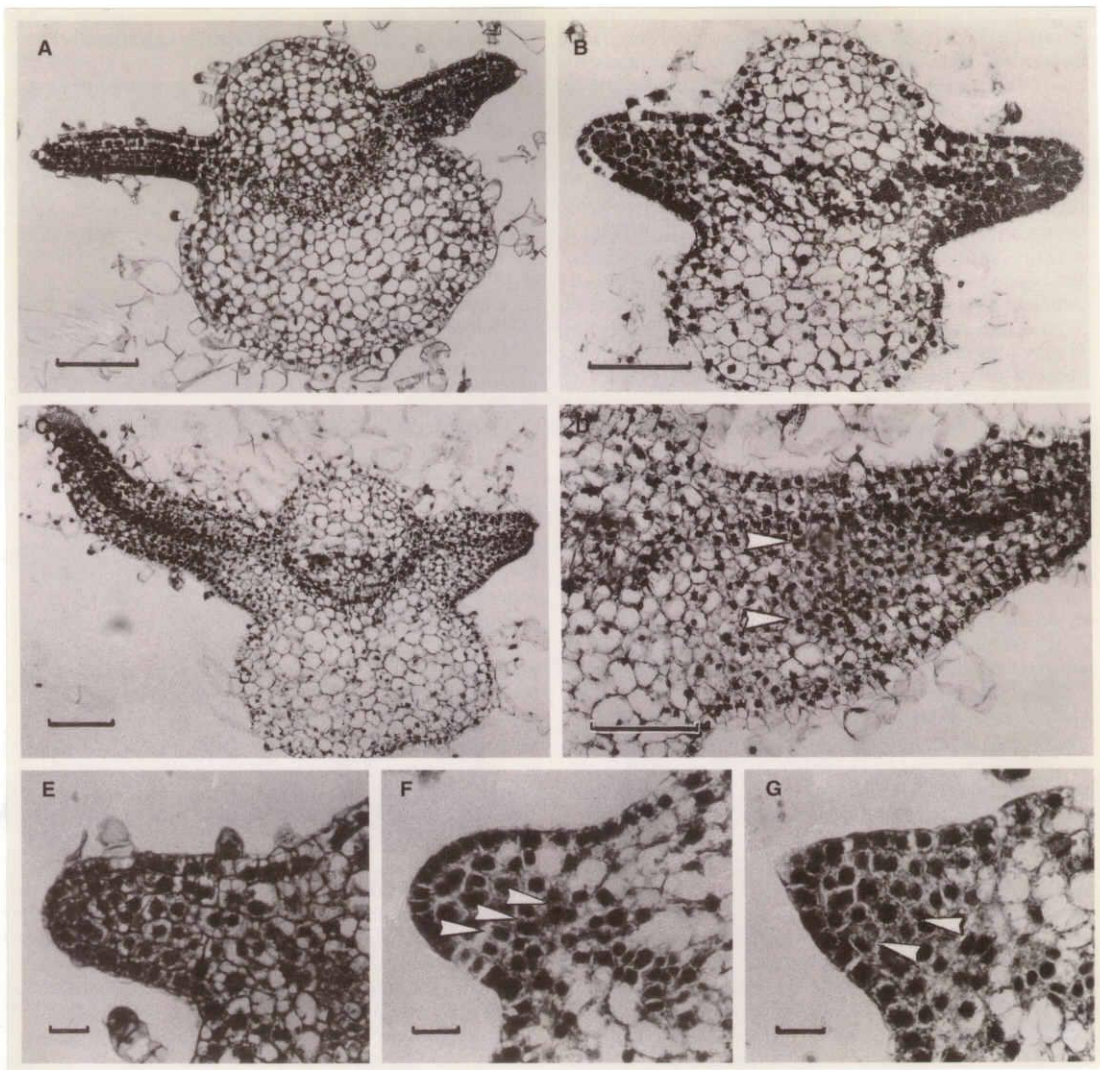

Fig. 2-7. Cross sections of the leaf primordia in T_0 and transgenic tobacco plants.

(A) a P4 leaf primordium of T_0 tobacco. (B) a P3 leaf primordium of transgenic tobacco. (C) a P5 leaf primordium of transgenic tobacco. (D) another P5 leaf primordium with abnormal meristematic cell clusters indicated by white arrowheads. (E) blade initiation in a P3 leaf primordium of T_0 tobacco. (F and G) blade initiation in P2 primordia of the transgenic tobacco. White arrowheads indicate abnormal periclinal cell divisions in the mesophyll cell layers. All transformant tissues shown were from plants with the severe phenotype. Bars indicate 0.1 mm in (A-D) and 20 μm in (E-G).

Chapter 3

A rice homeobox gene, *OSH1*, is expressed prior to organ differentiation in a specific region during early embryogenesis.

Introduction

The fundamental body plan in higher plants is established during the embryogenesis, although most morphogenetic events occur in the post-embryonic phase of the life cycle. In the early stage of embryogenesis, several body axes that cause apical-basal, dorsal-ventral and radial patterns are established, and two apical meristems (shoot and root) are formed. The apical meristems successively produce various tissues and organs throughout the plant life cycle, while maintaining themselves as stem-like cells. In species of the *Poaceae*, which have highly developed embryos, mature embryos contain almost all organs seen in the vegetative phase such as shoot apex, leaves, vascular systems, and root (Randolph, 1936; Hong et al., 1995). To elucidate the genetic control of the pattern formation and/or the organ differentiation during plant embryogenesis, many embryonic mutants have been isolated in *Arabidopsis* (Castle and Meinke, 1993; Errampalli et al., 1991; Jürgens et al., 1991), maize (Clark and Sheridan, 1991; Sheridan and Clark, 1987) and rice (Hong et al., 1995; Nagato et al., 1989). The study of available embryo mutants of rice indicate the existence of several major developmental processes taking place during early embryogenesis before morphogenetic events start (Kitano et al., 1993). Despite the intensive efforts by the workers in the field, little is known about the molecular mechanisms regulating these developmental processes.

One of the powerful approaches for understanding the molecular mechanisms involved in plant embryogenesis is to identify molecular markers which can be used to monitor cell specification events during early embryogenesis and to gain an entry into regulatory networks that are activated in different embryonic regions after fertilization (Goldberg et al., 1994). With this approach, it has been demonstrated that some genes are expressed in specific cell types, regions and organs of embryo (Goldberg et al., 1989;

Jofuku et al., 1989). The information gained from these studies helps the way to elucidate the functional roles of these genes.

In *Drosophila*, the principles of the genetic control during embryogenesis have been unraveled through the combined genetic and molecular approaches (reviewed in Ingham, 1988). These approaches demonstrate that the homeobox genes, which encode evolutionary conserved 61 amino acid domains called homeodomains, play important roles in cellular or regional differentiation of *Drosophila* embryo. In plants, homeobox genes have been isolated from several species such as maize (Vollbrecht et al., 1991; Bellmann and Werr, 1992), rice (Matsuoka et al., 1993; Tamaoki et al., 1995), *Arabidopsis* (Ruberti et al., 1991; Schena and Davis, 1992; Mattsson et al., 1992; Lincoln et al., 1994) and soybean (Ma et al., 1994). Plant homeobox genes, by analogy of the functional roles of animal homeobox genes,have been expected to encode transcriptional regulators that mediate important developmental processes during embryogenesis (Schena and Davis, 1992). It has not been demonstrated, however, that the plant homeobox genes are directly involved in embryogenesis, although ectopic expressions of the homeobox genes have caused the abnormal leaf development in the vegetative phase of the transgenic plants (Matsuoka et al., 1993; Lincoln et al., 1994; Schena et al., 1993; Sinha et al., 1993; Kano-Murakami et al., 1993). Only very recently, the expression of maize homeobox genes was observed at the localized region of developing maize embryo (Smith et al., 1995; Klinge and Werr, 1995).

To elucidate the possibility that plant homeobox genes are involved in embryo development, I examined the temporal and spatial expression of a rice homeobox gene, *OSH1*, during rice embryogenesis in wild type and in organless embryo mutant, *orl1*, which develops no embryonic organs (Hong et al., 1995). The results described here suggest that *OSH1* is not directly associated with shoot development, but may function to specify cell identity

and provide regional information for the formation of shoot and its adjacent tissues.

Experimental Procedures

Plant materials.

To observe developmental course of wild-type embryos and expression pattern of *OSH1*, embryos from the rice (*Oryza sativa* L.) cultivar Taichung 65 were used. I also used embryos from *orl1* mutant, a monogenic, recessive mutant of rice derived from chemical mutagenesis with *N*-methyl-*N*-nitroso-urea (Hong et al., 1995).

Preparation of rice embryo sections.

Developmental course of wild-type rice embryos was examined by standard paraffin method. For paraffin sectioning, seeds at various developmental stages were fixed in FAA (formalin/glacial acetic acid/70% ethanol, 5:5:90), dehydrated in graded ethanol series and embedded in paraffin. Samples were sectioned at 10μm and stained with hematoxylin.

In situ hybridization.

In situ hybridization with digoxigenin-labeled RNA produced from the *OSH1* coding region without poly A-region was conducted as described previously (Kouchi and Hata, 1993). Tissues were fixed with 4% (w/v) paraformaldehyde and 0.25% glutaraldehyde in 0.1M sodium phosphate buffer and embedded in Paraplast Plus. Microtome sections (7-10μm thick) were applied to slide glass treated with Vectabond (Vector Lab.). Hybridization and immunological detection of the hybridized probe was performed by the method of Kouchi and Hata, 1993.

Results

Expression of a rice homeobox gene, *OSH1*, during embryogenesis in wild-type plants.

Rice embryos develop much more quickly than those of other cereal plants such as maize and barley. They complete most of the morphogenetic events within one week under normal conditions. Globular stage lasts nearly three days after pollination (3 DAP) (Fig. 3-1A, B). Although organogenetic events are not observed before 3-4 DAP, a dorsiventral polarity is evident from the gradient of cell size in the late globular embryos at 2-3 DAP (Fig. 3-1B). The first morphological differentiation is recognized as a ventral protrusion of coleoptile at the late 3 DAP or early 4 DAP when the embryo reaches 100-110 μm long and comprises 800-900 cells (Fig. 3-1C). Shoot and radicle apices are first observed at 4 DAP (Fig. 3-1D). The first through third foliage leaves are formed successively at 5, 6, and 8 DAP, respectively, in an alternate phyllotaxis (Fig. 3-1E, F, G).

Based on the developmental course of rice embryo as described above, I performed *in situ* hybridization analysis on embryos at 2 DAP through 7 DAP to determine the expression pattern of *OSH1* during rice embryogenesis. When the sense-strand probe was used, no specific hybridization signal was observed in any experiments (data not shown). Therefore, signals with the antisense probe were caused by the specific hybridization between the *OSH1* transcripts and the probe.

I first examined the *OSH1* expression in globular embryos. The hybridization signals were first detected in globular embryos comprising around 100 cells and about 50-55 μm long at late 2 DAP or early 3 DAP (Fig. 3-2A). At this stage, embryos show no sign of organ differentiation. It is clear that the expression is restricted to a small region just below the center of the ventral region of the embryo, where the shoot apex arises later (Fig. 3-2A). In

the late globular through coleoptilar stages of embryos, *OSH1* was expressed in an enlarged ventral region of embryo (Fig. 3-2B, C). The signals were detected in the outermost several cell layers just below the coleoptilar protrusion extending to the basal (Fig. 3-2B) and inner part of the embryo corresponding to the expected epiblast and radicle, respectively (Fig. 3-2C).

At the shoot apex differentiation stage when embryos are 250-300 μm long (4 DAP), *OSH1* was expressed in the shoot apex, epiblast, radicle primordia, and their intervening tissues (Fig. 3-2D), but not in coleoptile, scutellum or a region where the first leaf would differentiate. The expression pattern in the radicle is different from that in the shoot. Serial sections of the embryo revealed that the *OSH1* expression in the radicle was observed in the cells surrounding the root apical meristem in a donut shape but not in the meristem (Fig. 3-2E). At a more advanced stage when the first leaf primordium was evident and embryos were 400-500 μm in length (5 DAP), the expression pattern of *OSH1* was basically the same as that in the previous stage (Fig. 3-2F). Enlarged view of the shoot apex shows that no signal was detected in the L1(tunica) layer of the meristem and the first leaf primordium (Fig. 3-2G). This spatial pattern of *OSH1* expression is maintained in the following stage when the second leaf primordium is formed, although the intensity of hybridization signals becomes much weaker (Fig. 3-2H), indicating that the *OSH1* expression is reduced and/or the *OSH1* transcripts become unstable at the late embryonic stage.

It is noteworthy that the onset of the *OSH1* expression is much earlier than that of organ differentiation and the expression is restricted to a specific region on the ventral side. Although the hybridization signals are detected in the shoot, epiblast, radicle (except the meristem) and the intervening tissues, clearly there is no relation in cell-lineage among them. This suggests that the *OSH1* expression does not reflect cell lineage, but may be related to regionalization in globular embryo. To clarify this possibility, I analyzed the

expression of *OSH1* in an embryo mutant which is defective in organ differentiation.

OSH1 expression in an embryo mutant, *orl1*, lacking embryonic organs

A rice embryo mutant, *orl1*, lacks embryonic organs including shoot and radicle, although the embryos develop relatively large (longer than 1000 μm) (Hong et al., 1995). At the globular stage (1-3 DAP), they do not show any abnormality and are indistinguishable from the wild-type embryo. At 4 DAP, a small coleoptile-like protrusion frequently appears on the ventral side of the embryo but the embryo continues growing without further organogenetic events (Fig. 3-3B). Microscopically, I can not detect any sign of shoot and radicle differentiation in the *orl1* embryo. At 4 DAP and later stage, *orl1* embryos are morphologically distinguishable from the wild-type embryos by the absence of shoot and radicle.

I also examined the *OSH1* expression in the *orl1* embryos by *in situ* hybridization to elucidate the epistatic relationship between the *OSH1* expression and organ differentiation. In this experiment, I used embryos set on heterozygous plants for *orl1*, since the homozygous *orl1* embryos became lethal. Consequently, I can expect the frequency of homozygous *orl1* embryos to be 25% in the panicles of the heterozygous plants. At the 3 DAP, all globular embryos examined showed the same pattern of hybridization signals as with the wild-type embryos, indicating that both temporally and spatially, the *OSH1* expression is normally regulated in the *orl1* embryos. At 4 DAP, *orl1* embryos, retaining globular shape (Fig. 3-3A) or showing small coleoptile-like protrusions (Fig. 3-3B), maintain a normal pattern of the *OSH1* expression, although neither shoot nor radicle is differentiated (Fig. 3-3B). Hybridization signals were detected in the ventral region corresponding to a place where shoot, epiblast and radicle would differentiate. At 6 DAP, the same expression

pattern was observed as at 4 DAP, but the expression level was reduced (Fig. 3-3C). In the large *orl1* embryos at 7 DAP, no signal was detected (Fig. 3-3D). Thus the *OSH1* transcript is decreasing in *orl1* embryo with the embryonic maturation as in the wild type embryo.

These results indicate that both temporal and spatial patterns of the *OSH1* expression are exactly maintained even in the *orl1* embryos lacking shoot and radicle. Consequently, the *OSH1* expression is not directly associated with organ differentiation. Taken together with the observation made in the wild type and mutant embryo, it is clear that *OSH1* is first expressed much earlier than the onset of morphological differentiation, and is considered to function in a regulatory process prior to or independent of organ determination.

Discussion

Do plant homeobox genes act to determine the regional and cellular identities during embryogenesis, like their animal homologs? Expression of plant homeobox genes in shoot meristems strongly suggested their involvement in organ formation from shoot meristems (Smith et al., 1992; Jackson et al., 1994; Matsuoka et al., 1995), but it has not been reported so far that plant homeobox genes also mediate some organ formation processes in embryogenesis as in animal embryos. For evaluating their functional significance in development, I need to monitor their expression going back to the embryonic phase. In this paper, I have examined the spatial and temporal expression patterns of rice homeobox gene, *OSH1*, during rice embryogenesis. *OSH1* expression was first detected in a specific ventral region of globular embryo. In embryos at this stage, however, no morphological differentiation is observed, although regional differentiation such as dorsiventral pattern is implied by the gradual change of cell size along the dorsiventral axis. This indicates that the cellular differentiation at the gene expression level has already occurred at this stage. Although I do not know anything about the initial signal for such cellular differentiation in embryo, it is plausible that *OSH1* may play an important role in the cellular differentiation preceding organ formation. Considering the possibility that the putative *in vivo* function of *OSH1* is a trans-acting factor, *OSH1* may function as a regulator switching on and off the developmental program of embryonic cells located in a specific region. With the advancement of embryonic maturation, the expression level of *OSH1* is reduced (Fig. 3-2H). The down regulation of *OSH1* expression at later stages suggests that its primary function resides in the early embryogenesis. This result also suggests a possibility that the main function of *OSH1* in embryo is to establish cellular identity in the ventral region at the globular stage. Once the ventral identity is established and then the

organogenesis is started, *OSH1* may finish its function in early embryogenesis and decrease its expression level.

OSH1 has been considered as a rice counterpart gene of maize *KN1* gene because the primary structures of the two genes are quite similar and the over-expression of the genes cause similar alterations in morphology in transgenic tobacco plants (Matsuoka et al., 1993). *KN1* is expressed in the vegetative shoot apex, except in the L1 layer and leaf primordia (Jackson et al., 1994). From the expression pattern of *KN1* in the wild-type and dominant *Kn1* mutant plants, Hake and her colleagues proposed a hypothesis that *KN1* functions to promote indeterminate growth and its down regulation is important for the entry of leaf founder cells into a determinate developmental pathway (Smith et al., 1992). Recently, they examined the expression of *KN1* during maize embryogenesis and showed that the *KN1* expression is closely associated with the shoot apex differentiation, since *KN1* expression is first detected when and where shoot apex primordium is anatomically visible (Smith et al., 1995). This observation with the *KN1* expression in maize embryo is different from my observation that the onset of *OSH1* expression occurs much earlier than the formation of shoot meristem, although the spatial expression pattern of *KN1* in embryo coincides with that of *OSH1* at the shoot apex-differentiation stage. This indicates that *OSH1* may function at much earlier stage during embryogenesis than *KN1* does, and therefore, there may be functional differences between *OSH1* and *KN1* .

Normal expression of *OSH1* in the organless *orl1* embryos (Fig. 3-3) strongly suggests that *OSH1* is not directly associated with shoot apex differentiation, but is related to a regulatory process operating prior to or independently of the shoot apex differentiation. By analyzing many rice embryo mutants, Kitano et al., 1993 presented a scheme for regulatory processes active during rice embryogenesis (Fig. 3-4). In this scheme, they have proposed several regulatory processes before morphogenetic events

take place: pattern formation (apical-basal, dorsal-ventral), determination of organ differentiation, positional regulation, and size regulation. Embryonic pattern is estimated to be determined quite early in embryogenesis, because the pattern-determining genes of Arabidopsis, such as *GNOM* and *MONOPTEROS*, function at the very early stage of globular embryo (Berleth and Jürgens, 1993; Mayer et al., 1993). My data on the *OSH1* expression in specific cells of ventral region suggest that *OSH1* is related to embryonic pattern, especially dorsiventral pattern. But *OSH1* is expressed from the middle globular stage (ca. 100-cell stage), so it would not be directly involved in the pattern formation, but rather may function in specifying cell identity or in the detailed regionalization after embryonic pattern is roughly established. Otherwise there is another possibility that the rice embryonic pattern could be established later than Arabidopsis.

To date, a loss of function mutation of *OSH1* has not been isolated. Consequently, I can not yet specify the exact function of *OSH1* during embryogenesis, although the temporal and spatial patterns of *OSH1* expression imply an important role of *OSH1* in early embryogenesis. An *Arabidopsis* mutation, *shoot meristemless1* (*stm1*), caused the loss of shoot apical meristem in embryo (Barton and Poethig, 1993). Recently, *STM1* gene has been characterized as a *KN1*-type homeobox gene (Long et al., 1996). Considering the fact that homeobox gene functions are often conserved among organisms as different as mice and *Drosophila*, the function of *OSH1* may also be involved in the formation of the shoot apex in embryo by providing regional information for shoot differentiation. In fact, among the rice embryo mutants that show abnormal *OSH1* expression pattern, a rice shoot-less mutant is included (unpublished data).

The present data also show that *OSH1* can be used as a temporal or region-specific marker of embryogenesis. Normal expression of *OSH1* in *orl1* embryo implies that *orl1* is a defect of a gene operating downstream of *OSH1*.

That is, in *orl1* embryo, pattern formation is normally accomplished, but the following organ differentiation would be impaired. My preliminary data suggests that the expression pattern of *OSH1* differs among embryo mutants exhibiting similar phenotypes (unpublished data). Thus, by examining the expression pattern of *OSH1*, I can characterize embryo mutants more precisely in relation to pattern formation, which, in turn, enriches my understandings on the functions of plant homeobox genes.

Summary

Homeobox genes encode a large family of homeodomain proteins that play a key role in the pattern formation of animal embryo. By analogy, homeobox genes in plants are thought to mediate important processes in their embryogenesis, but there is very little evidence to support this notion. Here I described the temporal and spatial expression patterns of a rice homeobox gene, *OSH1*, during rice embryogenesis. *In situ* hybridization analysis revealed that in the wild type embryo, *OSH1* was first expressed at the globular stage, much earlier than organogenesis started, in a ventral region where shoot apical meristem and epiblast would develop later. This localized expression of *OSH1* indicates that the cellular differentiation has already occurred at this stage. At later stages after organogenesis had initiated, *OSH1* expression was observed in shoot apical meristem (except L1 (tunica) layer), epiblast, radicle and their intervening tissues in descending strength of expression level with embryonic maturation. I also performed *in situ* hybridization analysis with a rice organless embryo mutant, *orl1*, which develops no embryonic organs. In the *orl1* embryo, the expression pattern of *OSH1* was the same as that in the wild type embryo in spite of the lack of embryonic organs. This shows that *OSH1* is not directly associated with organ differentiation, but may be related to a regulatory process prior to or independent of the organ determination. The results described here strongly suggest that, like animal homeobox genes, *OSH1* plays an important role in regionalization of cell identity during early embryogenesis.

References

Barton, M. K., and Poethig R. S. (1993) Formation of the shoot apical meristem in *Arabidopsis thaliana* - An analysis of development in the wild type and in the *shootmeristemless* mutant. *Development* **119**, 823-831.

Bellmann, R. ,and Werr, W. (1992) Zmhox1a, the product of a novel maize homeobox gene, interacts with the *Shrunken* 26 bp *feedback* control element. *EMBO J.* **11**, 3367-3374.

Berleth, T., and Jürgens, G. (1993) The role of the monopteros gene in organising the basal body region of the *Arabisopsis* embryo. *Development* **118**, 575-587.

Castle, L. A., and Meinke, D. (1993) Embryo-defetive mutants as tools to study essential functions and regulatory processes in plant embryo development.*Semin. Dev.Bio.* **4**, 31-39.

Clark, J. K., and Sheridan, W. F. (1991) Isolation and characterization of 51 *embryo-speific* mutations of maize. *Plant Cell* **3**, 935-951.

Errampalli, D., Patton, D., Castle, L., Hansen, K., Schnall, J., Feldmann, K., and Meinke D. (1991) Embryonic lethals and T-DNA insertional mutagenesis in *Arabidopsis*. *Plant Cell* **3**, 149-157.

Goldberg, R. B., Barker, S. J., and Perez-Grau, L. (1989) Regulation of gene expression during plant embryogenesis.*Cell* **56**, 149-160

Goldberg, R. B., Paiva, G., and Yadegari, R. (1994) Plant embryogenesis: zygote to seed. *Science* **266**, 605-614.

Hong, S. K., Aoki, T., Kitano, H., Satoh, H., and Nagato, Y. (1995) Phenotypic Diversity of 188 Rice Embryo Mutants. *Dev. Genet.* **16**, 298-310.

Ingham, P. W. (1988) The molecular genetics of embryonic pattern formation in *Drosophila.Nature* **335**, 25-34

Jackson, D., Veit, B., and Hake, S. (1994) Expression of maize *KNOTTED1* related homeobox genes in the shoot apial meristem predicts patterns of morphogenesis in the vegetative shoot. *Development* **120**, 405-413.

Jofuku, K. D., Schipper, R. D., and Goldberg, R. B. (1989) A Frameshift Mutation Prevents Kunitz Trypsin Inhibitor mRNA Accumulation in Soybean Embryos. *Plant Cell* **1**, 427-435.

Jürgens, G., Mayer, U., Ruiz, R. A. T., Berleth, T., and Miséra, S. (1991) Genetic analysis of pattern formation in the *Arabidopsis* embryo. *Development Suppl.* **1**, 27-38.

Kano-Murakami, Y., Yanai, T., Tagiri, A., and Matsuoka, M. (1993) A rice homeobox gene, *OSH1*, causes unusual phenotype in transgenic tobacco. *FEBS Lett.* **334**, 365-368.

Kitano, H., Tamura, Y., Satoh, H., and Nagato, Y. (1993) Hierarchical regulation of organ differentiation during embryogenesis in rice. *Plant J.* **3**, 607-610.

Klinge, B., and Werr, W. (1995) Transcription of the *Zea mays* Homeobox (*ZmHox*) Genes Is Activated Early in Embryogenesis and Restricted to Meristems of the Maize Plant. *Dev. Genet.* **16**, 349-357.

Kouchi, H., and Hata, S. (1993) Isolation and characterization of novel nodulin cDNAs representing genes expressed at early stages of soybean nodule development. *Mol. Gen. Genet.* **238**, 106-119.

Lincoln, C., Long, J., Yamaguchi, J., Serikawa, K., and Hake S. (1994) A *knotted1*-like Homeobox Gene in Arabidopsis Is Expressed in the Vegetative Meristem and Dramatically Alters Leaf Morphology When Overexpressed in Trangenic Plants. *Plant Cell* **6**, 1859-1876.

Long, J. A., Moan, E. I., Medford, J. I., and Barton, M. K. (1996) A member of the KNOTTED class of homeodomain proteins encoded by the *STM* gene of *Arabidopsis*. *Nature* **379**, 66-69.

Ma, H., McMullen, M. D., and Finer, J. J. (1994) Identification of a homeobox-containing gene with enhanced expression during soybean (*Glycine max* L.) somatic embryo development. *Plant Mol. Biol.* **24**, 465-473.

Matsuoka, M., Ichikawa, H., Saito, A., Tada, Y., Fujimura, T., and Kano-Murakami, Y. (1993) Expression of a Rice Homeobox Gene Causes Altered Morphology of Transgenic Plants. *Plant Cell* **5**, 1039-1048.

Matsuoka, M., Tamaoki, M., Tada, Y., Fujimura, T., Tagiri, A., Yamamoto, N., and Kano-Murakami, Y. (1995) Expression of rice *OSH1* gene is localized in developing vascular strands and its ectopic expression in transgenic rice causes altered morphology of leaf. *Plant Cell Rep.* **14**, 555-559.

Mattsson, J., Söderman, E., Svenson, M., Borkird, C., and Engstörm, P. (1992) A new homeobox-leucine zipper gene from *Arabidopsis thaliana*. *Plant Mol. Biol.* **18**, 1019-1022.

Mayer, U., Büttner, G., and Jürgens, G. (1993) Apical-basal pattern formation in the *Arabidopsis* embryo: studies on the role of the *gnom* gene. *Development* **117**, 149-162.

Nagato, Y., Kitano, H., Kamijima, O., Kikuchi, S. and Satoh, H. (1989) Developmental mutants showing abnormal organ differentiation in rice embryos. *Theor. Appl. Genet.* **78**,11-15.

Randolph, L. F. (1936) Developmental morphology of the caryopsis in maize. *J. Agric. Res.* **53**, 881-916.

Ruberti, I., Sessa, G., Lucchetti, S., and Morelli, G. (1991) A novel class of plant proteins containing a homeodomain with a closely linked leucine zipper motif. *EMBO J.* **10**, 1787-1791.

Schena, M., and Davis, R. W. (1992) HD-zip proteins: members of an *Arabidopsis* homeodomain protein superfamily. *Proc. Natl. Acad. Sci. USA* **89**, 3894-3898.

Schena, M., Lloyd, A. M., and Davis, R. W. (1993) The *HAT4* gene of *Arabidopsis* encodes a developmental regulator. *Genes Dev.* **7**, 367-379.

Sheridan, W. F., and Clark, J. K. (1987) Maize embryogeny: a promising experimental system. *Trends. Genet.* **3**, 3-6.

Sinha, N. R., Williams, R. E., and Hake, S. (1993) Overexpression of the maize homeo box gene, *KNOTTED-1*, causes a switch from determinate to indeterminate cell fates. *Genes Dev.* **7**, 787-795.

Smith, L. G., Greene, B., Veit, B., and Hake, S. (1992) A dominant mutation in the maize homeobox gene, *Knotted-1*, causes its ectopic expression in leaf cells with altered fates. *Development* **116**, 21-30.

Smith, L. G., Jackson, D., and Hake, S. (1995) Expression of *knotted1* Marks Shoot Meristem Formation During Maize Embryogenesis. *Dev. Genet.* **16**, 344-348.

Tamaoki, M., Tsugawa, H., Minami, E., Kayano, T., Yamamoto, N., Kano-Murakami, Y., and Matsuoka, M. (1995) Alternative RNA products from a rice homeobox gene. *Plant J.* **7**, 927-938

Vollbrecht, E., Veit, B., Sinha, N., and Hake, S. (1991) The developmental gene Knotted-1 is a member of a maize homeobox gene family. *Nature* **350**, 241-243.

Figures

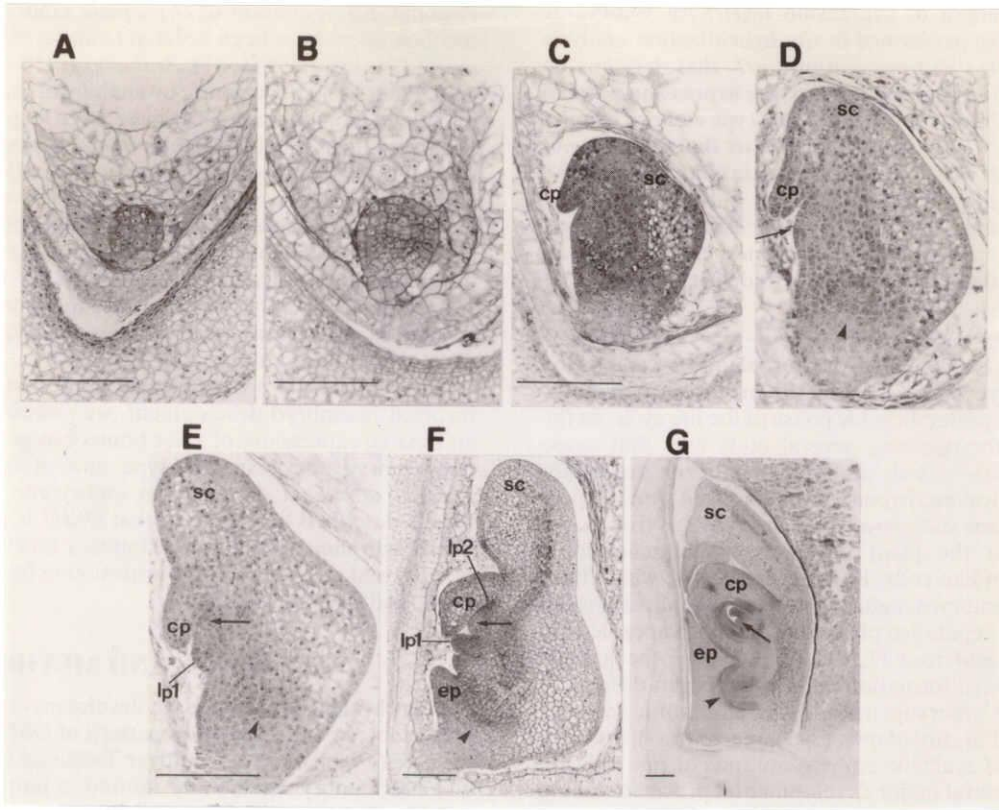

Fig. 3-1. Developmental course of wild-type rice embryo.

Micrographs shown are the median longitudinal sections. (A) Early globular stage (2 DAP). No morphological differentiation is observed. (B) Late globular stage (3 DAP). While a dorsiventral polarity is evident from the gradient of cell size, no organogenetic events are observed. (C) Coleoptilar stage (early 4 DAP). The first morphological differentiation is recognized as a ventral protrusion of coleoptile at this stage. (D) Apical meristem differentiation stage (4 DAP). Shoot and radicle apices are observed. (E) First leaf primordium differentiation stage (5 DAP). The shoot apical meristem is flat at this stage. (F) Second leaf primordium differentiation stage (6 DAP). The shoot apical meristem become dome-like at this stage. (G) Nearly mature embryo at 9 DAP. By this time, the first to third foliage leaves are formed successively in an alternate phyllotaxis. *Arrow*, shoot apex; *Arrowhead*, radicle apex; cp, coleoptile; sc, scutellum; ep, epiblast; lp1, first leaf primordium; lp2, second leaf primordium. Bar = 100 μm

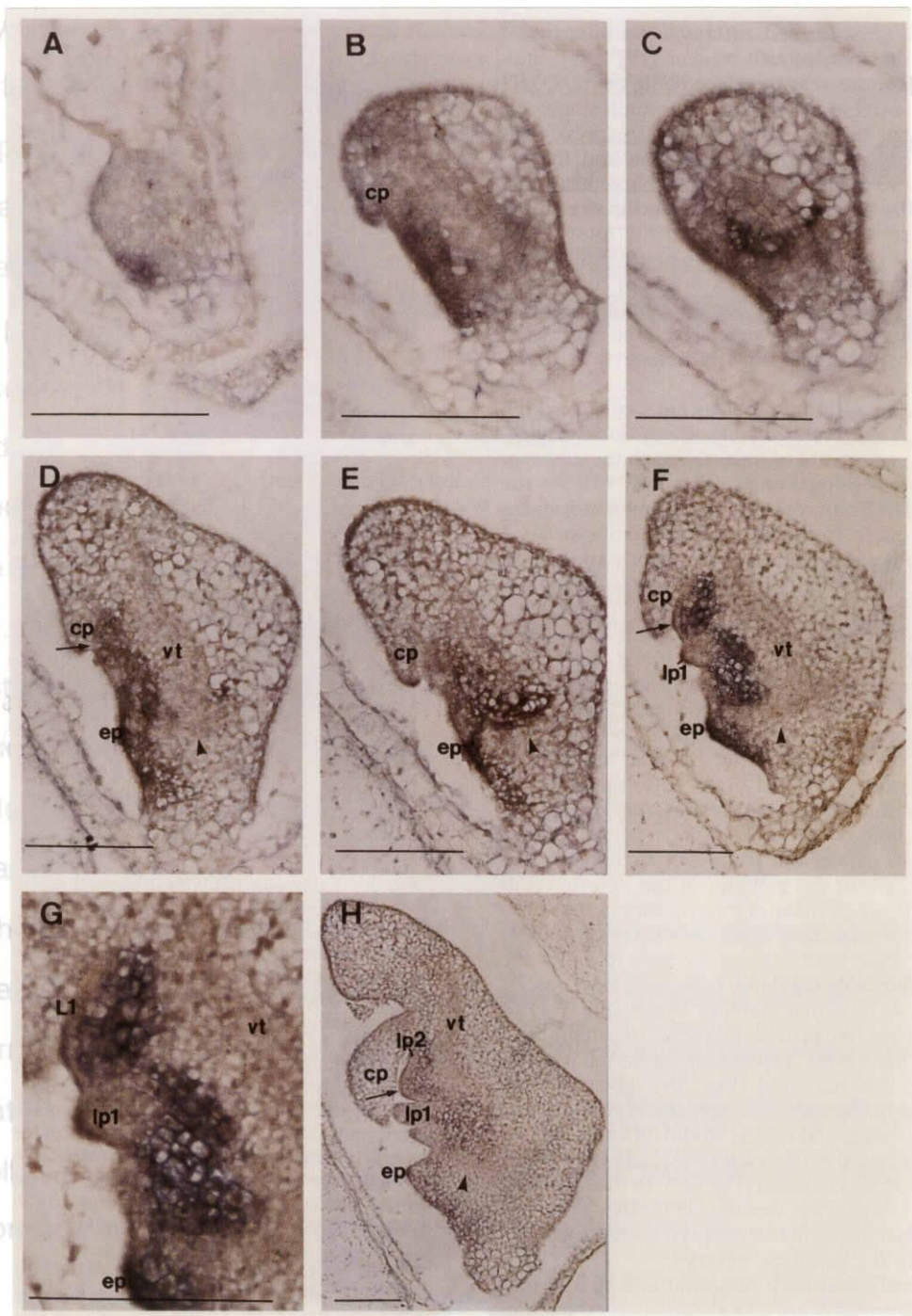
A
B
cp
C
D
cp
vt
ep
E
cp
ep
F
cp
vt
lp1
ep
G
L1
vt
lp1
ep
H
vt
lp2
cp
lp1
ep

Fig. 3-2. Detection of the *OSH1* transcript in wild-type rice embryos by *in situ* hybridization.

Median longitudinal sections of embryos are shown in the figures except (C) and (E) which are sectioned adjacent to the median longitudinal plane. Positive hybridization signals are indicated by blue to violet color. (A), Globular embryo at 3 DAP. Signals are localized in the ventral region of embryo, where shoot apex will differentiate later. (B), Coleoptilar stage embryo at early 4 DAP. Signals are visible in enlarged ventral region just below the coleoptilar protrusion. (C), The section of coleoptilar stage embryo at early 4 DAP adjacent to the median longitudinal plane. The hybridization pattern is different from that on the median section, and signals are observed in the inner part of the embryo corresponding to the region where radicle will arise. The section on the opposite side against the median plane shows the identical hybridization pattern. (D), Embryo at late 4 DAP in which shoot apex is being formed . Pattern of *OSH1* expression is similar to that in (B). (E), The section of the embryo at late 4 DAP which is swerved from the median longitudinal plane. Signals are observed at the region surrounding the root apical meristem like a donut shape. The swerved section of the opposite side against the median plane showed the hybridization pattern identical to this figure. (F), First leaf differentiating embryo at 5 DAP. Signals are visible in shoot apex, epiblast, the region at the ventral side of vascular tissue. (G), Enlarged view of the shoot apex region in (F). Signals are absent in both L1(tunica) layer and first leaf primordia. (H), Second leaf differentiating embryo at 7 DAP. Similar pattern to that in (F) is observed but the intensity of signals is much lower than that at 5 DAP. *Arrow*, shoot apex; *Arrowhead*, radicle apex; cp, coleoptile; sc, scutellum; ep, epiblast; L1, L1 (tunica) layer; vt; vascular tissue; lp1, first leaf primordium; lp2, second leaf primordium. Bar = 100 μm.

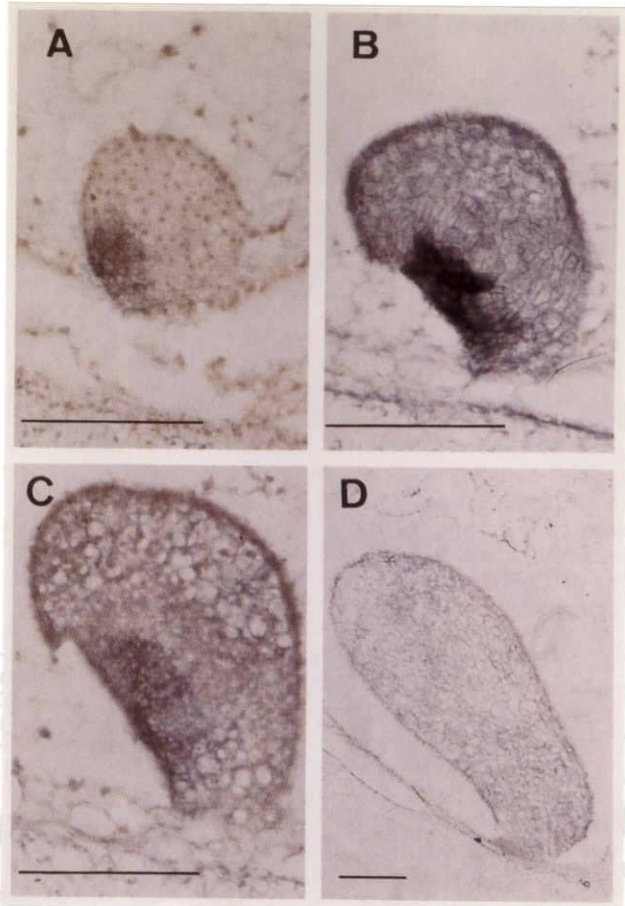

Fig. 3-3. Expression of *OSH1* in rice *orl1* mutant embryo showing no organ differentiation.

All figures shown are median longitudinal sections of *orl1* embryos. (A), Embryo at 4 DAP. The expression of *OSH1* is observed in the ventral side of the embryo. This pattern of expression is essentially the same as that in the wild-type embryo at 3 DAP (Fig. 3-2A). (B), Embryo with coleoptile-like protrusion at 4 DAP. In *orl1* mutant embryos, a small coleoptile-like protrusion frequently appears on the ventral side of the embryo. The embryo continues its growth without any further organogenetic events. The expression pattern of *OSH1* is similar to that observed in (A). (C), Embryo with coleoptile-like protrusion at 6 DAP. Comparing to the wild-type embryo at 6 DAP (Fig. 3-1F), the sever defect in organ differentiation is observed. The expression pattern of *OSH1* observed is similar to that in (B), but the expression level is reduced. (D), Embryo at 7 DAP. The embryo grows up with showing no organ differentiation. No *OSH1* expression is observed. Bar = 100 μm.

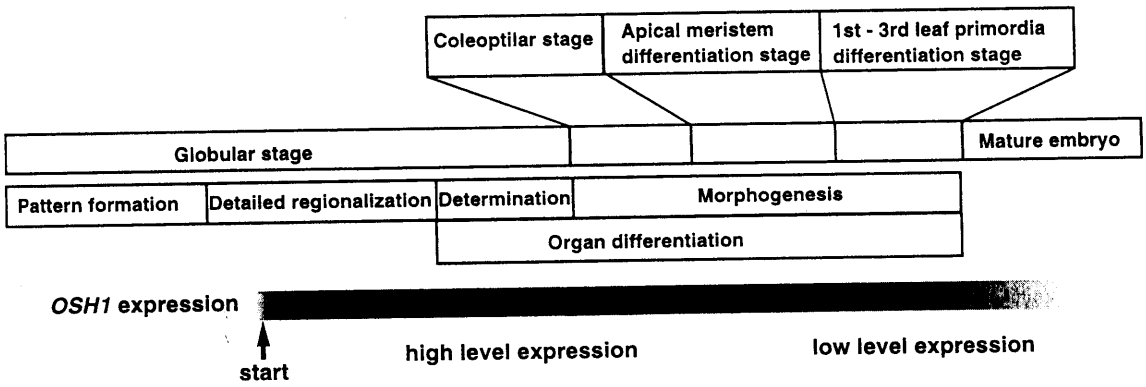

Fig. 3-4. *OSH1* expression and schematic representation of hypothetical regulatory processes during rice embryogenesis.

The *OSH1* expression is first observed in a specific region of the ventral side of the globular stage embryo which has no visible organ differentiation. The high level expression of *OSH1* keeps during the late globular stage to the first leaf primordia differentiation stage. Then, the expression of *OSH1* is reduced as the embryo maturation proceeds. From the observation in the *orl1* mutant, the localized expression of *OSH1* is not affected by the organ differentiation. These indicate that *OSH1* functions in the early stages of the embryogenesis and may play a role in the specification of cell identity or in the detailed regionalization after embryonic pattern formation is roughly established.

Chapter 4

Two separable functions of a rice homeobox gene, *OSH15*, in plant development.

Introduction

Although most plant morphogenetic events occur in the post embryonic development of plant life cycle, the basic body plan in higher plants is generated during embryogenesis. In the early stage of embryogenesis, several body axes such as apical-basal, radial, and dorso-ventral patterns are established. Based on the regional information determined by these axes, embryonic organs including two apical meristems (shoot and root) are formed at the correct positions. After seed germination, the apical meristems successively produce various tissues and organs throughout the plant life cycle while maintaining themselves as stem-like cells (Steeves and Sussex, 1989).

The process of axis establishment during embryogenesis has been the focus of many studies, regardless of plant or animal materials (Jürgens, 1995; Lawrence and Morata, 1994). Recent advances in studies on animal embryogenesis have established the genetic programs by which genes control patterning (Gehring et al., 1994; Lawrence and Morata, 1994), and many of the genes involved in this process have been cloned. Among them, homeobox genes, which encode an evolutionarily conserved 64 amino acid sequence called homeodomain, play important roles in developmental decisions that control cell specification or pattern formation.

In higher plants, the first homeobox gene was cloned by transposon tagging from the maize *Knotted1* (*Kn1*) mutant as *KNOTTED1* (*KN1*) gene (Vollbrecht et al., 1991). In the *Kn1* mutant, abnormal arrangements of lateral veins, sporadical outgrowths called knots, and ligule displacement are observed in leaf blades . It has been revealed that *Kn1* is a dominant mutation caused by ectopic expression of *KN1* in leaves, and that its ectopic expression results in the disorganization of the developmental program of leaf blades (Smith and Hake, 1994).

Many homeobox genes have been cloned from various plant species in an effort to address the biological functions of homeobox genes in plant development. Based on amino acid sequence similarities within the homeodomain or conserved protein motifs outside of the homeodomain, plant homeobox genes have been classified into five groups (Kerstetter et al., 1994; Lu et al., 1996). These include the KNOTTED-type homeodomain proteins, homeodomain zipper proteins (HD-ZIP), plant homeodomain finger proteins (PHD-finger), the GLABRA2 homeodomain protein, and the BELL1 homeodomain protein. In animals, families of related homeobox genes often specify related developmental processes (Gehring et al., 1994). Based on the observations that KNOTTED-type homeodomain proteins are expressed around the shoot apical meristem and overexpression of these genes affects the developmental program of the leaf blades, it has been suggested that genes of this class are involved in maintenance of the shoot apical meristem and/or the development of lateral organs (Smith et al., 1992).

Plant homeobox genes, by analogy to functional roles of animal homeobox genes, have been expected to encode transcriptional regulators that mediate important developmental processes during embryogenesis. Recently, the involvement of plant homeobox genes in embryogenesis are suggested by their expression patterns during embryogenesis (Sato et al., 1996a; Smith et al., 1995; Klinge and Werr, 1995; Long et al., 1996). Also loss-of-function mutations in an *Arabidopsis* homeobox gene, *STM* (Shoot Meristemless) result in the shoot meristemless phenotype of embryos. This finding has demonstrated directly the involvement of this gene in shoot formation or maintenance during embryogenesis (Long et al., 1996).

I am interested in elucidating the role of KNOTTED-type homeobox genes in plant development, especially in monocotyledonous plants. Toward this goal, I have isolated a family of KNOTTED-type homeobox genes from rice. Recently rice has become a model system in monocotyledonous plants

for plant biologists, mainly because of the accumulated mutants, the feasibility of efficient transformation, the creation of a highly saturated molecular genetic map, and the large-scale analysis of expressed sequence tags (Izawa and Shimamoto, 1996). So the isolation and characterization of KNOTTED-type genes from rice will permit further molecular and genetic analyses of this class of homeobox genes.

Here, I describe the cloning and characterization of a rice homeobox gene, *OSH15*. Ectopic expression experiments with *OSH15* in transgenic tobacco provide evidence that its gene product affects the developmental program of tobacco plants. The *in situ* mRNA localization analyses through the whole plant life cycle suggest that *OSH15* functions during embryogenesis, and around the vegetative shoots, infloresence shoots, and floral meristem. The biological functions of *OSH15* during the whole plant life cycle are dicussed.

Experimental Procedures

Amplification of homeodomain by PCR method

The genomic DNA from rice (*Oryza sativa* L.) cultivar Nippon-bare was amplified by PCR using two oligonucleotide primers corresponding to the conserved amino acids region of the homeodomain (5' AA(A/G)CT(A/C/G/T)CC(A/C/G/T)AA(A/G)GAGGC 3', and 5' TGGTTGATGAACCAGTTGTT 3'). Amplified fragments were cloned into pCRII (Invitrogen) and sequenced. One clone corresponding to *OSH15* was used as a probe for further screening for cDNA and genomic clones.

Screening of cDNA and genomic DNA libraries

A cDNA library constructed from rice rachis mRNA and a genomic library constructed from rice genomic DNA digested partially with *Sau*3AI were screened with a probe prepared as mentioned above. Hybridization was performed in 50 % Formamide, 6x SSC, 5x Denhardt's solution, 0.5 % SDS, and 0.1 mg/mL salmon sperm DNA at 42 Åé for 14 h and filters were washed in 2x SSC, 0.1 % SDS at room temperature and then further washed in 0.2x SSC, 0.1 % SDS at 65 Åé.

Sequencing analysis

Nucleotide sequences were determined by the dideoxynucleotide chain-termination method using an automated sequencing system (ABI373A). The cDNA and genomic clones were completely sequenced on both strands except for a large intron. Analysis of cDNA and amino acid sequences were carried out using GENETYX computer software (Software Kaihatsu Co., Japan)

Construction of chimeric genes

A DNA fragment containing the *35S* promoter was exised from pBI121 (Clontech Lab. Inc., CA, USA) at the *Hind*III/*Sma*I site and introduced into the same site of pUC18 to produce a plasmid designated p35S. A DNA fragment containing the noparine synthetase terminater (*nos*) was exised from pBI121 at the *Ssc*I/*EcoR*I site and introduced into the same site of p35S to produce a plasmid designated p35Snos. Then a DNA fragment containing the *35S* and *nos* sequences was exised from p35Snos at *Hind*III/*EcoR*I site and replaced the insert of pBI121 at the same site to produce a plasmid designated pBI35Snos. The cDNA clone encoding rice *OSH15* was exised at the *Xba*I/*EcoR*V site and introduced into the *Xba*I/*Sma*I site of pBI121 to construct the *35S-OSH15* fusion gene in the binary vector.

Transformation and regeneration of tobacco

The fusion construct was introduced into *Agrobacterium tumefaciens* LBA4404 by electroporation. Transformation of *Nicotiana tabacum* cv. Samsun NN was according to the leaf disc method as previously reported (Matsuoka & Sanada, 1991). Transformants were selected in medium containing 100 mg/L of kanamycin.

RNA gel blot analysis

Total RNAs from rice were separately prepared from various organs for RNA gel blot analysis. Fifteen μg of each RNA preparation was electrophoresed on a 1 % agarose gel, then transferred to Hybond N^+ membrane (Amersham) and hybridized with the entire *OSH15* insert as a probe. Hybridization was performed in 50% formamide, 6x SSC (1x SSC is 0.15 M NaCl, 15 mM sodium citrate), 5x Denhardt's solution (1x Denhardt's solution is 0.02% Ficoll, 0.02% PVP, 0.02% BSA), 0.5 % SDS, and 0.1 mg/mL salmon sperm DNA at 42Åé for 14 h. Each filter was washed in 2x SSC, 0.1 % SDS at room temperature and then further washed in 0.2x SSC, 0.1 %

SDS at 65Åé. In the analysis of the transgene expression level in transgenic tobacco plants, total RNA from leaves of wild and transgenic tobacco plants were extracted and ten μg of each total RNA was subjected to northern blot hybridization. The probe and hybridization, and washing procedures are the same as mentioned above.

Histological analysis

Plant materials were fixed in FAA solution and embedded in Technovit 7100 resin (Kulzer & Co. GmbH, Wehrheim, FRG). Microtome sections (3-5 μm) were stained with hematoxylin.

in situ hybridization

Plant materials were fixed in 4% (w/v) paraformaldehyde and 0.25% glutaraldehyde in 0.1 M sodium phosphate buffer, pH 7.4 overnight at 4°C, dehydrated through graded ethanol series and then *t*-butanol series (Sass, 1958), and finally embedded in Paraplast Plus (Sherwood Medical). Microtome sections (7-10 μm thick) were applied to glass slides treated with Vectabond (Vector Labs). *In situ* hybridization with digoxigenin-labeled sense or antisense RNA was conducted according to the method of Kouchi and Hata (1993). Double-target *in situ* hybridization was conducted according to the method of Kouchi et al. (1995).

Results

Cloning and sequencing of a rice homeobox containing gene, *OSH15*

To isolate new members of the KNOTTED type homeobox genes from rice, I designed degenerate oligonucleotide primers corresponding to the conserved amino acid sequences from the homeodomain region of previously reported KNOTTED-type homeobox genes (Kerstetter et al., 1994), and performed PCR amplification with rice genomic DNA as template. Several amplified fragments of different sizes were cloned and sequenced. Among them, one clone which was designated *OSH15* (*Oryza sativa* homeobox 15) was used for further screening of full size cDNA and genomic clones.

The isolated*OSH15* cDNA clone contains a 1065-bp open reading frame, capable of encoding a polypeptide of 355 amino acid residues, with a 93-bp 5' noncoding region and a 373-bp 3' noncoding region (Fig. 4-1 A). The open reading frame contains a conserved homeodomain (64 amino acids) at the C-terminus as is the case with other KNOTTED type homeobox genes. Comparing with other plant homeodomains, its deduced amino acid sequence is most similar to that of KNOTTED type homeobox genes such as *KN1* from maize (89 %), *OSH1* from rice (94 %), *NTH15* from tobacco (86 %), *STM* and *KNAT1* from *Arabidopsis* (86 % and 95 %, respectively) (Vollbrecht et al., 1991; Matsuoka et al., 1993; Tamaoki et al., 1997; Long et al., 1996; Lincoln et al., 1994). Furthermore the amino acid sequence is completely identical to that of maize *RS1* in the homeodomain region (Schneeberger et al., 1995).

The ELK region consisting of a conserved 21 amino acid region located immediately upstream of the KNOTTED type homeodomain is also found in *OSH15*. The N-terminus of the homeodomain, there is a cluster of positively charged amino acids that is often observed in proteins localized in the nucleus and might work for nuclear localization signal (Raikhel, 1992). It is also

noteworthy that there are three glycine stretches, three alanine stretches and one histidine stretch near the N-terminus of OSH15 (Fig. 4-1 A). Similar homopolymeric amino acid stretches are also observed in OSH1 (proline and glutamine), NTH15 (Aspargine and proline), KN1 (histidine) and RS1 (serine, alanine, glutamine and histidine). The biological role of these homopolymeric amino acid stretches has not been elucidated. However, it has been suggested that they may be involved in transcriptional activation because polyproline and polyglutamine stretches often act as activation domains in some trans-acting factors (Gerber et al., 1994). The presence of these clusters in the predicted OSH15 protein indicates that *OSH15* acts as a regulatory gene in rice. I also cloned and characterized the genomic DNA that completely covers the *OSH15* coding region. By comparing the genomic DNA sequence and cDNA sequence, it is revealed that *OSH15* consists of five exons and four introns. This exon/intron structure is also conserved among the KNOTTED type homeobox genes (Fig. 4-1 B) (Matsuoka et al., 1993; Lincoln et al., 1994).

Expression of the *OSH15* gene in different organs

To determine the expression pattern of *OSH15* in various organs of rice, I conducted an RNA gel blot hybridization analysis using the entire coding sequence of the*OSH15* cDNA as a probe (Fig. 4-2). Total RNA was extracted from leaf blades, vegetative shoot apices, inflorescence shoot apices, stems, roots, root tip, caryopsis, embryos (8 DAP: days after pollination), rachis, and suspension cells. A single strong band was detected in RNA from rachis and stems. The size of the band was approximately 1.6kb, almost the same size as the cDNA clone. A relatively weak band with the same size was also observed in RNA from vegetative shoots, inflorescence shoots and caryopsis, but not in leaf blades, roots, root tips, embryos, and suspension cells. Thus, the *OSH15* expression pattern shows strict organ specificity. To avoid cross-hybridization of the probe with other homeobox genes, I also performed the same

experiment with the 3' non-coding region as a probe. The blot pattern with faint signals was the same as that with the whole sequence of *OSH15*, demonstrating that the whole *OSH15* cDNA sequence specifically recognized the *OSH15* mRNA under strict hybridization conditions.

Expression of the *OSH15* coding sequence in tobacco

To analyze the biological functions of the *OSH15* gene, the cDNA clone was expressed ectopically in transgenic tobacco plants. The complete coding sequence of *OSH15* was transcriptionally fused to the cauliflower mosaic virus *35S* promoter (*35S*) in the sense orientation and introduced into wild-type tobacco plants (cv. Samsun NN) via Agrobacterium mediated gene transfer. More than fourty independent transformants were regenerated in this experiment. Most of the transformants showed abnormal morphologies such as an aberrant leaf morphology, a dwarf phenotype, and/or a formation of ectopic shoots on leaves. These transformants were divided into four phenotypic categories based on leaf morphology: (1) mild phenotype, (2) intermediate phenotype, (3) severe phenotype, (4) shooty phenotype.

Transformants in the mild category appeared to have normal growth except for an aberrant leaf morphology (Fig. 4-3 D, right side of G). The size of the leaves in this group was slightly small, the midrib was curved, and the shape of the leaves was wavy. I could not observe any abnormalities in the shape or the organ number of flowers in this category.

Transformants with the intermediate phenotype had severly wrinkled leaves with no definite mid veins in the center of leaves (Fig. 4-3 C, left side of G). Leaves in this category were fairly small (compare left and right in Fig. 4-3 G). The number of leaves in these plants was increased because of more phytomer with shorter internodes than those of wild type plants (Fig. 4-3 C). I could also observe abnormalities in the morphology of flowers on plants in this category (Fig. 4-3 H). They had waved petals and stamen filaments with

reduced length, whereas the length of pistils were normal. Consequently, the fertilities of those plants were low but pollen development was unaffected. Actually when I picked up anthers and pollinated the pistils by hand, fertility was recovered.

Leaves of the plants with severe phenotype showed quite aberrant morphologies (Fig. 4-3B and F). The leaves were very small and their veins could hardly be detected. Those plants were severely dwarfed. In this category, few plants produced flower buds. Also floral abscission occurred prematurely, so I could not observe the morphology of a mature flower.

In plants with the shooty phenotype, the size and the shape of leaves were similar to those with the severe phenotype. These plants were also severely dwarfed and showed weak apical dominance (Fig. 4-3A). The main difference in leaves between plants with the shooty phenotype and the severe phenotype was that ectopic shoots formed on the adaxial side of leaves (Fig. 4-3E, I, and J). Sections through ectopic shoots revealed that the layer structure of a leaf, in which six to seven cell layers were normally observed, was disturbed in leaves of the plants with severe or shooty phenotype and the differantiation of the palisade parenchyma was obscure (Fig. 4-3I and data not shown). In some cases, ectopic shoots grew and produced new leaves just like a new branch from an axillary bud (Fig. 4-3J). Interestingly, the phenotype of the leaves produced from ectopic shoots were not always the same as that of the original leaves. As shown in Fig. 4-3J, leaves from an ectopic shoot on the shooty leaf showed a relatively milder phenotype. The same phenomenon was also observed in branches from axillary buds. For example, a branch from a severe plant did not always produce leaves with the severe phenotype, but produced shooty or intermediate leaves (data not shown).

To test whether the expression levels of the *OSH15* transgene correlated with the severity of the phenotypes, I extracted total RNA from leaves of four individual transgenic plants in each phenotypic category and

from wild-type tobacco plants and performed RNA gel blot analysis. The *OSH15* transgene expression was easily detected in leaves of all transgenic plants showing abnormal morphology (Fig. 4-4, lanes 3-18), and no cross hybridization signal was detected in leaves of wild type tobacco plants (Fig. 4-4, lanes 1 and 2). There seemed to be a correlation between the expression level of the transgene and the phenotype of each transgenic line. In general, low levels of *OSH15* expression gave mild to intermediate phenotypes, plants with a moderate level of *OSH15* expression had an intermediate to severe phenotype and a high level of *OSH15* expression produced severe to shooty plants. But this correlation was not strict. For example, in lane 7, *OSH15* expression was high, but this plant showed a relatively mild phenotype.

In situ localization of *OSH15* mRNA during embryogenesis

To determine the spatial pattern of *OSH15* gene expression during different stages of plant development, I conducted *in situ* hybridization experiments with digoxygenin-, or fluorescein-labeled *OSH15* antisense RNAs as a probe (Fig. 4-5 to 4-7).

In Fig. 4-5, the expression patterns of *OSH15* during rice embryogenesis are shown comparing with those of another rice homeobox gene, *OSH1*, which we cloned and characterized before (Matsuoka et al., 1993; Sato et al., 1996a). After fertilization, rice embryos grow in a globular shape with relatively irregular cell divisions. In the early globular stage embryo (2DAP), embyos are composed of about 100 cells and the size is about 50 μm in length. Although I can not observe any sign of organ differentiation at this stage, the expression of *OSH1* was already observed in the ventral and basal part of the embryo where the shoot apical meristem would develop later in embryogenesis (Fig. 4-5B). But in the same section, *OSH15* gene expression was not detected (Fig. 4-5A). In the late globular stage embryo (3DAP), a dorsiventral polarity within the embryo become evident from the gradient of

cell size although no organogenetic events are yet observed, and *OSH1* mRNA accumulation continued in the ventral and basal part of the embryo (Fig. 4-5D). On the same histological section, one can see expression of *OSH1* as a pink signal from its fluorescein labeled probe (Fig. 4-5D); and in the same area the first appearance of *OSH15* by means of its digoxygenin labeled probe (Fig. 4-5C). Thus, the timing of the initiation of gene expression during the embryogenesis is different for the two genes, but both genes are expressed in the same region, that is, the future shoot region before any visible organ differentiation.

At the coleoptilar stage (4DAP), the first morphological differentiation is observed as a ventral protrusion of a coleoptile primordium. The initial of the shoot apical meristem is also recognized as a notch under the coleoptile primordium. At this stage, both *OSH15* and *OSH1* mRNA accumulations were observed in the ventral and basal part of the embryo including the initial of the shoot apical meristem (Fig. 4-5E and F, respectively). By this stage, expression of both genes overlap.

Differences in the expression pattern between *OSH15* and *OSH1* began to be observed in the embryo at 5DAP which had a developping coleoptile, shoot apical meristem, and provascular tissue. In the embryo at this stage, *OSH15* was expressed at the ventral side of the embryo, but the expression within the shoot apical meristem was down-regulated (Fig. 4-5G), whereas the expression of *OSH1* within the shoot apical meristem continued high (data not shown).

By 7DAP, rice embryos develop successively two primordia of embryonic leaves at the periphery of the shoot apical meristem in a distichous phyllotaxis and the root cap differentiates at the tip of the radicle primordium. In the embryo at this stage, differences of the expression patterns between *OSH15* and *OSH1* became clearer (Fig. 4-5H and I). *OSH1* expression stained with the digoxygenin labeled probe was observed in the shoot apical

meristem, in the ventral side around the provascular tissue, the epiblast (bud scale), and below it (Fig. 4-5I). On the other hand, the expression of *OSH15* on the same section stained with the fluorescein labeled probe was restricted around the boundaries between the two embryonic organs, that is, the scutellum and the coleoptile, the coleoptile and the second leaf primordium, the shoot apical meristem and the first leaf primordium, the first leaf primordium and the coleoptile, the coleoptile and the epiblast (indicated by arrowheads in Fig. 4-5H). At the tip of the epiblast, the expression of *OSH15* was also observed. As often observed in the class 1 type of the KNOTTED gene family, both the *OSH15* and *OSH1* expressions were strictly supressed in the leaf primordia even though they were embryonic leaves. To constitute the three dimensional image of *OSH15* expression in embryo, I observed it in the rectangular longitudinal sections of a rice embryo at 5 DAP. Fig. 4-6 A and B show the schematic representations of a longitudinal and a rectangular longitudinal section of a rice embryo. Line X in panel A indicates an approximate plane of the rectangular section shown in panel B. By overlaying the signal of *OSH15* expression observed in serial sections (panel C, D, and E), the spotted expression of *OSH15* localized around the boundaries between two different organs in the longitudinal section (Fig. 4-5H, and Fig. 4-6A) was revealed to be a ring shape (Fig. 4-6B).

OSH15 expression in an embryo mutant, *orl1*

The expression of *OSH15* during embryogenesis prior to morphological differentiation, in the area where the shoot apical meristem will develop indicates that *OSH15* functions at an earlier stage than the morphological differentiation of the shoot apical meristem. To elucidate the epistatic relationship between *OSH15* expression and shoot differentiation, I conducted *in situ* hybridization using the embryos of the rice embryogenesis defective mutant, *organless1* (*orl1*) which is caused by a single recessive mutation

(Hong et al., 1995). *orl1* lacks embryonic organs including shoot and radicle, although the embryo grows relatively large (larger than 1000μm). Before the late globular stage, I can not distinguish wild from *orl1* embryos under the microscope because both embryos show a globular shape without any organs. At 4 DAP and later stage, *orl1* embryos are morphologically distinguishable from wild-type embryos by the absence of the shoot and the radicle.

I examined the expression of *OSH15* in *orl1* embryos. At the globular stage, I could not identify which sections were those of the mutant embryo (homozygous *orl1* plants are lethal and I had to use embryos set on plants heterozygous for *orl1*). The expected frequency of homozygous *orl1* embryo is 25% in the panicle of heterozygous plants. More than fifty early globular embryos examined showed the same hybridization pattern as the wild type that marked the future shoot apical meristem region, indicating that *OSH15* expression is normally regulated in the *orl1* embryo (Fig. 4-5J). At 6DAP, the mutant embryos become larger but stay still in a globular shape. *OSH15* expression was maintained in the position where the shoot apical meristem would have developed in the wild-type embryo although neither shoot nor radicle is differentiated in mutant embryos. These results indicate that the expression patterns of *OSH15* are exactly maintained even in the *orl1* mutant embryos lacking a shoot apical meristem. This suggests that, in the wild type embryo at the globular stage, *OSH15* is first expressed earlier than the onset of morphological differentiation (see discussion).

In situ localization of *OSH15* mRNA around the shoot apex

After seed germination, expression of *OSH15* mRNA was localized specifically in a ring shaped pattern at a leaf insertion point of the vegetative shoot apical meristem (Fig. 4-7A and B). Fig. 4-7A shows a near median longitudinal section of a rice vegetative shoot. *OSH15* expression appears as

pairs of signals, each on opposite flanks of the shoot apical meristem. The cross section through the plane X in Fig. 4-7A revealed that those pairs of signals representing *OSH15* expression came from a ring shape (Fig. 4-7B). In the same section, the expression of *OSH1* was observed as disc shaped (Fig. 4-7C) because *OSH1* was expressed in the dome of shoot apical meristem (Matsuoka et. al. unpublished results). The expression of both genes were also observed in the axillary buds at the base of the second leaf primordium (indicated by arrowheads in Fig. 4-7B and C). The earliest appearance of *OSH15* expression in the shoot apical meristem was observed in two to four cells before any visible differentiation of P0 leaf (indicated by an arrowhead in Fig. 4-7A). From the observations mentioned above, *OSH15* expression in vegetative shoots appears to represent the boundary of each phytomer or the pre-patterning for the future internodes.

OSH15 expression continues after transition from the vegetative to the infloresence meristem. At the stage of primary rachis-branch primordia differentiation, *OSH15* expression was observed at the base area of each primary rachis-branch primordia as dividing the newly formed organs from the stem (Fig. 4-7D), whereas in the same section, *OSH1* expression was localized at the rachis-branch primordia itself and the vascular tissue (Fig. 4-7E). At the secondary rachis-branch differentiation stage, *OSH15* expression was observed as pairs of signal or stripes depending on the plane of its bisection (Fig. 4-7. G, H, and I). The observations of these serial sections demonstrate that *OSH15* was expressed in a ring shaped pattern at the boundary of each unit which produces a floral meristem. Later in floral development, *OSH15* was expressed in floral primordia and subtended lateral structures such as palea, lemma, and glumes in floral meristems (Fig. 4-7 F).

Discussion

A rice homeobox gene, *OSH15*, is a member of the class1 type of KNOTTED-type homeobox gene family.

The *OSH15* cDNA encodes a hypothetical protein with 355 amino acids that contains a homeodomain DNA binding motif at its C-terminal side. Homeodomains represent a highly conserved protein motif that recognize and bind specific DNA sequences (Kornberg, 1993). Based on this DNA binding property, homeodomain-containing proteins are believed to act as transcriptional factors to regulate the expression of specific target genes. Homeodomains consist of three α-helices, with helix 2 and helix 3 comprising a helix-turn-helix structure (Qian et al., 1989). Within the homeodomain, the recognition helix 3 is responsible for DNA-protein interaction. In the third helix, *OSH15* contains all four of the invariant amino acids conserved in all of the homeodomains, (W-52, F-53, N-55, R-57)(Wolberger et al., 1991; Gehring et al., 1994; Scott et al., 1989). Therefore, it is very likely that *OSH15* encodes a homeobox transcriptional factor. By comparing the *OSH15* homeodomain with other representatives of the major classes of plant homeodomains, I found that the *OSH15* homeodomain had the highest similarity to those of the class 1 type of the KNOTTED gene family. So I conclude that *OSH15* is a member of the KNOTTED-type class 1 genes.

The amino acid identity along a whole region of the predicted OSH15 protein shows high similarity to maize *RS1* (88 %) and, especially within the homeodomain, the amino acid sequences of both genes are perfectly identical. The amino acid sequece of *OSH15* also shows high degrees of similarity to the maize *KNOX4* gene with an exchange of an amino acid residue within the homeodomain. *RS1* and *KNOX4* are mapped at the two maize genomic region in which ancient duplications of the genome are thought to have occurred (Helentjaris et al., 1988). *OSH15* is mapped to the

long arm of the rice chromosome 7 (Sato et al. unpublished results), where synteny is observed between this region of the rice genome and those two maize genomic region (Ahn and Tanksley, 1993). These results indicate that *OSH15* may be an orthologous gene for maize *RS1* and/or *KNOX4*. Furthermore, the similarity of the expression patterns of both *OSH15* and *RS1* around the shoot apical meristem also supports this notion.

Morphological alterations of leaves in transgenic tobacco plants expressing *OSH15*

Ectopic expression of *OSH15* in transgenic tobacco plants induced abnormal morphologies of leaves and flowers. These morphological abnormalities are similar to the phenotypes observed in transgenic tobacco or *Arabidopsis* plants overproducing KNOTTED-type class 1 genes such as *KN1*, *OSH1*, *KNAT1*, and *NTH15* (Sinha et al., 1993; Kano-Murakami et al., 1993; Sato et al., 1996b; Chuck et al., 1996; Tamaoki et al., 1997; Müllar et al., 1995). This indicates that these genes share at least some common target genes when overexpressed.

The degree of abnormalities and the expression level of the *OSH15* transgene in transgenic tobacco plants generally correlates, but this correlation is not strict. This suggests that physiological conditions other than expression levels of the transgene affect the degree of the morphological abnormalities. Possibly, physiological conditions affect the stability of mRNA or the activity of the protein products of the transgene. Perhaps due to this reason leaves on ectopic shoots or axillary branches do not necessarily show the same phenotype as leaves on primary axes.

Phenotypes observed in the transgenic plants overexpressing *OSH15*, such as the formation of ectopic shoots on leaves and the shortening of stamen filaments, are similar to the phenotype observed in transgenic tobacco plants with artificially increased cytokinin concentrations (Smart et al., 1991; Li

et al., 1992) or in plants with reduced gibberellins levels (Pharis and King, 1985). In fact, in transgenic tobacco plants overexpressing *OSH1* or *NTH15* which show similar phenotypes to those overexpressing *OSH15*, increased levels of cytokinin and reduced levels of gibberellins have been reported (Kusaba et al., 1997; Tamaoki et al., 1997). Therefore, it is possible that these gene products alter some phytohormone concentrations via transcriptional regulation of genes involved in hormone metabolism, or are involved in hormonal perception by plant cells.

Two separable functions of *OSH15* durng embryogenesis

I reported previously that the expression of a rice homeobox gene, *OSH1*, is localized at the limited area where the shoot apical meristem will develop later, prior to any visible organ differentiation, during rice embryogenesis (Sato et al., 1996a) The same phenomenon is also observed in maize *KN1* (Smith et al., 1995), *Arabidopsis STM* (Long et al., 1996) and tobacco *NTH15* (Kyou et al., unpublished results). These findings indicate the involvement of this class of homeobox genes in the formation of shoots and their maintainance during embryogenesis and the later stages of plant development including vegetative and reproductive stages. The appearance of *OSH15* expression during embryogenesis was detected at the same region as *OSH1*, where the shoot apical meristem would develop later in embryogenesis. In the *orl1* mutant which can not form almost all organs including the shoot apical meristem, the expression patterns of *OSH1* and *OSH15* were the same as that in wild rice and localized at the area where the shoot apical meristem would form in wild type plants. This indicates that both genes are expressed prior to the onset of visible organ formation, and also suggests that *OSH15* may be involved in shoot apical meristem formation during early embryogenesis in cooperation with *OSH1*. However, the timing of the appearance of the *OSH15* expression was later than that of *OSH1*; Thus

there may be an epistatic relationship between these two genes. Some of the homeobox genes which are thought to be involved in shoot formation during embryogenesis such as *KN1*, *OSH1*, *OSH15*, *NTH15*, and *KNAT1* produce ectopic shoots on the leaves of transgenic tobacco or *Arabidopsis* plants overproducing these genes (Sinha et al., 1993; Kano-Murakami et al., 1993; Sato et al., 1996b; Chuck et al., 1996; Müller et al., 1995). It is possible that this formation of ectopic shoots may mimic the process of shoot formation in the natural context of embryogenesis.

By the coleoptilar stage before the differentiation of the shoot apical meristem, there is no observable difference in the expression patterns of *OSH1* and *OSH15*. At the first leaf primordium differntiation stage, however, the expression pattern of *OSH15* dramatically changes and becomes completely different from that of *OSH1*. At this stage, the expression of *OSH1* continues within the shoot apical meristem. This suggests that *OSH1* is involved in the maintainance of the indeterminate state of the shoot apical meristem as is the case for the *KN1* in maize (Smith et al., 1992). In contrast to *OSH1*, the expession of *OSH15* within the shoot apical meristem is down-regulated, and in turn, is localized at the boundaries of some embryonic organs as a ring shaped pattern (Fig. 4-6). This expression pattern is similar to those around the shoot apical meristem after seed germination. Thus, the expression pattern of *OSH15* changes dramatically before and after the formation of the shoot apical meristem during embryogenesis. The change in the pattern of *OSH15* expression may be an essential process for proper embryogenesis. In the *orl1* mutant without most organ differentiation including the shoot apical meristem, the change in the *OSH15* expression pattern did not occur. These observations indicate that *OSH15* may have at least two separable functions before and after the formation of the shoot apical meristem. *OSH15* may first function in the formation of the shoot apical meristem during embryogenesis in cooperation with *OSH1*. After shoot

formation, *OSH1* is involved in the maintainance of the shoot apical meristem, whereas *OSH15* is not. The function of *OSH15* after shoot formation in embryos is probably similar to those after seed germination, because the pattern and the site of the expression of *OSH15* are quite similar to those around the vegetative shoot (see below).

Expression of *OSH15* marks the segmental unit of the shoot axis.

A ring shaped pattern of *OSH15* expression is observed at each leaf insertion point around the vegetative shoots. A similar expression pattern is also observed in the infloresence meristem and the floral meristem. The position of the ring which indicates *OSH15* expression is always observed between two lateral organs newly formed from the vegetative, the infloresence, or the floral meristem. Such ring shaped expression pattern was clearly observed in the cross section of the shoot at the embryonic stage (Fig. 4-6). Such expression pattern indicates that *OSH15* may be involved in or respond to an early pattern forming event that defines the segmental units of the plant body designated phytomers as proposed in Schneeberger et al. (1995) for maize *RS1*. Looking at it another way, *OSH15* expression may mark the future internodes and may be involved in their differentiation. This is suggested by the fact that the ring shaped expression of *OSH15* around the vegetative shoot apical meristem is always observed in the region between two nodes where the development of the internodes will occur. It also supports this notion that all of the four loss-of-function alleles of *OSH15* which I identified show defects in internode elongation (Sato et al. unpublished results). I hope to clarify the functions of *OSH15* around the shoot apical meristem by further observations of the phenotypes of these recessive mutation alleles.

Summary

In many eukaryotic organisms including plants, homeobox genes are thought to be master regulators that establish the cellular or regional identities and specify the fundamental body plan. I isolated and characterized a cDNA designated *OSH15* (*Oryza sative* homeobox 15) that encodes a KNOTTED-type homeodomain protein. Transgenic tobacco plants overexpressing the *OSH15* cDNA showed a dramatically altered morphological phenotype caused by disturbance of specific aspects of tobacco development, thereby indicating the involvement of *OSH15* in plant development. To understand the function of *OSH15* in plant development better, I performed *in situ* hybridization analyses through the whole plant life cycle, comparing the expression pattern with that of another rice homeobox gene, *OSH1*. In early embryogenesis, both genes were expressed as the same pattern at a region where the shoot apical meristem would develop later. In late embryogenesis, the expression pattern of the two genes became different. Whereas the expression of *OSH1* continued within the shoot apical meristem, *OSH15* expression within the shoot apical meristem ceased but became observable in a ring shaped pattern at the boundaries of some embryonic organs. This pattern of expression was similar to that observed around vegetative or reproductive shoots, or the floral meristem in mature plants. Based on the above observations, I propose that *OSH15* plays at least two different roles in rice development. One may be involved in the establishment of the regional identity that is prerequisite for shoot formation and another may be involved in setting up morphogenetic boundaries of segmentation units of the plant body.

References

Ahn, S. and Tanksley, S. D. (1993) Comparative linkage map of the rice and maize genomes. *Proc. Natl. Acad. Sci. USA* **90**, 7980-7984.

Chuck, G., Lincoln, C. and Hake, S. (1996) *KNAT1* Induces Lobed Leaves with Ectopic Meristems When Overexpressed in *Arabidopsis*. *Plant Cell* **8**, 1277-1289.

Gehring, W. J., Affolter, M. and Bürglin, T. (1994) HOMEODOMAIN PROTEINS. *Annu. Rev. Biochem.* **63**, 487-526.

Gerber, H. P., Seipel, K., Georgiev, O., Höffere, M., Hug, M., Rusconi, S. and Schaffner, W. (1994) Transcriptional Activation Modulated by Homopolymeric Glutamine and Proline Stretches. *Science* **263**, 808-811.

Helentjaris, T., Weber, D. and Wright, S. (1988) Identification of the Genomic Locations of Duplicate Nucleotide Sequences in Maize by Analysis of Restriction Fragmet Length Polymorphisms. *Genetics* **118**, 353-363.

Hong, S. K., Aoki, T., Kitano, H., Satoh, H. and Nagato, Y. (1995) Phenotypic Diversity of 188 Rice Embryo Mutants. *Dev. Genet.* **16**, 298-310.

Izawa, T. and Shimamoto, K. (1996) Becoming a model plant: the importance of rice to plant science. *Trends plant sci.* **1**, 95-99.

Jürgens, G. (1995) Axis Formation in Plant Embryogenesis: Cues and Clues. *Cell* **81**, 467-470.

Kano-Murakami, Y., Yanai, T., Tagiri, A. and Matsuoka, M. (1993) A rice homeobox gene, *OSH1*, causes unusual phenotype in transgenic tobacco. *FEBS lett.* **334**, 365-368.

Kerstetter, R., Vollbrecht, E., Lowe, B., Veit, B., Yamaguchi, J. and Hake, S. (1994) Sequence Analysis and Expression Patterns Divide the

Maize *knotted1*-like Homeobox Genes into Two Classes. *Planat Cell* **6**, 1877-1887.

Klinge, B. and Werr, W. (1995) Transcription of the *Zea mays* Homeobox (*ZmHox*) Genes Is Activated Early in Embryogenesis and Restricted to Meristems of the Maize Plant. *Dev. Genet.* **16**, 349-357.

Kornberg, T. B. (1993) Understanding the Homeodomain. *J. Bio. Chem.* **268**, 26813-26816.

Kouchi, H. and Hata, S. (1993) Isolation and characterization of novel nodulin cDNAs representing genes expressed at early stages of soybean nodule development. *Mol. Gen. Genet.* **238**, 106-119.

Kouchi, H., Sekine, M. and Hata, S. (1995) Distinct Class of Mitotic Cyclins Are Differentially Expressed in the Soybean Shoot Apex during the Cell Cycle. *Plant Cell* **7**, 1143-1155.

Kusaba, S., Kano-Murakami, Y., Matsuoka, M., Tamaoki, M., Sakamoto, T., Yamaguchi, I., Fukumoto, M. (1997) Alteration of hormone levels in transgenic tobacco plants overexpressing a rice homeobox gene, *OSH1*. *Plant Physiol.* in press.

Lawrence, P. A. and Morata, G. (1994) Homeobox genes: Their Function in Drosophila Segmentation and Pattern Formation. *Cell* **78**, 181-189.

Li, Y., Hagen, G. and Guilfoyle, T. J. (1992) Altered Morphology in Transgenic Tobacco Plants That Overproduce Cytokinins in Specific Tissues and Organs. *Dev. Biol.* **153**, 386-395.

Lincoln, C., Long, J., Yamaguchi, J., Serikawa, K. and Hake, S. (1994) A *knotted1*-like Homeobox Gene in Arabidopsis Is Expressed in the Vegetative Meristem and Dramatically Alters Leaf Morphology When Overexpressed in Trangenic Plants. *Plant Cell* **6**, 1859-1876.

Long, J. A., Moan, E. I., Medford, J. I. and Barton, M. K. (1996) A member of the KNOTTED class of homeodomain proteins encoded by the *STM* gene of *Arabidopsis*. *Nature* **379**, 66-69.

Lu, P., Porat, R., Nadeau, J. A. and O'Neill, S. D. (1996) Identification of a Meristem L1 Layer-Specific Gene in Arabidopsis That Is Expressed during Embryonic Pattern Formation and Defines a New Class of Homeobox Genes. *Plant Cell* **8**, 2155-2168.

Matsuoka, M., Ichikawa, H., Saito, A., Tada, Y., Fujimura, T. and Kano-Murakami, Y. (1993) Expression of a Rice Homeobox Gene Causes Altered Morphology of Transgenic Plants. *Plant Cell* **5**, 1039-1048.

Matsuoka, M. and Sanada, Y. (1991) Expression of photosynthetic genes from the C4 plant, maize, in tobacco. *Mol. Gen. Genet.* **225**, 411-419.

Müller, K. J., Romano, N., Gerstner, O., Garcia-Maroto, F., Pozzi, C., Salamini, F. and Rohde, W. (1995) The barley *Hooded* mutation caused by a duplication in a homeobox gene intron. *Nature* **374**, 727-730.

Pharis, R., P. and King, R., W. (1985) Gibberellins and Reproductive Development in Seed Plants. *Annu. Rev. Plant Physiol.* **36**, 517-568.

Qian, Y., Q., Billeter, M., Otting, G., Müller, M., Gehring, W. J. and Wüthrich K. (1989) The Structure of the *Antennapedia* Homeodomain Determined by NMR Spectroscopy in Solution: Comparison with Prokaryotic Repressors. *Cell* **59**, 573-580.

Raikhel, N. V. (1992) Nuclear Targeting in Plants. *Plant Physiol.* **100**, 1627-1632.

Sass, A. E. (1958) Botanical micro technique, 3rd edn. Iowa State University Press, Ames.

Sato, Y., Hong, S. K., Tagiri, A., Kitano, H., Yamamoto, N., Nagato, Y. and Matsuoka, M (1996a) A rice homeobox gene, *OSH1*, is expressed before organ differentiation in a specific region during early embryogenesis. *Proc. Natl. Acad. Sci. USA* **93**, 8117-8122.

Sato, Y., Tamaoki, M., Murakami, T., Yamamoto, N., Kano-Murakami, Y. and Matsuoka, M. (1996b) Abnormal cell divisions in leaf primordia caused by the expression of the rice homeobox gene,

OSH1, lead to altered morphology of leaves in transgenic tobacco. *Mol. Gen. Genet.* **251**, 13-22.

Schneeberger, R. G., Becraft, P. W., Hake, S. and Freeling, M. (1995) Ectopic expression of the *knox* homeobox gene *rough sheath1* alters cell fate in the maize leaf. *Genes Dev.* **9**, 2292-2304.

Scott, M. P., Tamkun, J. W. and Hartzell, G. W. III (1989) The structure and function of the homeodomain. *Biochem. Biophys. Acta.* **989**, 25-48.

Sinha, N. R., Williams, R. E. and Hake, S. (1993) Overexpression of the maize homeo box gene, *KNOTTED-1*, causes a switch from determinate to indeterminate cell fates. *Genes Dev.* **7**, 787-795.

Smart, C. M., Scofield, S. R., Bevan, M. W. and Dyer, T. A. (1991) Delayed leaf senescence on tobacco plants transformed with *tmr*, a gene for cytokinin production in *Agrobacterium. Plant Cell* **3**, 647-656.

Smith, L. G., Greene, B., Veit, B. and Hake, S. (1992) A dominant mutation in the maize homeobox gene, *Knotted-1*, causes its ectopic expression in leaf cells with altered fates. *Development* **116**, 21-30.

Smith, L. G. and Hake, S. (1994) Molecular genetic approaches to leaf development: *Knotted* and beyond. *Can. J. Bot.* **72**, 617-625.

Smith, L. G., Jackson, D. and Hake, S. (1995) Expression of *knotted1* Marks Shoot Meristem Formation During Maize Embryogenesis. *Dev. Genet.* **16**, 344-348.

Steeves, T. A. and Sussex, I. M. (1989) Patterns in Plant Development. Cambridge University Press.

Tamaoki, M., Kusaba, S., Kano-Murakami, Y. and Matsuoka, M. (1997) Ectopic Expression of a Tobacco Homeobox Gene, *NTH15*, Dramatically Alters Leaf Morphology and Hormone Levels in Transgenic Tobacco. Plant Cell Physiol. 38, 917-927.

Vollbrecht, E., Veit, B., Sinha, N. and Hake, S. (1991) The developmental gene Knotted-1 is a member of a maize homeobox gene family. *Nature* **350**, 241-243.

Wolberger, C., Vershon, A. K., Liu, B., Johnson, A. D. and Pabo, C. O. (1991) Crystal Structure of a MATα2 Homeodomain-Operator Complex Suggests a General Model for Homeodomain-DNA Interactions. *Cell* **67**, 517-528.

Figures

A

```
GAGCTCCAGGAGGAAGAAGAGAGAGAGCCTAGCTGCTAGGGTTTCCATCGGATTTGGTTTTTTATTTTCTTTTTGTTTCTTGTGTGTGTT     90

TTGATGGATCAGAGCTTTGGGAATCTTGGAGGAGGAGGAGGAGCAGGGGGGAGCGGCAAGGCGGCGGCGTCGTCGTTCCTGCAGCTGCCG    180
   M  D  Q  S  F  G  N  L  G  G  G  G  G  G  A  G  G  S  G  K  A  A  A  S  S  F  L  Q  L  P

CTGTCCACGGCGGCGGCGGCCACCGCGTACTACGGCACGCCGCTCGCCTTGCACCAGGCGGCGGCCGCGGCTGGCCCGTCGCAGTACCAC    270
L  S  T  A  A  A  A  T  A  Y  Y  G  T  P  L  A  L  H  Q  A  A  A  A  A  A  G  P  S  Q  Y  H

GGTCACGGTCACCCCCACCACGGCGGCGGCCACCACCACAGCAAGCACGGCGGCGCCGGTGGTGGGGAGATCTCGGCGGCGGAGGCCGAG    360
G  H  G  H  P  H  H  G  G  G  H  H  H  S  K  H  G  G  A  G  G  G  E  I  S  A  A  E  A  E

TCCATCAAGGCCAAGATCATGGCGCACCCCCAGTACTCCGCCCTCCTCGCAGCCTACCTCGACTGCCAGAAAGTCGGAGCGCCGCCGGAG    450
S  I  K  A  K  I  M  A  H  P  Q  Y  S  A  L  L  A  A  Y  L  D  C  Q  K  V  G  A  P  P  E

GTGCTGGAGAGGCTGACCGCCACGGCGGCAAAGCTGGACGCCCGCCCTCCCGGCCGCCACGACGCGCGCGACCCGGAGCTCGACCAGTTC    540
V  L  E  R  L  T  A  T  A  A  K  L  D  A  R  P  P  G  R  H  D  A  R  D  P  E  L  D  Q  F

ATGGAGGCGTACTGCAACATGCTGGCCAAGTACAGGGAGGAGCTGACGCGGCCGATCGACGAGGCCATGGAGTTCCTCAAGAGGGTGGAG    630
M  E  A  Y  C  N  M  L  A  K  Y  R  E  E  L  T  R  P  I  D  E  A  M  E  F  L  K  R  V  E

TCGCAGCTCGACACCATCGCCGGCGGCGCCCATGGCGGCGGCGCCGGCTCGGCGCGCCTCCTCCTCGCCGATGGTAAATCTGAATGTGTT    720
S  Q  L  D  T  I  A  G  G  A  H  G  G  G  A  G  S  A  R  L  L  L  A  D  G  K  S  E  C  V

GGTTCTTCTGAGGATGACATGGACCCAAGTGGCCGCGAAAACGAGCCGCCTGAGATCGACCCGCGCGCTGAGGATAAGGAGCTCAAGTTT    810
G  S  S  E  D  D  M  D  P  S  G  R  E  N  E  P  P  E  I  D  P  R  A  E  D  K  E  L  K  F

CAGCTTCTGAAGAAGTACAGTGGCTACTTGAGCAGCCTAAGGCAAGAATTTTCCAAGAAAAAGAAGAAAGGAAAGCTGCCTAAGGAGGCC    900
Q  L  L  K  K  Y  S  G  Y  L  S  S  L  R  Q  E  F  S  K  K  K  K  K  G  K  L  P  K  E  A

AGGCAGAAGCTGCTTCACTGGTGGGAGCTGCACTACAAGTGGCCTTACCCCTCAGAGACGGAGAAGATTGCGCTTGCGGAATCGACAGGA    990
R  Q  K  L  L  H  W  W  E  L  H  Y  K  W  P  Y  P  S  E  T  E  K  I  A  L  A  E  S  T  G

CTAGATCAGAAGCAGATCAACAACTGGTTCATCAACCAGAGGAAACGGCACTGGAAGCCATCGGAGGACATGCCGTTCGTCATGATGGAA   1080
L  D  Q  K  Q  I  N  N  W  F  I  N  Q  R  K  R  H  W  K  P  S  E  D  M  P  F  V  M  M  E

GGTTTTCACCCACAGAATGCTGCTGCATTGTACATGGATGGCCCGTTCATGGCAGATGGAATGTACCGCCTCGGTTCGTGAACCTCGATC   1170
G  F  H  P  Q  N  A  A  A  L  Y  M  D  G  P  F  M  A  D  G  M  Y  R  L  G  S  *

TCGATCATCGGCGTGTTTGATGAGAGATCCAATGCCAAGATAAATTGATCATGGAATGTATTCAGCATGCGTTGCAATGCATGGACATTG   1260

TTATGGAATTTTTGGTTTATTTACCTTTCACCGTGGATTGACAAGGTCTCGATCATGTTAGTGTTGACGGTCCATAGTTCTCCAGTAATG   1350

TTGTTGTTTTTCCTTTCGATGGCTTGTAAAAGTTTAGGCGTATCGGAATTTCGATCAACTTGCTCGTACGCTGGTAATTAATTTGGTGAT   1440

GGTCTATATGTTGTATGGTTGTGCGTTTCAGATTGGTGTTCAAAGTTGCCTATCTGAAACAATTATATATATTTATATTGCTTCTCATTT   1530

T(A)n
```

B

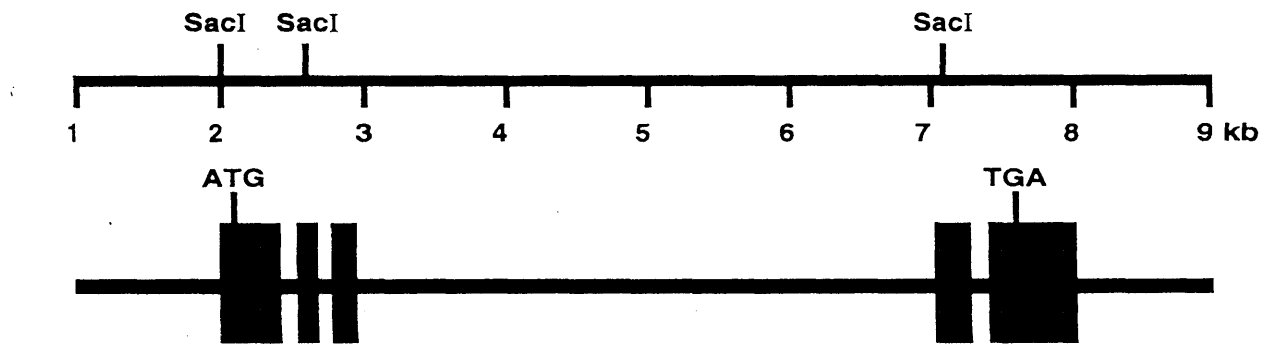

Fig. 4-1. Structure of the *OSH15* gene. (A) Nucleotide and deduced amino acid sequences of *OSH15*. A bold underline indicates the homeodomain. The ELK region is represented with a dashed underline. The homopolymeric amino acids streches such as poly alanines, histidines,or glycines, are indicated by thin underlines. The insertion sites of introns are indicated by filled triangles. Numbers at the right side indicate the nucleotide positions. (B) Genomic structure of *OSH15*. The scale bar and the *Sac*I recognition sites are presented at the top. Exons and introns are indicated by boxes and lines, respectively. ATG and TGA indicate the locations of the initiation and the termination codons of the gene, respectively.

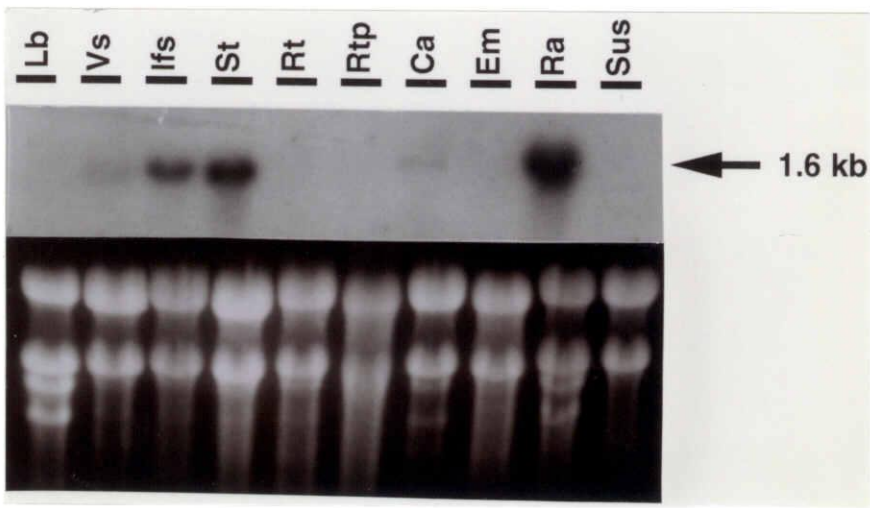

Fig. 4-2. RNA gel blot analysis of *OSH15* expression in various organs of wild-type rice. RNA was isolated from leaf blades (Lb), vegetative shoots (Vs), infloresence shoots (Ifs), stems (St), roots (Rt), root tips (Rtp), caryopsis (Ca), embryos (Em), rachis (Ra), and suspension cells (Sus). Fifteen μg of total RNA were loaded per lane. The blot was probed with *OSH15* cDNA. The approximate size of transcripts was indicated at right. In the lower case, Ethidium bromine stained RNAs corresponding to the above lanes are shown for the control of RNA loading.

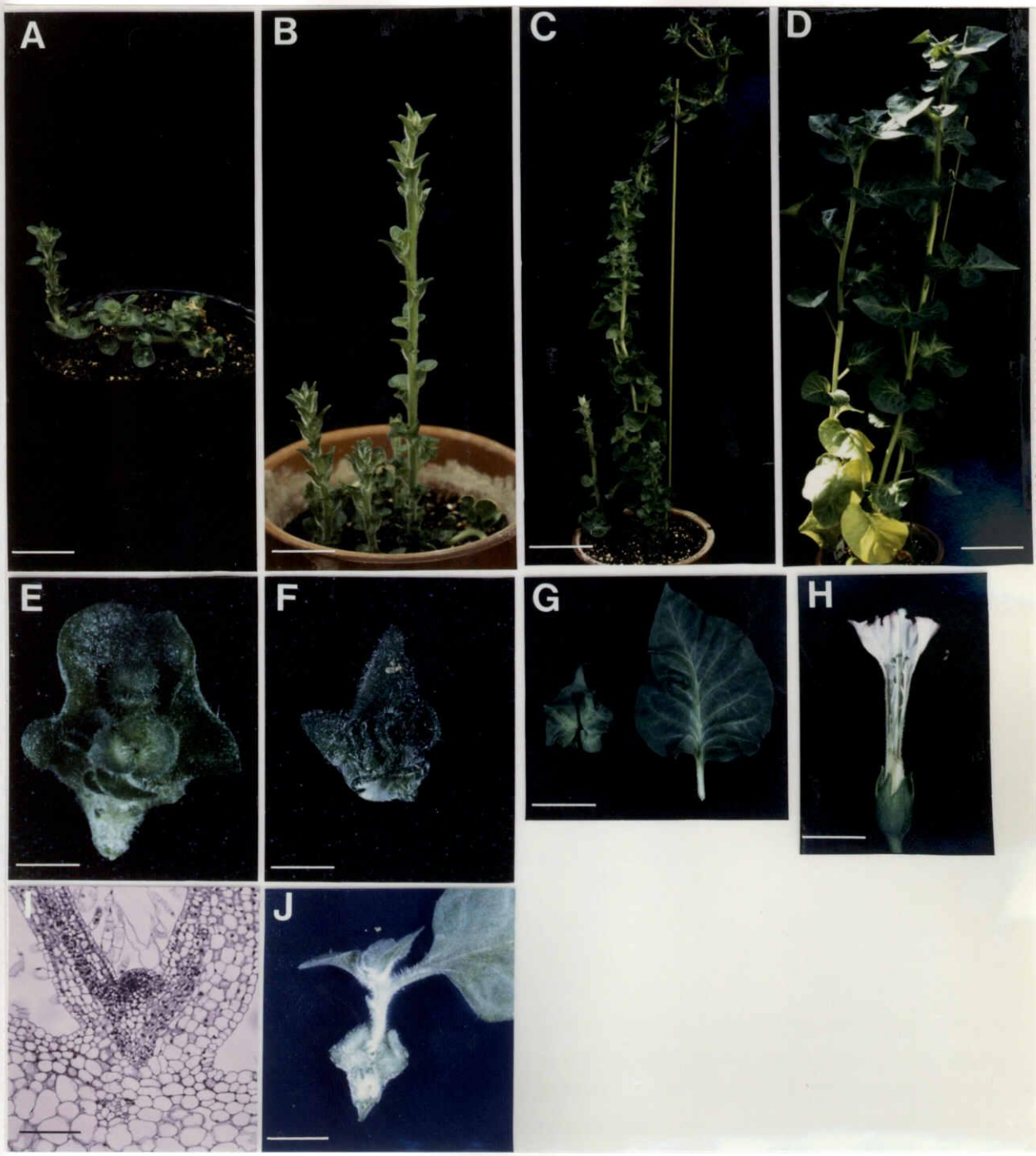
A
B
C
D
E
F
G
H
I
J

Fig. 4-3. Phenotypes of transgenic plants carrying the *35S-OSH15* gene. (A) A typical transgenic plant with shooty phenotype (Bar = 3 cm). (B) A typical transgenic plant with severe phenotype (Bar = 3 cm). (C) A typical transgenic plant with intermediate phenotype (Bar = 10 cm). (D) A typical transgenic plant with mild phenotype (Bar = 10 cm). (E) A leaf from a shooty phenotype plant (Bar = 5 mm). (F) A leaf from a severe phenotype plant (Bar = 4 mm). (G) A typical leaf of intermediate phenotype plants (left), and a typical leaf of mild phenotype plants (right) (Bar = 5 cm). (H) A typical flower from intermediate phentype plants (Bar = 1 cm). (I) A section through an ectopic shoot on the leaves of the plants with shooty phenotype (Bar = 150 μm). (J) In some cases, ectopic shoots grow and produce some leaves. This panel shows an example that leaves of ectopic shoots are not always as abnormal as original leaves (Bar = 4 mm).

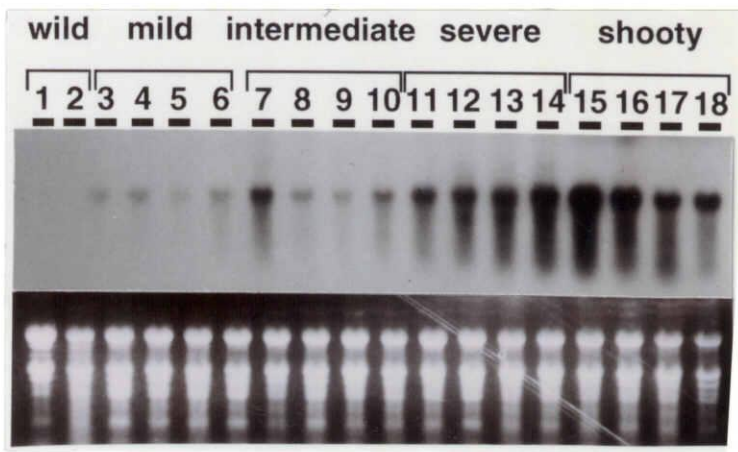

Fig. 4-4. Transgene expression in leaves of *35S-OSH15* transformants. RNA was isolated from leaves of two independent wild-type and sixteen independent transgenic tobacco plants. Lanes 1 and 2, wild-type leaves; lanes 3-6, leaves from mild phenotype; lanes 7-10, leaves from intemediate phenotype; lanes11-14, leaves from severe phenotype; lanes 15-18, leaves from shooty phenotype. The blot was hybridized with the same probe as used in Fig. 4-2. The appoximate size of transcripts is 1.6 kb. Ten μg of total RNA were loaded in each lane. In the lower case, Ethidium bromine stained RNAs corresponding to the above lanes are shown for the control of RNA loading.

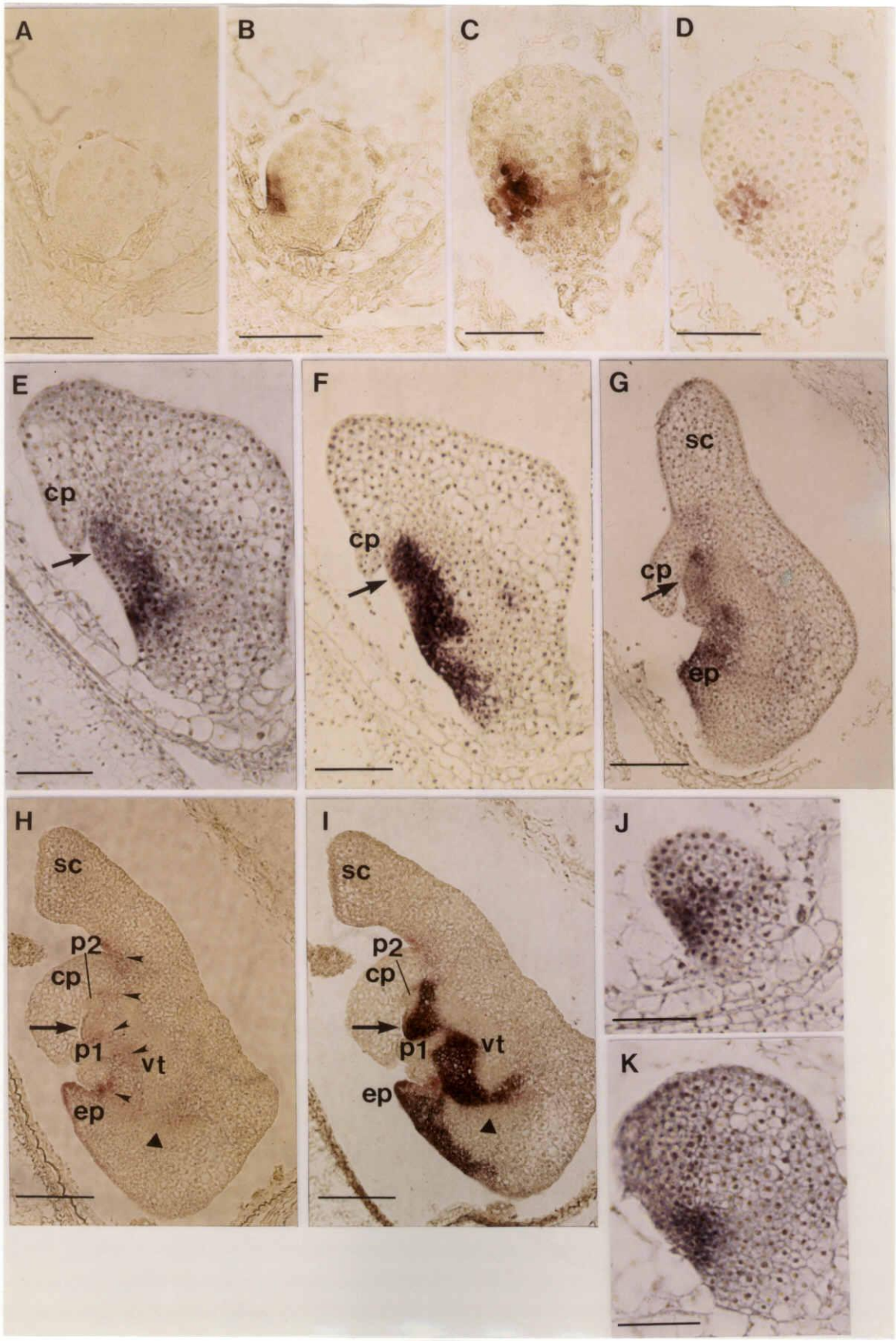
A
B
C
D
E
cp
F
cp
G
sc
cp
ep
H
sc
p2
cp
p1
vt
ep
I
sc
p2
cp
p1
vt
ep
J
K

Fig. 4-5. *in situ* mRNA localization of *OSH15* and *OSH1* in developing embryos of wild-type and in *orl1* mutant embryo. Longitudinal sections through the embryo were hybridized with an *OSH15* and/or an *OSH1* antisense probe. Panel (A) and (B), (C) and (D), and (H) and (I) are double-labeling of the same sections for *OSH15* and *OSH1.* Probes were labeled with digoxigenin-UTP or fluorescein-UTP and the transcript-specific hybridization signal is visualized as either purple or pink color, respectively. Panel (E), (F), (G), (J), and (K) are single-labeling for *OSH15* (E, G, J, and K) or *OSH1* (F). Probes were labeled with digoxigenin-UTP and the trascript-specific hybridization signal is visualized as purple color. (A) Single staining of fluorescein labeled*OSH15* antisense probe (pink) in the globular stage embryo (2DAP). In this stage, no hybridization signal of *OSH15* was observed. (B) Double staining of mixtures of fluorescein labeled*OSH15* (pink) and digoxigenin labeled *OSH1* (purple) antisense probe in the same section as in (A). (C) Double staining of mixtures of fluorescein labeled*OSH1* (pink) and digoxigenin labeled *OSH15* (purple) antisense probe in the late globular stage embryo (3DAP). (D) Single staining of fluorescein labeled*OSH1* antisense probe (pink) in the same section as in (C). (E) Single staining of digoxigenin labeled *OSH15* antisense probe (purple) in the coleoptilar stage embryo (4DAP). (F) Single staining of digoxigenin labeled *OSH1* antisense probe (purple) in the coleoptilar stage embryo (4DAP). (G) Single staining of digoxigenin labeled *OSH15* antisense probe (purple) in the first leaf primordium differentiation stage embryo (5DAP). (H) Single staining of fluorescein labeled*OSH15* antisense probe (pink) in the second leaf primordium differentiation stage embryo (7DAP). Arrowheads indicate the expression of *OSH15* observed in the boundaries of some embryonic organs. (I) Double staining of mixtures of fluorescein labeled*OSH15* (pink) and digoxigenin labeled *OSH1* (purple) antisense probe in the same section as in (H). (J) Single staining of digoxigenin labeled *OSH15* antisense probe (purple) in the *orl1* mutant embryo (4DAP). (K) Single

staining of digoxigenin labeled *OSH15* antisense probe (purple) in the *orl1* mutant embryo (6DAP). Bars in (A, B, C, D, J, and K) = 100 μm. Bars in (E and F) =100 μm. Bar in (G) = 160 μm. Bars in (H and I) = 200 μm. cp, coleoptile; ep, epiblast; sc, scutellum; vt, vascular tissue; p1, the first leaf primordium; p2, the second leaf primordium; arrow, shoot apex; filled triangle, radicle apex.

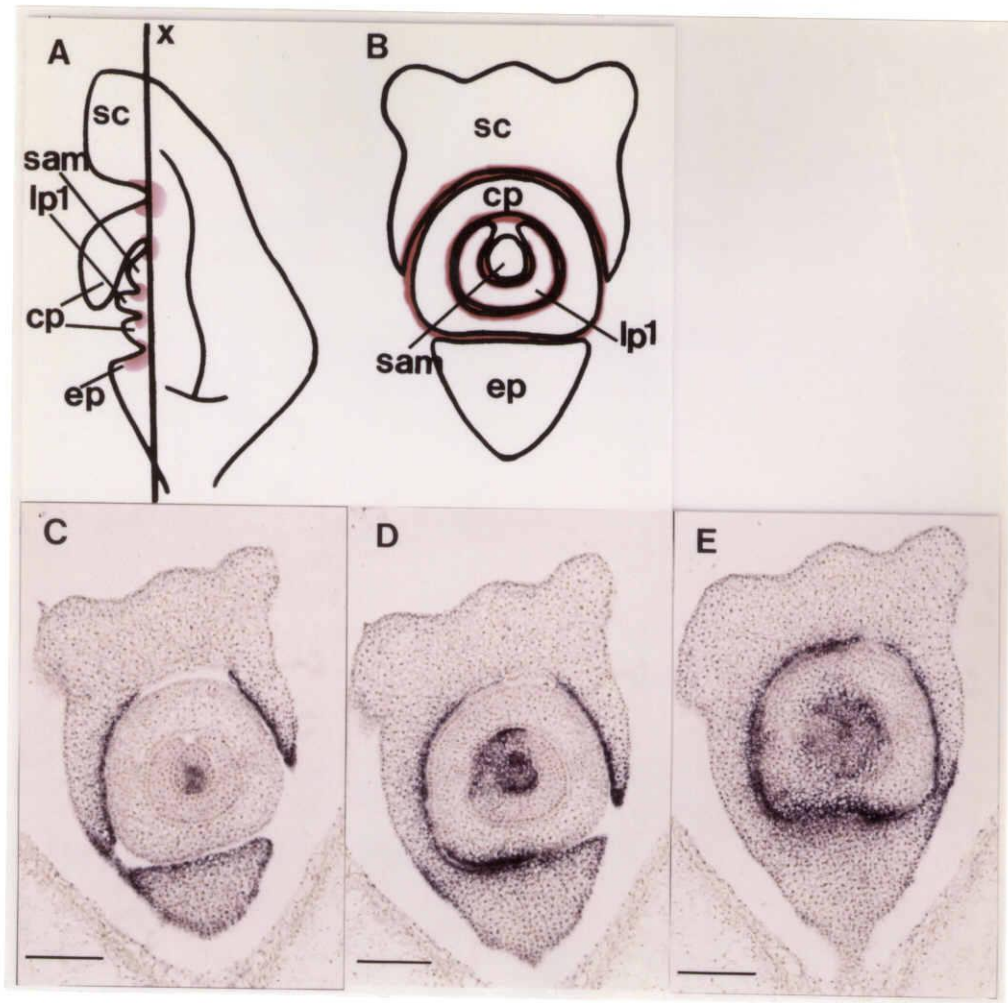

Fig. 4-6. *in situ* mRNA localization of *OSH15* in the rectangular longitudinal sections of wild-type embryo. (A) Schematic representation of a longitudinal section of a rice embryo at 5 DAP. Line x indicate the plane of rectangular bisection. Pink signal represents the spotted pattern of *OSH15* expression. (B) Schematic representation of a rectangular longitudinal section of a rice embryo at 5 DAP. (C, D, and E) Single staining of digoxigenin labeled *OSH15* antisense probe (purple) in the ractangular longitudinal sections of a wild-type rice embryo at 5 DAP. (C), (D), and (E) are sectioned sequencially from the left side to the right side in panel (A). Bars = 60 μm, cp, coleoptile; ep, epiblast; sc, scutellum; lp1, the first leaf primordium; sam, shoot apical meristem.

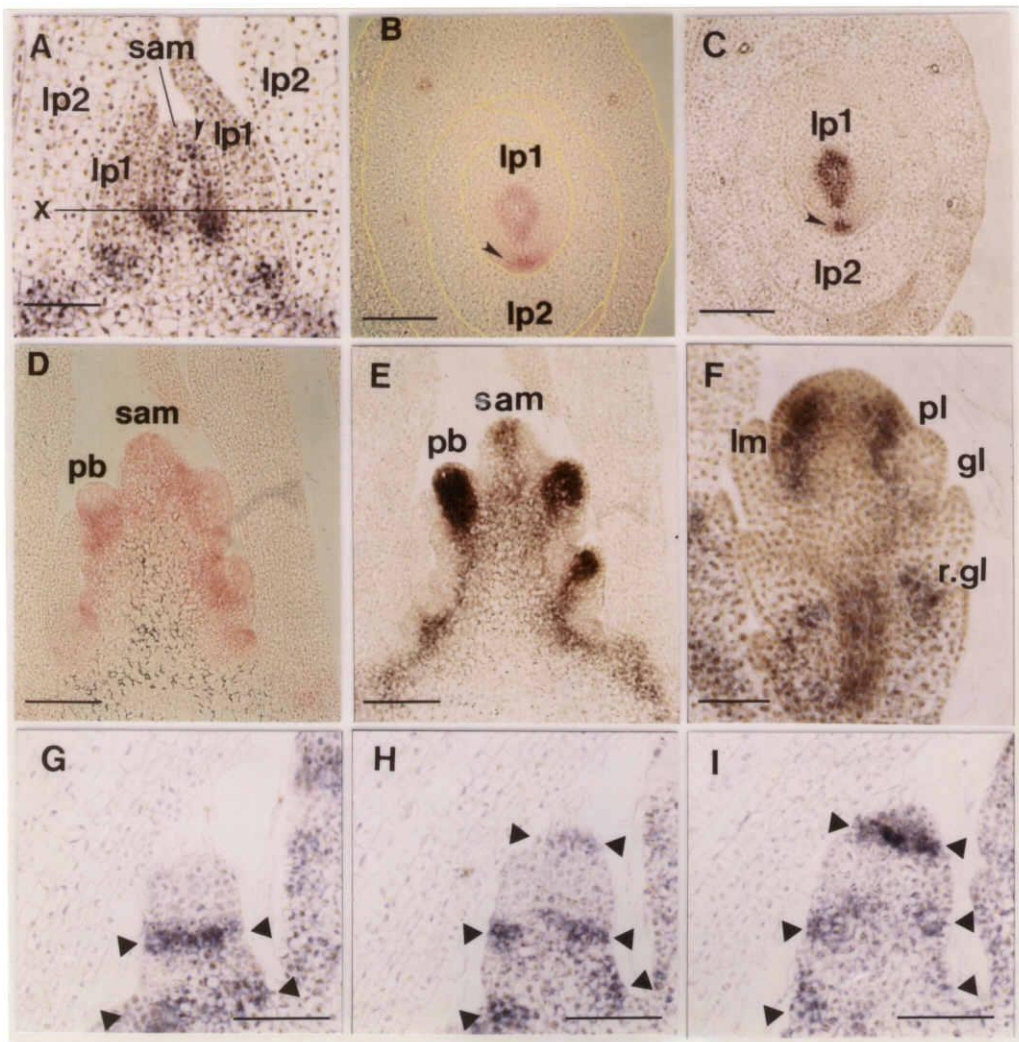
A
sam
lp2
lp2
lp1
lp1
x
B
lp1
lp2
C
lp1
lp2
D
sam
pb
E
sam
pb
F
pl
lm
gl
r.gl
G
H
I

Fig. 4-7. *in situ* mRNA localization of *OSH15* around the vegetative and infloresence shoot apical meristem and the floral meristem. (A) Single staining of digoxigenin labeled *OSH15* antisense probe (purple) in the longitudinal section of the vegetative shoot apical meristem. Line x indicates the approximate plane of bisection shown in (B and C). (B) Single staining of fluorescein labeled*OSH15* antisense probe (pink) in the cross section around th vegetative shoot apical meristem. The yellow outlines show the border of leaves. An arrowhead indicate the expression of *OSH15* in the axillary bud. (C) Double staining of mixtures of fluorescein labeled*OSH15* (pink) and digoxigenin labeled *OSH1* (purple) antisense probe in the same section as in (B). An arrowhead indicate the expression of *OSH15* in the axillary bud. (D) Single staining of fluorescein labeled*OSH15* antisense probe (pink) in the infloresence shoot of the primary rachis-branch primordia differentiation stage. (E) Double staining of mixtures of fluorescein labeled*OSH15* (pink) and digoxigenin labeled *OSH1* (purple) antisense probe in the same section as in (D). (F) Single staining of digoxigenin labeled *OSH15* antisense probe (purple) in the longitudinal section of the floral meristem. (G) Single staining of digoxigenin labeled *OSH15* antisense probe (purple) in the longitudinal section of the secondary rachis-branch primordium. (H) Single staining of digoxigenin labeled *OSH15* antisense probe (purple) in the serial section of (G). (I) Single staining of digoxigenin labeled *OSH15* antisense probe (purple) in the serial section of (H). sam, shoot apical meristem; lp1, leaf primordium 1; lp2, leaf primordium 2; pb, primary rachis branch primordium; lm, lemma; pl, palea; gl, glume; r. gl, rudimentary glume; filled triangles, the site of *OSH15* expression as a ring shaped pattern. Bars in (A and F) = 50 μm. Bar in (B, C, D, and E) = 100 μm. Bars in (G, H, and I) = 30 μm.

Chapter 5

Loss-of-function mutations in a rice homeobox gene, *OSH15*, are defective in internode elongation caused by the abnormal shape and arrangements of epidermal and hypodermal cells.

Introduction

The entire ground portion of a plant body is an assembly of shoot units termed phytomeres, which consist of an axillary bud, a stem and a leaf. The shoot apical meristem (SAM) continuously produces these units, at the same time maintaining itself as a collection of indeterminate stem cells (Steeves and Sussex, 1989). The mechanisms governing SAM activity are just beginning to be determined. For example, recent genetic and molecular studies on SAM formation and maintenance suggest that two genes, designated *CLV1* and *STM*, function in a competitive manner in the maintenance of indeterminate cells (Clark et al., 1995). *CLV1* has been shown to encode a receptor kinase, suggesting the involvement of a signal transduction pathway operating via extracellular ligands to regulate SAM activity (Clark et al., 1997). Further, *STM* has been shown to encode a *KNOTTED*-type homeobox gene and to function in meristem maintenance (Long et al., 1996).

The first higher plant homeobox gene to be cloned was *KNOTTED1 (KN1)* from the maize *Knotted1* (*Kn1*) mutant (Vollbrecht et al., 1991). Leaf blades of *Kn1* mutants exhibit abnormal arrangements of lateral veins, sporadic outgrowths called knots, and ligule displacements. *Kn1* has been shown to be a dominant mutation, caused by ectopic expression of *KN1* in leaves, that results in the disorganization of the developmental program of leaf blades (Smith and Hake, 1994). Many homeobox genes have subsequently been cloned from various plant species in an effort to address the biological functions of these genes in plant development. Based on amino acid sequence similarities within the homeodomain or conserved protein motifs outside of the homeodomain, plant homeobox genes have been classified into five groups (Kerstetter et al. 1994; Lu et al. 1996). These include the KNOTTED-type homeodomain proteins, homeodomain zipper proteins (HD-

ZIP), plant homeodomain finger proteins (PHD-finger), the GLABRA2 homeodomain proteins, and the BELL1 homeodomain protein.

In the functional analysis of plant homeobox genes, several approaches have been adopted, including the analysis of gene expression patterns, ectopic expression analysis, introduction of antisense RNA, inducible gene expression systems, identification of loss-of-function mutants, and others. The combination of these efforts has led to the characterization of functions of plant homeobox genes. For the *KNOTTED*-type homeobox genes, ectopic expression in tobacco, *Arabidopsis*, and tomato, and dominant mutations in maize, barley, or tomato often cause severe morphological abnormalities (Smith and Hake, 1994; Sinha et al., 1993; Matsuoka et al., 1993; Tamaoki et al., 1997; Chuck et al., 1996; Hareven et al., 1996; Schneeberger et al., 1995; Müller et al., 1995; Chen et al., 1997). However, it is difficult to determine the function(s) of these genes in the wild-type context from the phenotype of transgenic plants or dominant neomorphic mutations.

Recently, loss-of-function alleles of *KN1* were reported (Kerstetter et al., 1997). Although, perhaps due to the high genetic redundancy in maize, some of the phenotypes were not clear or exhibited poor penetrance, these mutations have revealed a role for *KN1* in meristem maintenance. In animals, families of related homeobox genes are often involved in related developmental processes (Gehring et al. 1994). Based on the observation that most of the *KNOTTED*-type homeobox genes are expressed around the SAM (Smith et al., 1992; Jackson et al., 1994; Lincoln et al., 1994; Tamaoki et al., 1997), and from the phenotypes of the loss-of-function mutations in *KN1* and *STM* (Kerstetter et al., 1997; Long et al., 1996), it has been suggested that genes of this class are involved in maintenance of the shoot apical meristem and/or the development of lateral organs.

Rice has become a model plant for the study of monocotyledonous plants because of the feasibility of transformation, its relatively small genome

size, the high saturation of molecular markers on the rice genome, and large-scale analysis of expressed sequence tags (Izawa and Shimamoto, 1996). Furthermore, the gene knock-out system using a rice retrotransposon, *Tos17*, has been recently exploited (Hirochika et al. 1996). Transpositions of *Tos17* are activated during tissue culture and some copies of *Tos17* can be inserted into the rice genome. In this system, it is possible to screen for mutants with insertion of *Tos17* into genes of interest from a large pool of plants regenerated after a few months of tissue culture.

I have isolated six rice homeobox genes grouped into the class1-type of the *KNOTTED*-like homeobox gene family. Most of these genes are expressed around the SAM and their expression patterns suggest that some of the genes may play a role in maintaining indeterminacy in the meristem and/or differentiation of lateral organs. A crucial step in determining the normal function(s) of the *KNOTTED*-type homeobox genes from rice is the isolation of recessive mutation alleles of these genes. I report here the isolation and characterization of loss-of-function mutants of the rice homeobox gene, *OSH15*. I have analyzed the phenotype of plants carrying loss-of-function mutations in *OSH15* and demonstrate a new function of the *KNOTTED*-type homeobox gene family outside of meristem formation and/or maintenance.

Experimental procedures

Plant growth conditions

Rice plants were grown in the field or in the greenhouse at 30 ℃ (day) and 24 ℃ (night). Rice mutants (*d6-1*, *d6-tankanshirasasa*, *d6-ID6*) were described in Kinoshita (1982) and Nagao and Takahashi (1963).

PCR amplification and sequencing

For screening for loss-of-function mutants, DNA fragments in which *Tos17* had inserted into the rice homeobox genes were amplified by PCR using transposon-specific primers designated LTR4S and LTR4A and a gene-specific primer designated KN31 from 300 ng of rice genomic DNA sampled from a pool of 23 or 24 plants. PCR products were gel purified and cloned into the pCRII vector (Invitrogen).

For sequencing of the entire coding region of *d6-ID6* and shiokari, exon and exon/intron border sequences were amplified by PCR from 30 ng of rice genomic DNA using primers PF2-I2R, I2F-I3R, and I3F-RR. To avoid PCR artifacts, I carried out three independent PCR reactions with each primer set. PCR products were gel purified and cloned separately into pCRII. Primer sequences are listed below.

LTR4S: CTGGACATGGGCCAACTATACAGT,

LTR4A: ACTGTATAGTTGGCCCATGTCCAG,

KN31: CCGAATTCTGGTTGATGAACCAGTTGTT,

PF2: ATCTTCAAACTTTAATTCCTCC,

I2R: CATGAACGATATATGAACTGG,

I2F: GGGTTGATTAATCGGAATCG,

I3R: GGGGATGGATGATTGGTTG,

I3F: AACATGGTCATGACTGAAGC,

RR: AACATGATCGAGACCTTGTC.

Nucleotide sequences were determined by the dideoxynucleotide chain-termination method using an automated sequencing system (ABI373A). Analysis of the nucleotide sequences was carried out using GENETYX computer software (Software Kaihatsu Co., Japan).

Genomic DNA isolation and southern blot hybridization

Rice genomic DNA was isolated from leaf tissue and 1 μg was digested with restriction enzymes, transferred onto Hybond N^+ membranes (Amersham) under alkaline conditions and analyzed by Southern hybridization. A cDNA probe specific for *OSH15,* which consisted of the fourth and part of the fifth exon, was amplified by PCR using the primers OSH15d (GATGGTAAATCTGAATGTG) and KN31. Hybridization was performed as described in Church and Gilbert (1984) except that membranes were hybridized at high stringency (68 C).

RNA isolation and northern blot hybridization

Total RNA was isolated from rice rachis tissues and 10 μg were electrophoresed in a 1% agarose gel, then transferred to a Hybond N^+ membrane (Amersham) and analyzed by northern blot hybridization. The probe and hybridization conditions were the same as those used in the Southern analysis.

Complementation analysis

To construct pBI-OSH15, a restriction fragment covering the 14 kbp region of the *OSH15* genomic locus was cloned into the *Hind*III/*Sal*I site of the hygromycin resistant binary vector pBI101-Hm3. This vector was a modification of pBI-H1 (Ohta et al. 1990) and contains a unique *BamH*I site in

the multiple cloning site. pBI-cont, which was used as a control vector and contained no insert, was constructed from pBI101-Hm3 by digestion with *Sal*I and religation. Binary vectors were introduced into *Agrobacterium tumefaciens* strain EHA101 by electroporation. Rice transformation was performed as described in Hiei et al. (1994).

Histological analysis

Plant materials were fix in FAA (formalin:acetic acid:70% ethanol, 1:1:18), embedded in ice on a cryostat, cut into 20 μm sections and stained with safranin. For hematoxylin staining, plant materials fixed in FAA were dehydrated through a graded ethanol series and embedded in Technovit 7100 resin (Kulzer & Co. GmbH, Wehrheim, FRG). Microtome sections (3-5 μm) were stained with hematoxylin.

In situ hybridization analysis

In situ hybridization with digoxigenin-labeled RNA, produced from the *OSH15* coding region without a poly-A tail, was conducted as described previously (Kouchi and Hata 1993). Tissues were fixed with 4% (w/v) paraformaldehyde and 0.25% glutaraldehyde in 0.1 M sodium phosphate buffer and embedded in Paraplast Plus. Microtome sections (7-10 μm thick) were applied to glass slides treated with Vectabond (Vector Lab.). Hybridization and immunological detection of the hybridized probe were performed using the method of Kouchi and Hata (1993).

Results

Screening for loss-of-function mutations in the rice homeobox genes

Rare insertions of a transposable element into a gene can be detected by PCR-based screening. If an insertion of a transposable element occurs in the gene of interest, a suitable template will be generated which can be amplified exponentially by PCR using gene-specific and transposon-specific primers. My general approach for screening for loss-of-function mutations in the rice homeobox gene is depicted in Fig. 5-1A. I designed transposon-specific primers from the long terminal repeat (LTR) of *Tos17* in sense (LTR4S) and antisense (LTR4A) orientations, and a gene-specific primer (KN31) from the conserved region of the *KNOTTED*-type homeodomain. Using either LTR4S or LTR4A plus KN31, I performed PCR-based screening. For efficient screening, I adopted a pool sampling system in which plants were arranged in a two-dimensional matrix. Genomic DNA was isolated from leaves sampled in pools consisting of either a column or a row. In this way, the genomic DNA from each plant is represented in a unique combination of a row and a column. I screened 47 DNA pools consisting of 24 columns and 23 rows. These pools contained genomic DNA from about 550 plants in which transposition of the rice retrotransposon *Tos17* had been induced and random insertion had occurred. A range of amplification products was obtained (Fig. 5-1B).

From these amplification products, discrete bands with the same size in a column and row were cloned and sequenced. DNA sequencing analysis revealed that the amplified DNA fragment derived from the pooled genomic DNA corresponding to column 5 and row I contained the sequences of *Tos17* and the rice homeobox gene *OSH15*, which belongs to the class1-type of the *KNOTTED* family homeobox genes. Since *Tos17* was inserted into the fourth

exon of *OSH15*, just upstream of the homeodomain region (Fig. 5-1C), this transposon-tagged gene was predicted to be a loss-of-function allele.

To confirm that the insertion of *Tos17* had occurred in the *OSH15* gene and was transmitted germinally, I performed genomic Southern blot analysis with individuals of the progeny of this plant. Genomic DNA was isolated, digested with *Xho*I and hybridized with a probe specific for *OSH15* (Fig. 5-2A). Among 40 individuals tested, three patterns of hybridizing bands were observed. These were a single 6.4 kbp band, two bands of 6.4 kbp and 4.5 kbp or a single 4.5 kbp band. The number of individuals showing each pattern was 9, 21, and 10, respectively. The ratio of these numbers fits the theoretical 1:2:1 predicted for Mendelian inheritance. In wild-type rice, only a band with 6.4 kbp in size was detected (Fig. 5-5A, right panel, lanes 4 and 5). This corresponds to the size predicted from a restriction map of the *OSH15* genomic clone which I isolated previously (Fig. 5-5B). Alternatively, a band of 4.5 kbp was predicted to be generated from the insertion allele of *OSH15* based on the restriction maps of *OSH15* and *Tos17*. Consequently, individuals showing a single band of 4.5 kbp were homozygous (-/-), those with two bands of 4.5 and 6.4 kbp were heterozygous (+/-) for the insertion, and those with a single band of 6.4 kbp were wild-type (+/+). These observations confirmed that the insertion of *Tos17* had occurred in *OSH15* and was transmitted germinally.

To ensure that no normal *OSH15* transcript was generated from the mutant allele, total RNA was isolated from the rachis and subjected to northern blot analysis. As shown in Fig. 5-2B, no transcript was detected in the homozygous plants (-/-). This also suggests that the *Tos17* insertion represents a loss-of-function allele. Although signals corresponding to the *OSH15* transcript were detected in both wild-type (+/+) and heterozygous (+/-) plants, the intensity of signal in wild-type (+/+) plants was about twice as

strong as that in heterozygotes (+/-). Thus the expression level of *OSH15* was controlled in a dose dependent manner.

I next observed the phenotype caused by loss-of-function of *OSH15*. Although no abnormality in morphology was observed in plants heterozygous for the insertion or wild-type plants under normal growing conditions, all the plants homozygous for the insertion displayed a dwarf phenotype (Fig. 5-3A), indicating that the insertion of *Tos17* into *OSH15* was genetically linked to the dwarf phenotype.

Identification of allelic mutations in *OSH15*

To confirm that the dwarf phenotype was caused by the loss-of-function of *OSH15*, I identified allelic mutations in *OSH15*. Because of their agronomic importance, a large number of dwarf rice mutants have been isolated and characterized. These mutants are categorized into six groups based on the elongation pattern of the upper four to five internodes (Fig. 5-4, redrawn from Takeda 1977). In this diagram, the ratios of each internode length to total culm length are drawn schematically. In the *dn* type mutant, the ratio is very similar to that of wild-type but the length of each internode is shortened. In the *dm* type mutant, the length of the second internode is specifically shortened. In the *d6* type mutant, internodes below the second are shortened. In the *nl* type mutant, the fourth internode is relatively longer but the first internode is shortened. In the *sh* type mutant, the first internode is specifically shortened.

In order to fit the *OSH15* loss-of-function mutant into this classification scheme of rice dwarf mutants, I measured the length of the upper four internodes and panicle of the loss-of-function mutants and compared them with those of wild-type plants (Fig. 5-3B). Although no difference was observed between the mutant and the wild-type plant in the length of the panicle and the first internode, the lengths of the second, third, and fourth internodes were shortened to approximately 25 %, 27 %, and 15 %, respectively. By comparing

this internode elongation pattern to the previously described six groups of dwarf mutants, I determined that the *OSH15* loss-of-function mutants clearly fit into the *d6* group of dwarf mutants (Fig. 5-4).

Mutations in at least two loci can result in a *d6* phenotype (Kitano et al. unpublished results). At one locus, which is mapped at the telomere end of the short arm of chromosome 7, three allelic mutants designated *d6-1*, *d6-ID6*, and *d6-tankanshirasasa* (Kinoshita and Shinbashi, 1982; Nagao and Takahashi, 1963), have been identified. All of these mutants are recessive and they are often used as tester lines for this chromosome. In addition, *OSH15* maps to a position 8.3 cM from the telomere end of the short arm of chromosome 7 (data not shown).

In order to test the possibility that the three *d6* type dwarf mutants also contain mutations in *OSH15*, I performed Southern blot analysis (Fig. 5-5A). Genomic DNA was extracted from *d6-tankanshirasasa* (lane 1), *d6-1* (lane 2), *d6-ID6* (lane 3), and from two different wild-type rice cultivars, T-65 (a parental line of *d6-1*, lane 4) and shiokari (a parental line of *d6-ID6*, lane 5). These samples were digested with either *Sac*I or *Xho*I and hybridized with an *OSH15*-specific probe consisting of all of exon 4 and part of exon 5. In genomic DNA from wild-type plants digested with *Sac*I or *Xho*I, two bands of 4.5 kbp and 5.0 kbp or a single band of 6.4 kbp were observed, respectively (Fig. 5-5A lanes 4 and 5). In contrast, no hybridizing bands were observed in genomic DNA from *d6-tankanshirasasa* or *d6-1* digested with either enzyme (Fig. 5-5A lanes 1 and 2). Similarly, no hybridizing bands were detected when the 5' region upstream of *OSH15* was used to probe DNA from the dwarf mutants, whereas a specific band was detected in wild-type DNA (data not shown). This indicates that, in *d6-tankanshirasasa* and *d6-1*, a deletion occurred in the region of the *OSH15* gene. In the case of *d6-ID6*, hybridizing bands of the same size as those of wild-type plants were observed in *Sac*I-digested genomic DNA (Fig. 5-5A, left panel, lanes 3, 4, and 5). However, in

*Xho*I-digested genomic DNA, a novel band of approximately 18 kbp was detected. This contrasts with the 6.4 kbp band detected in genomic DNA from wild-type plants (Fig. 5-5A, right panel, lanes 3, 4, and 5). To identify the mutation in *d6-ID6*, I cloned and sequenced the entire coding region and the junctions of exons and introns from *d6-ID6*. By comparing the sequences of the *d6-ID6* to its parental line, shiokari, I determined that a deletion of about 700 bp including the entire first exon, the 5' upstream region and part of the first intron had occurred (Fig. 5-5B). As an *Xho*I site exists in the first exon of the wild-type gene, the *Xho*I-digested genomic DNA from *d6-ID6* showed a polymorphism compared to that from wild-type plants. Thus, all of the alleles of the *d6* locus contained deletions in the *OSH15* gene. This strongly suggests that loss-of-function of the *OSH15* gene causes the *d6*-type dwarf phenotype in rice.

Molecular complementation analysis of *d6* by *OSH15*

I also used complementation analysis to study *d6-1* by introduction of a wild-type *OSH15* gene. When I introduced a control vector which carries no rice genomic DNA to *d6-1*, no change in the culm length was observed (Fig. 5-6, right). However, when a 14 kbp DNA fragment containing the entire wild-type *OSH15* gene was introduced, the normal phenotype was restored (Fig. 5-6, left), confirming that the *d6* dwarf mutant is caused by the loss-of-function mutation in the *OSH15* gene.

Anatomy of the *d6* mutant internode

Plants homozygous for a loss-of-function allele of *OSH15* displayed an abnormal pattern of internode elongation which resulted in a dwarf phenotype. All four alleles showed the same pattern of internode elongation.

Under normal growth conditions, the shoot apical meristem (SAM) exists near the base of the ground portion of the plant body during the

vegetative stage. In wild-type rice plants, after the change from vegetative to reproductive growth, the upper four to six internodes elongate in succession from base to top. When an internode elongates, the intercalary meristem (IM) differentiates at the base of the internode. Internode elongation is caused by mitotic activity in cells of the IM and by the elongation of these cells in the elongation zone immediately above the IM.

Fig. 5-7 shows the mature fourth internode of a wild-type plant and the third and fourth internodes of a *d6-1* mutant. Although differentiation of nodes and internodes is obvious in both cases, internode elongation was severely affected in the *d6-1* mutant.

In order to understand the cellular basis of the *d6* mutant internode phenotype, I prepared sections of internodes from wild-type and mutant plants and observed them microscopically. In longitudinal sections of wild-type mature fourth internodes at 2-3 mm above the node, cells of the IM were observed to be closely packed and small-sized (Fig. 5-8A). Similar results were obtained with the *d6* mutant (Fig. 5-8B), demonstrating that differentiation of the IM was not affected in the *d6* mutant. In the upper region of the internode of wild-type plants, parenchyma cells were longitudinally elongated (Fig 5-8C), whereas, in the *d6* mutant, parenchyma cell elongation was not apparent (Fig. 5-8D). In cross sections of internodes from the elongated region of the stem of wild-type plants, epidermal cells and sclrenchymatous cell layers (hypodermal cell layers) were observed in the outermost part and outer part of the stem, respectively. Sclerenchymatous cells were very long (often reaching 1 mm in length) and slender, and had well developed secondary cell walls (Fig. 5-9B). Fourteen or fifteen small vascular bundles were arranged concyclically at the inside of the sclrenchymatous cell layer. Large vascular bundles were also arranged concyclically in the inner region and air spaces were located between them. The central region of the stem consisted of a large lacuna (cavity) (Fig. 5-9A).

In *d6-1*, the organization of small vascular bundles was severely disrupted whereas the arrangement of large vascular bundles and air spaces was similar to that seen in wild-type plants (Fig. 5-9C). In addition, epidermal cells of mutant internodes were obviously enlarged and sclrenchymatous cells, characterized by well developed secondary walls, were absent. In place of sclerenchymatous cells, vacuolate cells resembling parenchyma cells were observed (compare Fig. 5-9 B and D). The ring shaped arrangement of large vascular bundles and air spaces was not changed. Finally, the number of cell layers from the epidermis to the air spaces (8 to 9 layers) or to the large vascular bundles (13 to 15 layers) that constituted the outer part of an internode were similar in wild-type and mutant internodes. These observations suggest that radial pattern formation was not affected, but that differentiation of sclrenchymatous cell layers was defective in *d6-1* internodes.

Epidermal cell shape was observed in sections taken parallel to the epidermis using Nomarsky optics. In wild-type internodes, long, rectangular cells with a wavy margin, termed long cells were observed. Amongst the long cells were seen pairs of oval cells, termed silica and cork cells, which derived from a single cell termed a short cell (Fig. 5-10 A and B). In internodes of *d6-1* mutants, the shape of epidermal cells was quite different from that in wild-type. I observed large, distorted cells with smooth margins which probably correspond to the long cells in wild-type plants. In addition, small cells were also seen which probably correspond to short cells. However, differentiation of silica and cork cells was rarely observed (Fig. 5-10 C and D). This abnormal epidermal cell morphology is specific to the *d6* mutant. Epidermal cells of other dwarf mutants defective in internode elongation, such as *d18* or *d1*, did not show this phenotype (data not shown). Therefore, such abnormal epidermal cell morphology is not caused by the defect in internode elongation but rather may cause it (see Discussion).

Expression pattern of the *OSH15* gene

Since the loss-of-function mutation of *OSH15* affects the development of epidermal and hypodermal cells, I predicted that the expression of *OSH15* might be restricted to the differentiating protodermal cells of the internode. To address this possibility, I performed *in situ* hybridization to observe the localization of *OSH15* mRNA. In longitudinal sections, *OSH15* expression was localized just below the leaf insertion points and at the primordia of axillary buds (Fig. 5-11A). In cross sections through planes at different levels, *OSH15* mRNA seen below the leaf insertion point in longitudinal sections was observed to lie in a ring-shaped pattern (Fig. 5-11 B, C, and D). This localized expression of *OSH15* between two nodes corresponds well to the pattern of defects observed in the loss-of-function mutants.

Discussion

Targeted inactivation of the rice homeobox gene, *OSH15*

Identification of a loss-of-function mutation in a gene of interest is a powerful tool for understanding its function. To gain an understanding of the biological function of a rice homeobox gene, I screened for loss-of-function mutants. I identified one such mutation in *OSH15* from about 550 plants which were mutagenized with random insertions of the rice retrotransposon, *Tos17*. Such a high knock-out efficiency may be due to the selective transposition of *Tos17* into transcribed regions (Hirochika et al., 1996), and indicates the effectiveness of *Tos17* as a tool for targeted gene inactivation.

All the plants homozygous for the insertion of *Tos17* into the *OSH15* gene showed a dwarf phenotype with properties similar to the conventional dwarf mutants, *d6*. I conclude that this dwarf phenotype was caused by the loss-of-function of *OSH15* from the following experiments. First, all conventional *d6* mutants have complete or partial deletions in the *OSH15* gene which caused its loss-of-function. Second, the *d6* dwarf phenotype was complemented by the introduction of a wild-type *OSH15* gene.

The *OSH15* gene in rice encodes a member of the *KNOTTED*-type of the homeobox transcription factors (Sato et al. 1998). Homeobox genes encode a highly conserved protein motif, the homeodomain, which acts as a sequence-specific DNA binding motif (Gehring et al. 1992). Based on the deduced amino acid sequence around the homeodomain of *OSH15*, this gene is classified into the class1-type of the *KNOTTED* gene family. *OSH15* is most similar to maize *RS1* and *KNOX4* (Kerstetter et al., 1994), and its map position is 8.3 cM on rice chromosome 7, where synteny to the maize chromosome regions of both *RS1* and *KNOX4* is observed (Ahn and Tanksley, 1993). These results indicate that *OSH15* may be an orthologue of maize *RS1* and *KNOX4*. The presence of two *OSH15* orthologues in maize may be due to

the genetic redundancy in this species (Helentjaris et al., 1988). In fact, I have isolated six distinct class1-type *KNOTTED*-like homeobox genes from rice, and in most cases, the rice gene has two probable orthologues in maize.

Most class1-type genes of the *KNOTTED*-like homeobox gene family are expressed around the SAM and thought to be involved in SAM formation and/or maintenance. Loss-of-function alleles have been identified in *KN1* from maize (Kerstetter et al., 1997) and *STM* from *Arabidopsis* (Long et al., 1996). In both of these mutants, defects related to meristem maintenance, such as abnormal branching pattern and lateral organ formation, or maintenance of the SAM in the embryo were observed. In contrast to these previous observations, I could not identify any abnormality related to meristem formation or maintenance in the *OSH15* loss-of-function mutant. In fact, *OSH15* is not expressed in the center of the SAM during vegetative and reproductive growth (Sato et al. 1998). This indicates that, in contrast to *KN1* and *STM*, *OSH15* has roles other than meristem formation and/or maintenance.

The role of *OSH15* in internode elongation

I found that the loss-of-function mutations in *OSH15* resulted in a *d6*-type dwarf phenotype. In *d6* mutants, the abnormalities that I observed were restricted to the development of epidermal and hypodermal cells (Fig. 5-8, 9, and 10). From observations of dwarf mutants unrelated to the *d6* mutation, such abnormalities are not general characteristics of dwarf mutants but rather are specific to the *d6* mutants. Therefore, these abnormalities may likely be responsible for the defect in internode elongation in *d6* mutants.

Based on the phenotype of the loss-of-function mutants and the expression pattern of *OSH15*, I considered how *OSH15* might function in rice development. *OSH15* expression was observed just below the leaf insertion point, where the internode would later develop, before any visible

differentiation of the node or the internode had occurred (Fig. 5-11). *OSH1* mRNA was present in a ring-shaped pattern which delineated the several cell layers destined to become the outer part of the future internode. Thus, *OSH15* responds to positional cues that determine the outer several cell layers of the developing internode. The loss-of-function phenotype of the *d6* mutant internode demonstrates that the differentiation of the sclrenchymatous cell layers and the morphogenesis of the epidermal cells are affected by the product of *OSH15* within the developing internode. Taken together, these results indicate that *OSH15* may interpret positional information, and controls the differentiation and/or the morphogenesis of the hypodermal sclrenchymatous cell layers and epidermal cells.

How loss-of-function of *OSH15* could change the morphology and/or differentiation of epidermal or hypodermal cells may be interpreted as follows. One possibility is that gene(s) required for the morphogenesis of these cells are regulated by the products of *OSH15*. Cell morphology is determined by regulated cell expansion. Expansion of plant cells involves coordinated assembly of the cytoskelton and cell wall. The orientation of microtubules is believed to play an important role in determining the direction of expansion (Carpita and Gibeaut, 1993). In the outer cell layers of wild-type internodes in the elongation zone, the orientation of cortical microtubules was clearly horizontal, enabling these cells to elongate vertically, whereas in internodes of *d6* mutants, microtubule orientation was irregular (data not shown). Thus, *OSH15* may function in the regulation of genes involved in the organization of cortical microtubules in the outer cell layers of the internode.

Another possibility is that *OSH15* may act as a developmental switch by which cells in the hypodermal cell layers direct the formation of sclrenchymatous cells. In this hypothesis, it is conceivable that, in the loss-of-function mutant, the development of sclrenchymatous cells was blocked and the cells instead developed into parenchyma-like cells. This possibility is

supported by the fact that, in the first internode of the *d6* mutants, abnormalities in the development of hypodermal cell layers were also observed (data not shown). While internodes of *d6* mutants exhibited nearly normal elongation, they also showed a weak fasciation and distortion, and were somewhat thicker than wild-type internodes. Cross sections of the first internodes revealed that the differentiation of sclrenchymatous cell layers was blocked as in the lower abnormal internodes. These observations indicate that *OSH15* functions in the same manner in the first internode as in other internodes, even though normal internode elongation occurs. The elongation of the first internode may be compensated by some unknown factor(s) present in the first internode but not in other lower internodes.

Interestingly, in the first internode of *d6* mutants, epidermal cell shape was relatively normal (data not shown). This suggests that *OSH15* may not be directly involved in the development of epidermal cells. The reason that epidermal cells showed abnormal cell morphology in unelongated lower internodes of *d6* mutant plants may be explainable by the cell-cell interactions between the epidermal cells and the adjacent inner cell layers. Examples of such cell-cell interactions have been reported for the *FAS* gene from tomato (Szymkowiak and Sussex 1992) and the *KNOTTED* homeobox genes from maize (Hake, 1992). In *fas* (*fasciated*) tomato mutants, a larger meristem is formed, resulting in an increased number of floral organs. In studies of periclinal chimeras in which the L1 and L2 layers of the SAM consisted of wild-type cells and the inner layers were the *fas* genotype, it was found that the underlying *fas* tissue could induce abnormal cell divisions in the wild-type L1 layer (Szymkowiak and Sussex 1992). The interpretation of this result is that the FAS protein normally functions in preventing the meristem from overexpansion by repressing a diffusible signal.

The second example is *KN1* in maize. In dominant *Kn1* leaves caused by ectopic production of KN1 proteins in leaves, the abnormalities observed

in epidermal cells were not caused by the genotype of those cells (Hake, 1992). In this case, cell-cell interaction is thought to be mediated by the movement of KN1 protein and *KN1* mRNA through the plasmodesmata (Lucas et al., 1995).

In wild-type rice internodes, expression of *OSH15* in the inner cell layers may regulate epidermal cell morphology through the action of a signal generated in the inner cell layers or the OSH15 protein itself on epidermal cells. In the *d6* mutant, defects in the development of the sclrenchymatous cell layers were observed in other tissues such as the rachis and pedicel (data not shown). These tissues also showed a weak fasciation and distortion. *In situ* hybridization analysis revealed that *OSH15* was also expressed in the inflorescence and in floral meristems in a ring-shaped pattern where the rachis and pedicel would eventually develop (Sato et al. 1998). These observations strongly suggest that *OSH15* consistently functions as a developmental cue for the sclrenchymatous cells throughout most of the plant life cycle. Such a role of *OSH15* is in agreement with the notion that homeobox genes are master regulatory genes that specify the body plan and control the development of many eukaryotic organisms. The identifications of further loss-of-function mutations in plant homeobox genes will provide more clues to the general function(s) of plant homeobox genes in plant development.

Summary

The rice homeobox gene *OSH15* is a member of the *KNOTTED*-type homeobox gene family. Although the *KNOTTED*-type homeobox genes are thought, based on the phenotypes of gain-of-function mutants with ectopic expression of the genes, to be involved in the development and/or maintenance of the shoot apical meristem (SAM), it is difficult to know the actual function(s) of these genes in wild-type plants. A crucial step in determining the function of plant homeobox genes is the isolation of recessive mutant alleles of the genes. I report here the identification and characterization of a loss-of-function mutation in *OSH15* from a library of retrotransposon tagged lines of rice. Based on the phenotype and map position, I have further identified three independent deletion alleles of the locus from conventional morphological mutants. All of these recessive mutations, which are considered to be null alleles, exhibited defects in internode elongation. Introduction of a 14 kbp genomic DNA fragment which includes all exons, introns, and 5'- and 3'- flanking sequences of *OSH15* complemented the defects in internode elongation, confirming that they were caused by the loss-of-function of the *OSH15* gene. Internodes of the mutants had abnormal shaped epidermal and hypodermal cells and showed an unusual arrangement of small vascular bundles. These mutations demonstrate a role for *OSH15* in the development of rice internodes. This is the first evidence that the *KNOTTED*-type homeobox genes have roles in plant development outside of SAM formation and/or maintenance.

References

Ahn, S. and Tanksley, S. D. (1993) Comparative linkage map of the rice and maize genomes. *Proc. Natl. Acad. Sci. USA* **90**: 7980-7984.

Carpita, N. C. and Gibeaut, D. M. (1993) Structural models of primary cell walls in flowering plants: Consisteny of molecular structure with the physical properties of the walls during growth. *Plant J.* **3**: 1-30.

Chen, J. J., Janssen, B. J., Williams, A. and Sinha, N. (1997) A gene fusion at a homeobox locus: alterations in leaf shape and implications for morphological evolution. *Plant Cell* **9**: 1289-1304.

Church, G. and Gilbert, W. (1984) Genomic sequencing. *Proc. Natl. Acad. Sci. USA* **81**: 1991-1995.

Clark, S. E., Jacobsen, S. E., Levin, J. Z., and Meyerowitz, E. M. (1996) The *CLAVATA* and *SHOOT MERISTEMLESS* loci competitively regulate meristem activity in *Arabidopsis. Development* **122**: 1567-1575.

Clark, S. E., Williams, R. W., and Meyerowitz, E. M. (1997) The *CLAVATA1* Gene Encodes a Putative Receptor Kinase That Controls Shoot and Floral Meristem Size in Arabidopsis. *Cell* **89**: 575-585.

Chuck, G., Lincoln, C. and Hake, S. (1996) *KNAT1* Induces Lobed Leaves with Ectopic Meristems When Overexpressed in *Arabidopsis. Plant Cell* **8**: 1277-1289.

Gehring, W. J. (1992) The homeobox in perspective. *Trends Biochem. Sci.* **17**: 277-280.

Gehring, W. J., Affolter, M. and Bürglin, T. (1994) HOMEODOMAIN PROTEINS. *Annu. Rev. Biochem.* **63**: 487-526.

Hake, S. (1992) Unraveling the knots in plant development. *Trends Genet.* **8**: 109-114.

Hareven, D., Gutfinger, T., Parnis, A., Eshed, Y., and Lifschitz, E. (1996) The Making of a Compound Leaf: Genetic Manipulation of Leaf Architecture in Tomato. *Cell* **84**: 735-744.

Helentjaris, T., Weber, D. and Wright, S. (1988) Identification of the Genomic Locations of Duplicate Nucleotide Sequences in Maize by Analysis of Restriction Fragmet Length Polymorphisms. *Genetics* **118**: 353-363.

Hiei, Y., Ohta, S., Komari, T. and Kumashiro, T. (1994) Efficient transformation of rice (*Oryza sativa* L.) mediated by *Agrobacterium* and sequence analysis of the boundaries of the T-DNA. *Plant J.* **6**: 271-282.

Hirochika, H., Sugimoto, K., Otsuki, Y., Tsugawa, H., and Kanda, M. (1996) Retrotransposons of rice involved in mutations induced by tissue culture. *Proc. Natl. Acad. Sci. USA* **93**: 7783-7788.

Izawa, T. and Shimamoto, K. (1996) Becoming a model plant: the importance of rice to plant science. *Trends plant sci.* **1**: 95-99.

Jackson, D., Veit, B., and Hake, S. (1994) Expression of maize *KNOTTED1* related homeobox genes in the shoot apical meristem predicts patterns of morphogenesis in the vegetative shoot. *Development* **120**: 405-413.

Kerstetter, R. A., Laudencia-Chingcuanco, D., Smith, L. G., and Hake, S. (1997) Loss-of-function mutations in the maize homeobox gene, *knotted1*, are defective in shoot meristem maintenance. *Development* **124**: 3045-3054.

Kerstetter, R., Vollbrecht, E., Lowe, B., Veit, B., Yamaguchi, J. and Hake, S. (1994) Sequence Analysis and Expression Patterns Divide the Maize *knotted1*-like Homeobox Genes into Two Classes. *Planat Cell* **6**: 1877-1887.

Kinoshita, T. and Shinbashi, N. (1982) Identification of dwarf genes and their character expression in the isogenic background. *Japan. J. Breed.* **32**: 219-231.

Kouchi, H. and Hata, S. (1993) Isolation and characterization of novel nodulin cDNAs representing genes expressed at early stages of soybean nodule development. *Mol. Gen. Genet.* **238**: 106-119.

Lincoln, C., Long, J., Yamaguchi, J., Serikawa, K., and Hake, S. (1994) A *knotted1*-like Homeobox Gene in Arabidopsis Is Expressed in the Vegetative Meristem and Dramatically Alters Leaf Morphology When Overexpressed in Transgenic Plants. *Plant Cell* **6**: 1859-1876.

Long, J. A., Moan, E. I., Medford, J. I. and Barton, M. K. (1996) A member of the KNOTTED class of homeodomain proteins encoded by the *STM* gene of *Arabidopsis*. *Nature* **379**: 66-69.

Lu, P., Porat, R., Nadeau, J. A. and O'Neill, S. D. (1996) Identification of a Meristem L1 Layer-Specific Gene in Arabidopsis That Is Expressed during Embryonic Pattern Formation and Defines a New Class of Homeobox Genes. *Plant Cell* **8**: 2155-2168.

Lucas, W. J., Bouché-Pillon, S., Jackson, D. P., Nguyen, L., Baker, L., Ding, B., and Hake, S. (1995) Selective Trafficking of KNOTTED1 Homeodomain Protein and Its mRNA Through Plasmodesmata. *SCIENCE* **270**: 1980-1983.

Matsuoka, M., Ichikawa, H., Saito, A., Tada, Y., Fujimura, T. and Kano-Murakami, Y. (1993) Expression of a Rice Homeobox Gene Causes Altered Morphology of Transgenic Plants. *Plant Cell* **5**: 1039-1048.

Müller, K. J., Romano, N., Gerstner, O., Garcia-Maroto, F., Pozzi, C., Salamini, F. and Rohde, W. (1995) The barley *Hooded* mutation caused by a duplication in a homeobox gene intron. *Nature* **374**: 727-730.

Nagao, S. and Takahashi, M. (1963) Trial construction of twelve linkage groups in Japanese rice. Genetical studies on rice plant, XXVII. *J. Fac. Agr. Hokkaido Univ. Sapporo* **53**: 72-130.

Ohta, S., Mita, S., Hattori, T. and Nakamura, K. (1990) Construction and expression in tobacco of a β-glucuronidase (GUS) reporter gene containing an intron within the coding sequence. *Plant Cell Physiol.* **31**: 805-813.

Sato,Y., Sentoku, N., Nagato, Y., and Matsuoka, M. (1998) Two separable functions of a rice homeobox gene, *OSH15*, in plant development. *Plant J.* Submitted.

Schneeberger, R. G., Becraft, P. W., Hake, S. and Freeling, M. (1995) Ectopic expression of the *knox* homeobox gene *rough sheath1* alters cell fate in the maize leaf. *Genes Dev.* **9**: 2292-2304.

Sinha, N. R., Williams, R. E. and Hake, S. (1993) Overexpression of the maize homeo box gene, *KNOTTED-1*, causes a switch from determinate to indeterminate cell fates. *Genes Dev.* **7**: 787-795.

Smith, L. G., Greene, B., Veit, B. and Hake, S. (1992) A dominant mutation in the maize homeobox gene, *Knotted-1*, causes its ectopic expression in leaf cells with altered fates. *Development* **116**: 21-30.

Smith, L. G. and Hake, S. (1994) Molecular genetic approaches to leaf development: *Knotted* and beyond. *Can. J. Bot.* **72**: 617-625.

Steeves, T. A. and Sussex, I. M. (1989) Patterns in Plant Development. Cambridge University Press.

Szymkowiak, E. J. and Sussex, I. M. (1992) The internal meristem layer (L3) determines floral meristem size and carpel number in tomato periclinal chimeras. *Plant Cell* **4**: 1089-1100.

Takeda, K. (1977) Internode elongation and dwarfism in some gramineous plants. *Gamma Field Sym.* **16**: 1-18.

Tamaoki, M., Kusaba, S., Kano-Murakami, Y. and Matsuoka, M. (1997) Ectopic Expression of a Tobacco Homeobox Gene, *NTH15*, Dramatically Alters Leaf Morphology and Hormone Levels in Transgenic Tobacco. Plant Cell Physiol. **38**: 917-927.

Vollbrecht, E., Veit, B., Sinha, N. and Hake, S. (1991) The developmental gene Knotted-1 is a member of a maize homeobox gene family. *Nature* **350**: 241-243.

Figures

A

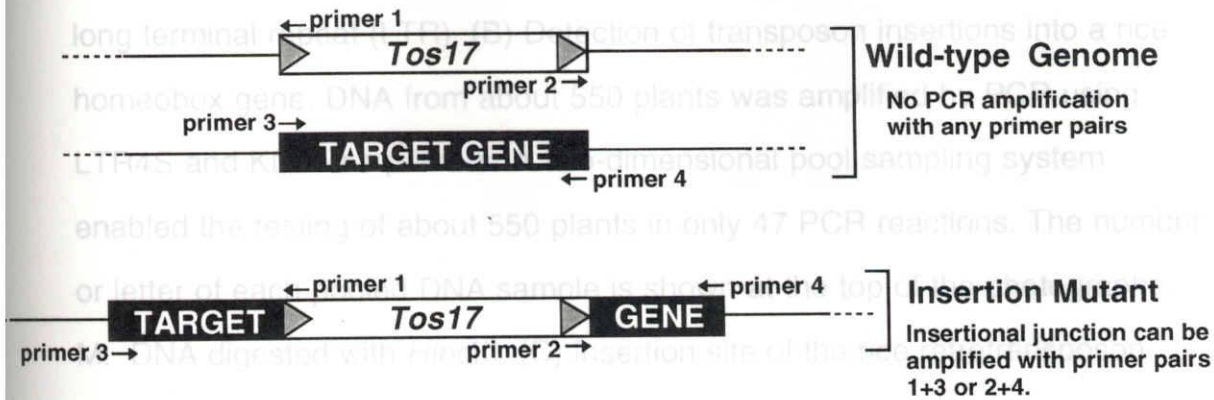
primer 1
Tos17
primer 2
primer 3
TARGET GENE
primer 4
Wild-type Genome
No PCR amplification with any primer pairs
primer 1
primer 4
TARGET
Tos17
GENE
primer 3
primer 2
Insertion Mutant
Insertional junction can be amplified with primer pairs 1+3 or 2+4.

B

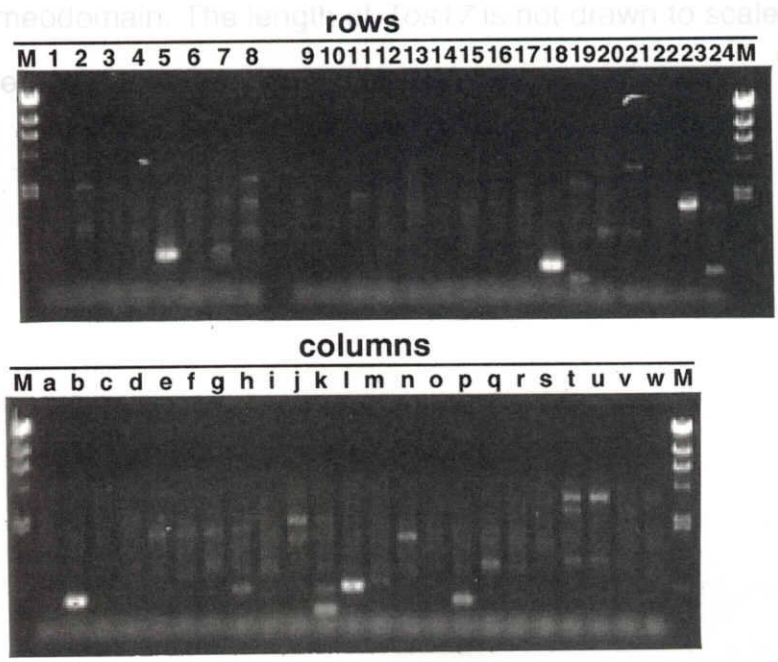
rows
M 1 2 3 4 5 6 7 8 9 10 11 12 13 14 15 16 17 18 19 20 21 22 23 24 M
columns
M a b c d e f g h i j k l m n o p q r s t u v w M

C

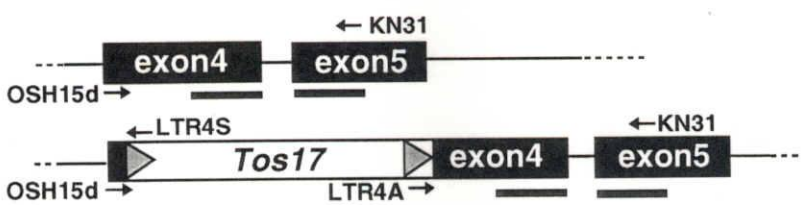
KN31
exon4
exon5
OSH15d
LTR4S
KN31
Tos17
exon4
exon5
OSH15d
LTR4A

Fig. 5-1. (A) General approach for detecting transposon insertions. An insertion of the rice retrotransposon *Tos17* into a target gene can be detected by PCR amplification using primer pairs 1+3 or 2+4. Triangles indicate the long terminal repeat (LTR). (B) Detection of transposon insertions into a rice homeobox gene. DNA from about 550 plants was amplified by PCR using LTR4S and KN31 as primers. A two-dimensional pool sampling system enabled the testing of about 550 plants in only 47 PCR reactions. The number or letter of each pooled DNA sample is shown at the top of the photographs. M: DNA digested with *Hind*III. (C) Insertion site of the rice retrotransposon *Tos17* into the fourth exon of the rice homeobox gene *OSH15*. Filled boxes indicate exons, and bold underlining indicates the approximate position of the homeodomain. The length of *Tos17* is not drawn to scale; *Tos17* is 4.3 kbp whereas the homeodomain is 190 bp.

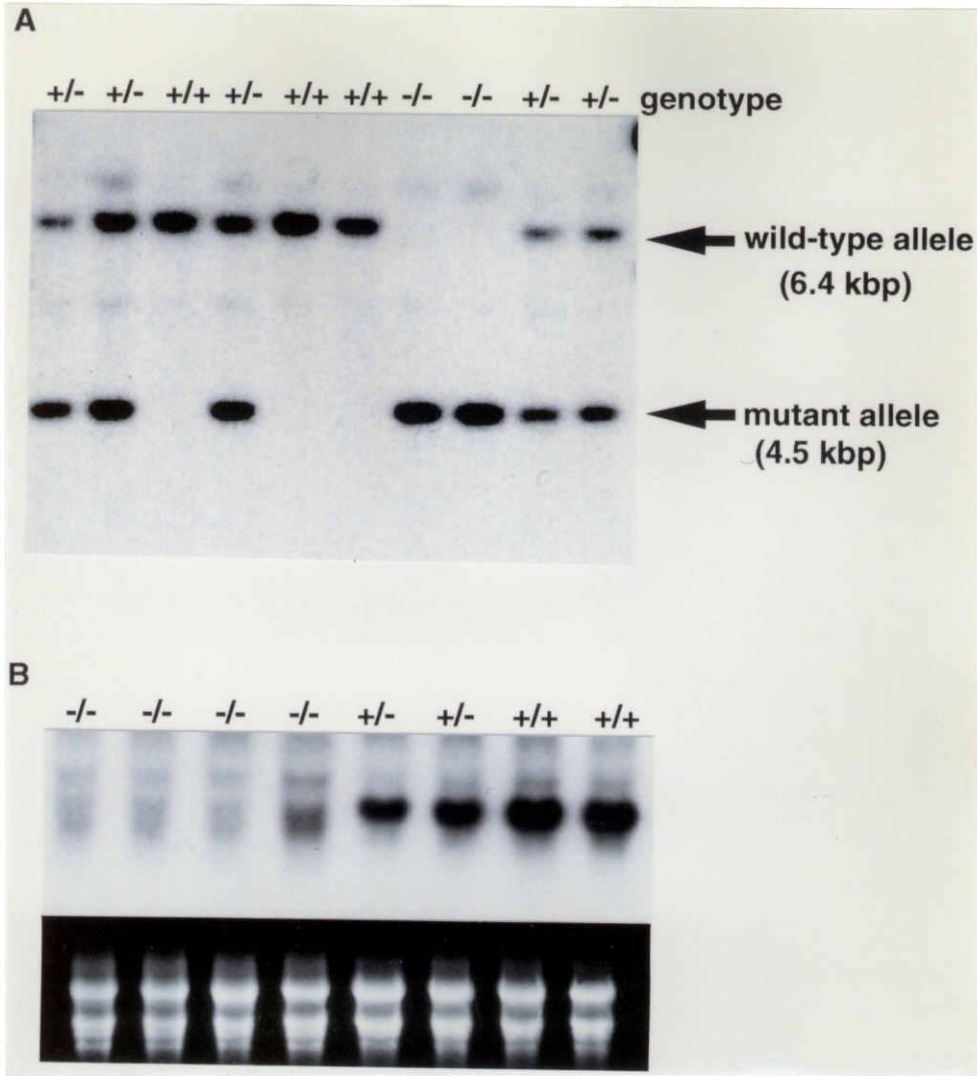

Fig. 5-2. (A) Cosegregation analysis by genomic Southern blot hybridization. Each lane contains 1 µg of genomic DNA digested with *Xho*I. In wild-type plants, a single 6.4 kbp band was detected (lanes +/+). A 4.5 kbp band was predicted, based on restriction maps of *Tos17* and *OSH15*, to be detected in *Xho*I digests containing the mutant allele . Therefore, individuals with only a single band at 4.5 kbp represent homozygotes for the insertion (-/-) and those showing bands at 6.4 kbp and 4.5 kbp represent heterozygotes (+/-). (B) Northern blot analysis of RNA from the rachis of homozygous (-/-), heterozygous (+/-) and wild-type (+/+) plants. A single band at 1.6 knt, corresponding to *OSH15* transcripts, was detected in heterozygous (+/-) and wild-type (-/-) plants but not in homozygous (-/-) plants. The lower panel shows ethidium bromide stained RNA corresponding to the above lanes to illustrate RNA loading levels.

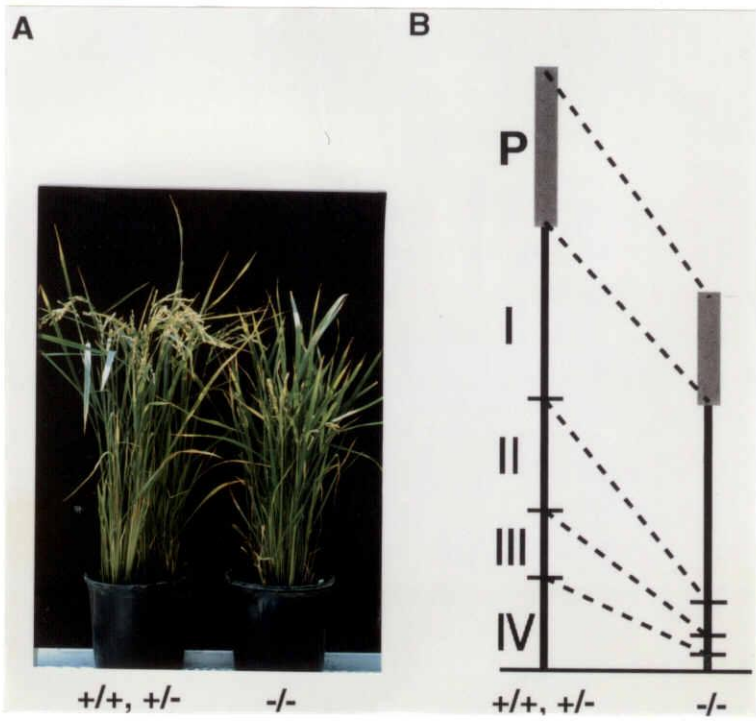

Fig. 5-3. (A) The appearance of homozygous (-/-), heterozygous (+/-) and wild-type (+/+) plants. All homozygous(-/-) plants exhibited a dwarf phenotype (compare the height of the positions of the panicles). (B) Comparison of the length of panicles and the upper four internodes of homozygous (-/-), heterozygous (+/-) and wild-type (+/+) plants. Lengths of panicles and upper four internodes were measured based on the average length of ten culms from twenty plants of each genotype and are summarized in the diagram. In mutants, the lengths of the second, third and fourth internodes were severely reduced.

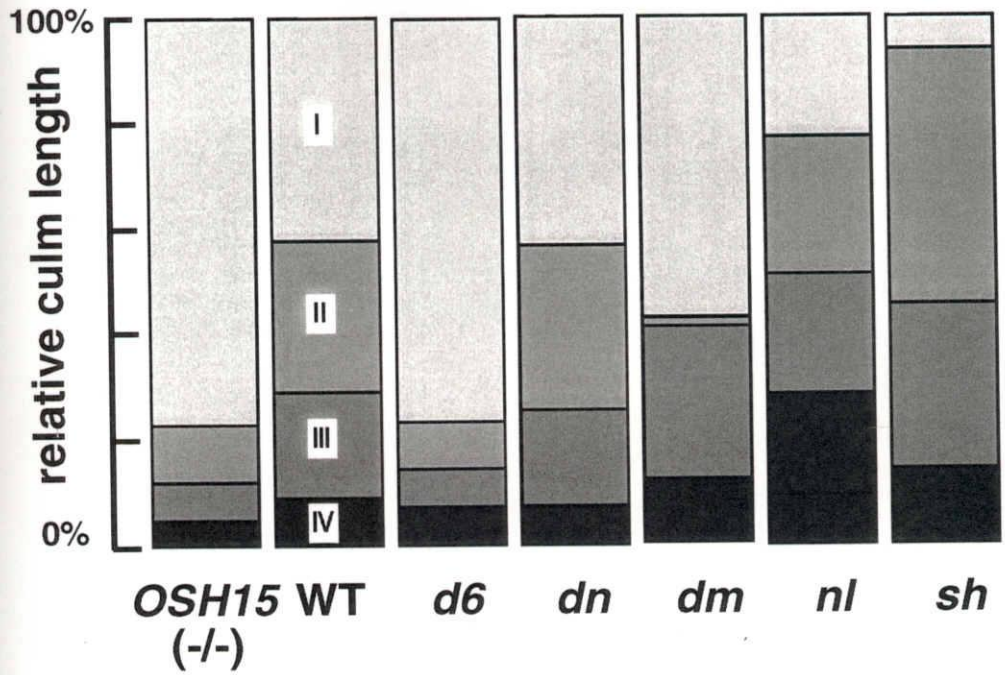

Fig. 5-4. Patterns of internode elongation of rice dwarf mutants (redrawn from Takeda 1977).

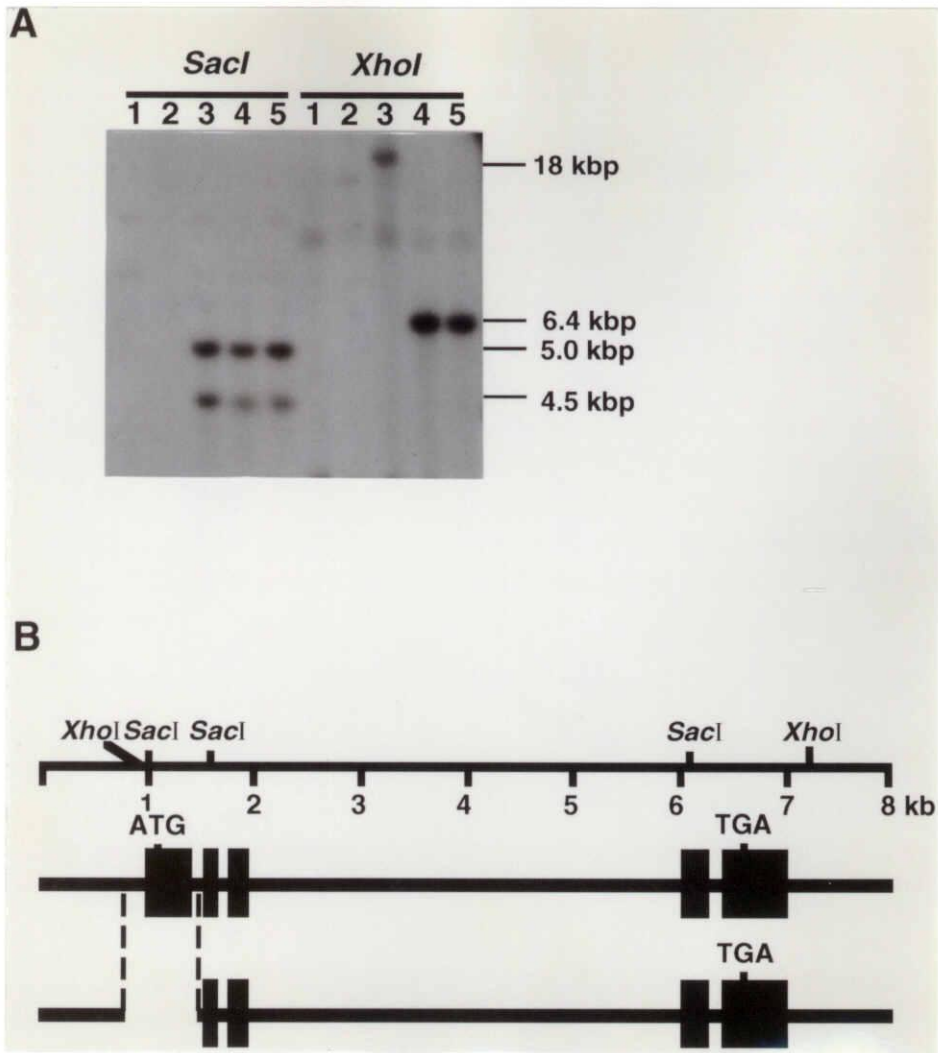

Fig. 5-5. (A) Detection of mutations in the *OSH15* genes of the three *d6* type mutants by genomic Southern analysis. Each lane contains 1 μg of genomic DNA digested with either *Sac*I or *Xho*I. Numbers at right indicate the approximate sizes of the specific bands. Lanes 1, *d6-tankanshirasasa*; lanes 2, *d6-1*; lanes 3, *d6-ID6*; lanes 4, T-65; lanes5, shiokari. (B) Genomic structure around the *OSH15* gene in wild-type and *d6*-ID6. Boxes and bold lines indicate exons, and introns plus untranslated regions, respectively. *Sac*I and *Xho*I restriction sites are indicated at the top. ATG and TGA indicate the position of the start and stop codons, respectively.

Fig. 5-6. Complementation analysis of the *d6* phenotype. A 14 kbp wild-type genomic DNA fragment containing the entire 8 kbp *OSH15* coding region (plus introns) and 6 kbp of upstream DNA was used to transform *d6-1* dwarf rice mutants (left plant). As a control, the vector without insert was also introduced (right plant). The normal phenotype was clearly restored in plants transformed with the *OSH15* gene.

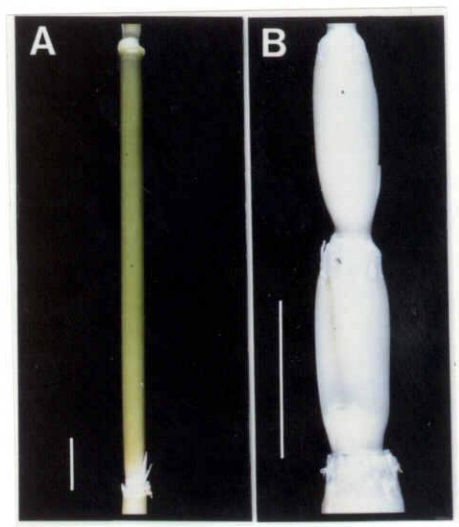

Fig. 5-7. The appearance of internodes from *d6* and wild-type plants. Surface views of the fourth internode of a wild-type plant (A), and the third and fourth internodes of a *d6* dwarf mutant (B). Bar = 1 cm.

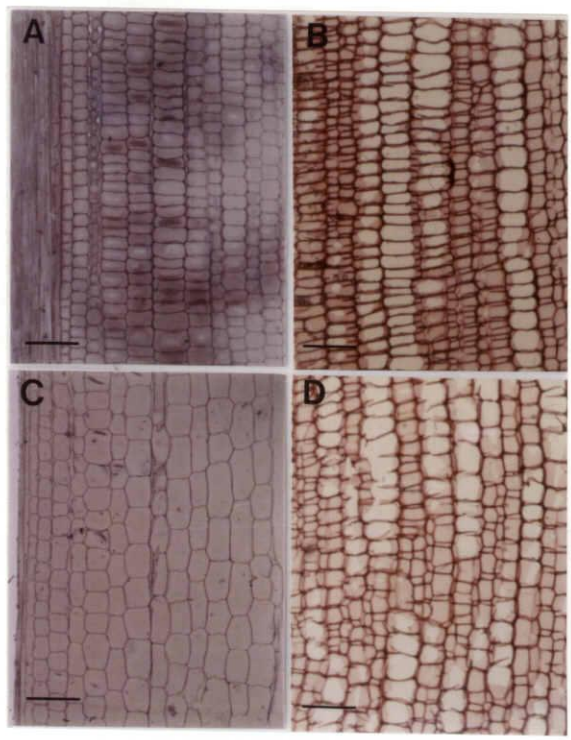

Fig. 5-8. Longitudinal sections of the fourth internodes of wild-type and *d6* dwarf mutant plants. (A) Longitudinal section through the IM of the fourth internode of a wild-type plant. (B) Longitudinal section through the IM of the fourth internode of a *d6* mutant plant. (C) Longitudinal section through the elongated zone of the fourth internode of a wild-type plant. (D) Longitudinal section through the elongated zone of the fourth internode of a *d6* mutant plant. Bar = 100 μm.

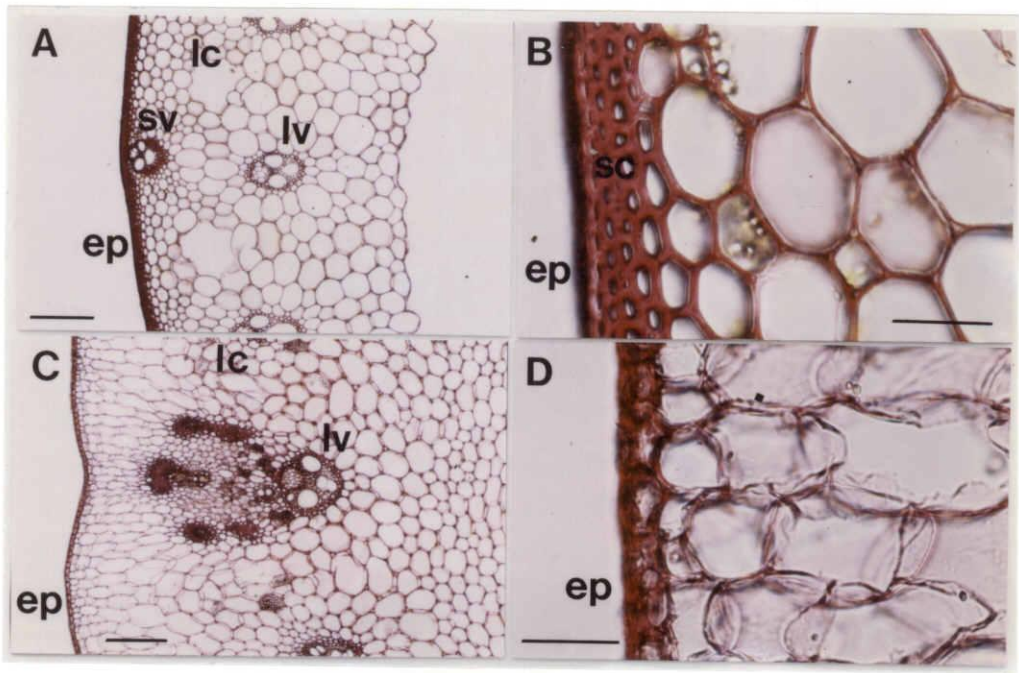

Fig. 5-9. Cross sections of the fourth internodes of wild-type and *d6* dwarf mutant plants. (A) Wild-type. Bar = 100 μm. (B) Higher magnification of (A). Bar = 30 μm. (C) *d6*. Bar = 100 μm. (D) Higher magnifications of (C). Bar = 30 μm. ep, epidermis; sc, sclrenchymatous cell layers; sv, small vascular bundles; lv, large vascular bundles; lc, lacuna (air spaces).

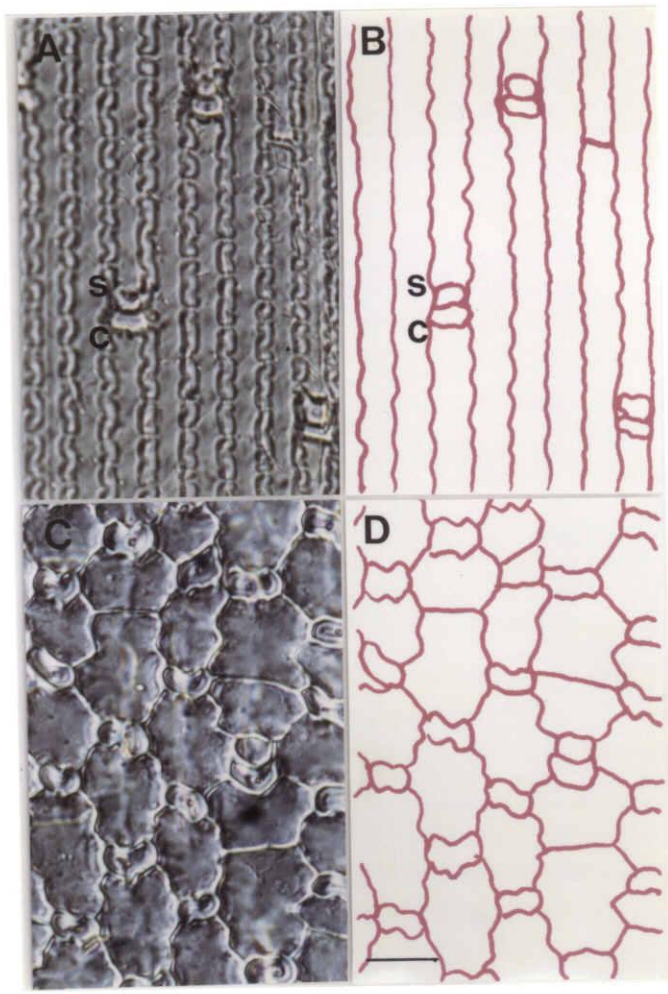

Fig. 5-10. Epidermal cells of wild-type and *d6* dwarf mutant plants. (A and B) Epidermal cells of the fourth internode of a wild-type plant. (C and D) Epidermal cells of the fourth internode of a *d6* mutant plant. Bar = 20 μm. s, silica cell; c, cork cell.

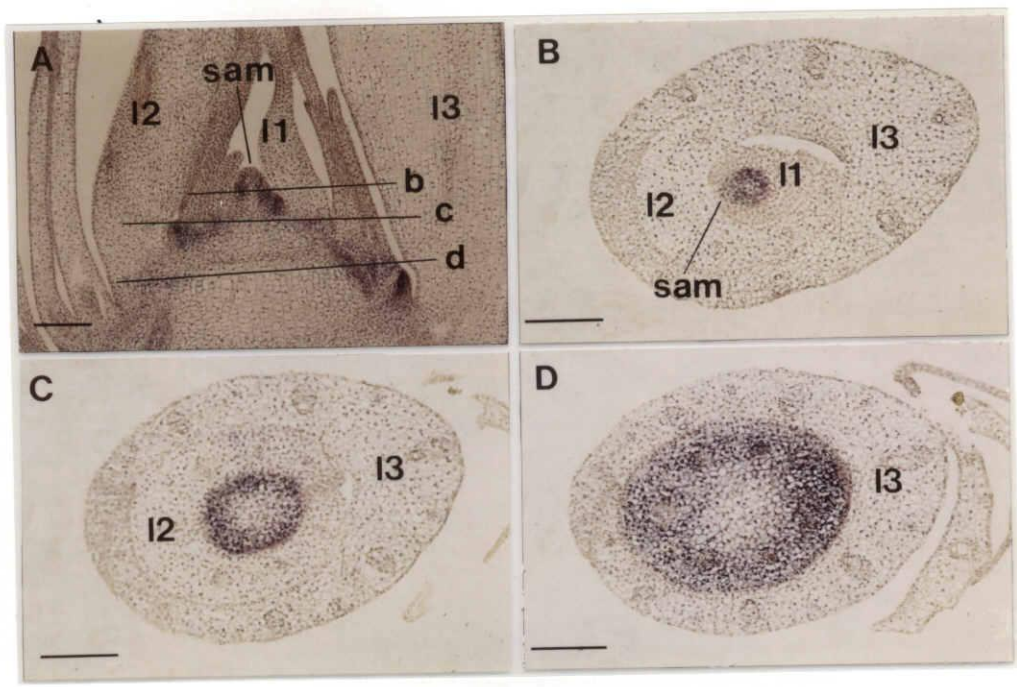

Fig. 5-11. *In situ* localization of *OSH15* mRNA in the rice vegetative shoot. (A) Longitudinal section of a rice vegetative shoot. Lines b, c, and d indicate the plane of cross sections corresponding to panels (B), (C) and (D). Bar = 100 μm. sam, shoot apical meristem; I1, I2, and I3 indicate leaf 1, 2, and 3, respectively.

Chapter 6

General Discussion

In this thesis, I analyzed the function of rice homeobox genes, *OSH1* and *OSH15*. It has been known that *KNOTTED*-type homeobox genes often cause severe morphological abnormalities in leaves when the genes are overexpressed with constitutive promoters such as the cauliflower mosaic virus *35S* promoter in transgenic plants. However, it has been difficult to ascertain the site or timing of the action of the transgenes. In the second chapter, I tried to express *OSH1* in transgenic tobacco plants in the timing at my disposal by driving it under the control of the *PR1a* promoter which can induce the expression of downstream genes by treatment of a chemical inducer. Although this inducible gene expression system did not work as I had expected, It was revealed that the *OSH1* expression in mature leaf was not necessary for the abnormal leaf development and such abnormal leaf morphology was induced by irregular periclinal cell divisions in incipient leaves. Based on these observations, I discussed the role of *OSH1* in transgenic tobacco as to affect the mechanism controlling the pattern of cell division. However, it should be noted that the ectopic expression experiments is always difficult to discuss the *bona fide* function of genes of interest in the wild-type context, that is, the function of *OSH1* around the rice SAM.

Recently, the inducible functional expression system using an animal gluococorticoid receptor has been developed (Lloyd et al., 1994). In this system, genes of interests are translationally fused to the animal glucocorticoid receptor (GR) and expressed constitutively in transgenic plants. In the normal growing condition, the fusion proteins are inactive because GR is trapped with heat shock proteins (HSPs), but when plants are exposed to dexamethasone, a steroid ligand of GR, the fusion proteins become active because GR is activated and is released from HSPs. In this inducible system, functions of genes of interest can be induced temporally and spatially at ones disposal. This system has been applied to some genes related to the plant development, such as an *Arabidopsis* homeobox gene, *ATHB1* (it is not the

KNOTTED-type) and *Arabidopsis* flowering-time gene, *CONSTANS* (Aoyama et al., 1995; Simon et al. 1996). In both cases, the focus of these studies are on the set of genes or genetic systems regulated by these genes rather than the function of these genes in wild-type context.

In the third chapter, I analyzed the expression pattern of *OSH1* during embryogenesis. Recently, analyses of the expression pattern of plant homeobox genes during embryogenesis (Smith et al., 1995; Long et al., 1996; Klinge and Werr, 1995; Lu et al., 1996; Sato et al., 1996) become focused by following reasons. In the first, by analogy of the function of animal homeobox genes, it is plausible that plant homeobox genes may also act in the regionalization of the embryo or the determination of the site of the organogenesis during embryogenesis. In the second, since the most of the *KNOTTED*-type homeobox genes are expressed around the SAM, these genes are thought to be useful molecular markers for the SAM development during embryogenesis. In the third, among the embryogenesis defective mutations in *Arabidopsis*, it was revealed that one mutation designated *stm* was caused by a loss-of-function of a *KNOTTED*-type homeobox gene, *STM*. In *stm*, almost all the embryonic organs such as cotyledons, hypocotyl, and radicle are formed normally during embryogenesis, but SAM is not observed. As a result, seeds of *stm* can germinate but can not grow thereafter. Based on the phenotype of the *stm* mutant and the expression pattern of *STM* during the wild-type embryogenesis, *STM* are thought to act in the maintenance of the SAM.

From the expression pattern of *OSH1* in the early embryogenesis of wild-type and the *orl1* mutant, in which most of the differentiations of embryonic organs are not observed and it grows relatively large in a globular shape, I revealed that *OSH1* is expressed both before and after the SAM formation. Based on these observations, I hypothesized that *OSH1* may be involved in the development and the maintenance of the SAM during

embryogenesis. To confirm this hypothesis, it is necessary to observe the phenotype of the loss-of-function mutation of *OSH1* during embryogenesis. But to date, such mutation in *OSH1* has not been identified. *KN1* from maize is thought to be an orthologue of *OSH1* because both genes show high similarities in the DNA sequence and the expression pattern and are mapped to the region where the synteny between the maize and rice is observed (Ahn and Tanksley,. 1993). Recently, loss-of-function mutations in *KN1* were reported (Kerstetter et al., 1997). These mutants were not embryogenesis defective, whereas *KN1* is expressed in a similar pattern to *OSH1* or *STM* during embryogenesis, and the functions of *KN1* and *OSH1* during embryogenesis are still unclear. This may be due to the fact that most of the maize genomes are duplicated (Helentjaris et al., 1988) or other genes may act in the same way as *KN1* (see later).

In the fourth and fifth chapters, I focused on the analyses of *OSH15.* To understand the function of *OSH15* in rice development, I performed *in situ* hybridization analyses. Based on the expression pattern of *OSH15*, I proposed that *OSH15* might play at least two different roles in rice development. One may be very similar to that of *OSH1* in the early embryogenesis. Another may be involved in the determination of the segmentation of shoot units or in the development of nodes or internodes. On the function of *OSH15* during the post embryogenesis stage of development, the validity of the latter possibility is proved by the isolation of the loss-of-function mutations in *OSH15* . The loss-of-function mutants of *OSH15* showed abnormal pattern of internode elongation. In the mutant internodes, moreover, the differentiation of hypodermal cell layers were obscure. Because the site of defects observed in the loss-of-function mutant well correspond with the regions of the ring shaped expression of *OSH15* around SAM, I considered that *OSH15* is involved in the differentiation of the hypodermal sclrenchymatous cell layers.

Many plant homeobox genes have been cloned from various plant species since the first plant homeobox gene, *KN1*, was cloned. Among them, only few genes have been elucidated their roles in plant development. Identification of the recessive mutation alleles of genes of interest is one of the powerful ways for understanding its function. In the plant homeobox genes, phenotypes of the loss-of-function mutants were reported on *KN1, STM, BELL1, GL2, and OSH15* (Kerstetter et al., 1997; Long et al., 1996; Reiser et al., 1995; Rerie et al., 1994). Among them, *STM, BELL1*, and *GL2* genes were cloned from recessive mutation alleles and their functions were discussed based on the phenotypes of the mutants. This kind of approach is called "forward genetics". On the other hand, the recessive mutation alleles of the *KN1* were produced genetically. Intragenic suppressors were identified from the heterozygous dominant *Kn1* mutants and among the progeny of these suppressors, the recessive *KN1* alleles were selected. Identification of recessive mutation alleles of *OSH15* is the first example in which the knock out line was screened based on the DNA sequence of a gene. This kind of approach is called "reverse genetics". Recently, targeted gene inactivation in plants has become practical. Insertionally mutagenized lines with T-DNA or (retro)transposons have been generated in *Arabidopsis*, maize, *Petunia*, and rice. Using these lines, it is possible to screen knock out lines of genes of interest systematically by the PCR. Another possibility to obtain knock out lines is the homologous recombination method. Indeed, some examples of the gene disruption based on the homologous recombination have also been reported in *Arabidopsis* (Miao and Lam, 1995). Now, large scale genome projects in *Arabidopsis* or rice are progressing and enormous sequence information is released. Establishment of the methods or the materials for targeted gene inactivation enables further the analysis of functions of genes by reverse genetics.

As mentioned repeatedly, *KNOTTED*-type homeobox genes are thought to be involved in the related developmental processes since most of this class of genes are expressed around the SAM. But the recessive mutation alleles of the *KNOTTED*-type homeobox genes reported so far (*STM*, *KN1*, and *OSH15*) showed completely different phenotypes. Since both *KN1* and *OSH15* were expressed in the early embryo, the loss-of-function mutants of these genes had been thought to be embryogenesis defective as was the case for *STM*. But both mutants did not show any defect in embryogenesis, therefore, the functions of both genes during embryogenesis are still unclear. It would be often observed that the loss-of-function of a single gene do not exhibit any phenotype, if there are many genes similar in sequences and in expression patterns like *KNOTTED*-type homeobox genes, or in the plants with duplicated genome like maize. The reason why in the loss-of-function mutants of *KN1* or *OSH15* embryogenesis defective was not observed is probably due to those mentioned above. To solve this problem, one is to use a plant material which have less duplicated genome like *Arabidopsis* or rice, and another is to analyze the double, triple or more mutant which has mutations simultaneously in homeobox genes with similar structure and expression pattern.

On the other hand, if the knock out mutant shows embryo lethal phenotype like *stm*, it would be difficult to observe the function of a gene of interest after embryogenesis. In such cases, analysis of the weak alleles may enable the analysis after embryogenesis. Or if the conditional gene targeting become applicable in plant, it would be more easier in such cases.

In this thesis, I tried to analyze the function of *KNOTTED*-type rice homeobox genes. Only a few part of the functions of *KNOTTED*-type homeobox genes in plant development become elucidated. Combined genetics and molecular biology (reverse and forward genetics) will enable further identification of functions of these genes. Although it is still in black box, further analysis, such as how the expression of those homeobox genes are

regulated, or what is the target gene(s) of the homeobox genes, will shed light on the genetic regulatory systems for the plant development in which the homeobox genes are engaged.

References

Ahn, S. and Tanksley, S. D. (1993) Comparative linkage map of the rice and maize genomes. *Proc. Natl. Acad. Sci. USA* **90**, 7980-7984.

Aoyama, T., Dong, C. H., Wu, Y., Carabelli, M., Sessa, G., Ruberti, I., Morelli, G. and Chua, N. H. (1995) Ectopic expression of the Arabidopsis transriptional activator Athb-1 alters leaf cell fate in tobacco. *Plant Cell* **7**, 1773-1785.

Helentjaris, T., Weber, D. and Wright, S. (1988) Identification of the Genomic Locations of Duplicate Nucleotide Sequences in Maize by Analysis of Restriction Fragmet Length Polymorphisms. *Genetics* **118**, 353-363.

Kerstetter, R. A., Laudencia-Chingcuanco, D., Smith, L. G. and Hake, S. (1997) Loss-of-function mutations in the maize homeobox gene, *knotted1*, are defective in shoot meristem maintenance. *Development* **124**, 3045-3054.

Klinge, B. and Werr, W. (1995) Transcription of the *Zea mays* Homeobox (*ZmHox*) Genes Is Activated Early in Embryogenesis and Restricted to Meristems of the Maize Plant. *Dev. Genet.* **16**, 349-357.

Lloyd, A. M., Schena, M., Walbot, V. and Davis, R. W. (1994) Epidermal Cell Fate Determination in Arabidopsis: Patterns Defined by a Steroid-Inducible Regulator. *SIENCE* **266**, 436-439.

Long, J. A., Moan, E. I., Medford, J. I. and Barton, M. K. (1996) A member of the KNOTTED class of homeodomain proteins encoded by the *STM* gene of *Arabidopsis*. *Nature* **379**, 66-69.

Lu, P., Porat, R., Nadeau, J. A. and O'Neill, S. D. (1996) Identification of a Meristem L1 Layer-Specific Gene in Arabidopsis That Is Expressed during Embryonic Pattern Formation and Defines a New Class of Homeobox Genes. *Plant Cell* **8**, 2155-2168.

Miao, Z. H. and Lam, E. (1995) Targeted disruption of the TGA3 locus in *Arabidopsis thaliana*. *Plant J.* **7**, 359-365.

Reiser, L., Modrusan, Z., Margossian, L., Samach, A., Ohad, N., Haughn, G. W. and Fischer, R. L. (1995) The *BELL1* Gene Encodes a Homeodomain Protein Involved in Pattern Formation in the Arabidopsis Ovule Primordium. *Cell* **83**, 735-742.

Rerie, W. G., Feldmann, K. A. and Marks, D. M. (1994) The *GLABRA2* gene encodes a homeo domain protein required for normal trichome development in *Arabidopsis*. *Genes Dev.* **8**, 1388-1399.

Sato, Y., Hong, S. K., Tagiri, A., Kitano, H., Yamamoto, N., Nagato, Y. and Matsuoka, M (1996) A rice homeobox gene, *OSH1*, is expressed before organ differentiation in a specific region during early embryogenesis. *Proc. Natl. Acad. Sci. USA* **93**, 8117-8122.

Simon, R., Igeño, M. I. and Coupland, G. (1996) Activation of floral meristem identity genes in *Arabidopsis*. *NATURE* **384**, 59-62.

Smith, L. G., Jackson, D. and Hake, S. (1995) Expression of *knotted1* Marks Shoot Meristem Formation During Maize Embryogenesis. *Dev. Genet.* **16**, 344-348.

Acknowledgment

I wish to express my deepest sense of gratitude to Dr. Makoto Matsuoka, Professor of BioScience Center, Nagoya University, for accepting me as a graduate student and for his keen interest, active help, persistent guidance, and sympathetic suggestions.

I am also thankful to Mrs. Akemi Tagiri for her excellent technical assistance of *in situ* hybridization, and to Dr. Masanori Tamaoki and Mr. Naoki Sentoku for their constant help and discussion throughout this work.

I am most grateful to Drs. Yasuo Nagato, Hidemi Kitano, Hirochika Hirohiko, Hitoshi Mori, Junji Yamaguchi, and Yutaka Takeda for their invaluable discussions in connection with this investigation.

My heartfelt many thanks are for members in my laboratory, Miyako Tanaka-Ueguchi, Yoshio Miura, Nobuhiro Nagasawa, Kazutsuka Sanmiya, Tomoaki Sakamoto, Asuka Nishimura, Hiroki Ito, Marino Yamashita, Yumiko Aoki, and Chizuko Yamamuro. I also thanks to all members of the BioScience Center, Nagoya University for their friendliness and help.

Lastly, I express my heartfelt thanks to my parents and Ms. Sae Shimizu for their encouragement and patience during the nine years of my study in Nagoya University.

January 1998

Yutaka Sato

List of Publications

(1) **Sato, Y., Tamaoki, M., Murakami, T., Yamamoto, N., Kano-Murakami, Y., and Matsuoka, M.** (1996) Abnormal cell divisions in leaf primordia caused by the *OSH1* expression lead to altered morphology of leaves in transgenic tobacco. *Mol. Gen. Genet.* **251**, 13-22.

(2) **Sato, Y., Hong, S. K., Tagiri, A., Kitano, H., Yamamoto, N., Nagato, Y., and Matsuoka, M.** (1996) A rice homeobox gene, *OSH1*, is expressed before organ differentiation in a specific region during early embryogenesis. *Proc. Natl. Acad. Sci. USA.* **93**, 8117-8122.

(3) **Sato, Y., Sentoku, N., Nagato, Y., and Matsuoka M.** (1997) Two separable functions of a rice homeobox gene, *OSH15*, in plant development. *Plant J.* Submitted.

(4) **Sato, Y., Sentoku, N., Miura, Y., Kitano, H., Hirochika, H., and Matsuoka, M.** (1998) Loss-of-function mutations in a rice homeobox gene, *OSH15*, are defective in internode elongation caused by the abnormal shape and arrangements of epidermal and hypodermal cells. *Genes & Dev.* Submitted.

List of Publications (Appendix)

(1) **Tamaoki, M., Sato, Y., and Matsuoka, M.** (1997) Dorsoventral pattern formation of tobacco leaf involves spatial expression of a tobacco homeobox gene, *NTH15*. *Genes Genet. Syst.* **72**, 1-8.

(2) 佐藤　豊、千徳　直樹、松岡　信、　(1997)「総説・高等植物の胚発生時におけるホメオボックス遺伝子の発現様式と機能」　蛋白質 核酸 酵素　**42** (11), 1866-1874.